Persistent free radicals in asphaltenes and their reactions

by

Alili Aytan

A thesis submitted in partial fulfillment of the requirements for the degree of

Master of Science
in
Chemical Engineering

Department of Chemical and Materials Engineering
University of Alberta

© Alili Aytan, 2019

ABSTRACT

Asphaltenes, defined as a solubility class, are soluble in toluene and insoluble in paraffinic solvents such as C_5 and C_7. Asphaltenes have high heteroatom and a low H/C ratio compared to bitumen's other fractions. Moreover, they have a complex structure, high molecular weight, and high melting point that give rise to its poor quality and therefore, asphaltenes have a low value as a product. Consequently, not much attention has been paid to the processing of asphaltenes. It is known that asphaltenes have high radical concentration that ranges between 10^{18} to 10^{20} spins/g, which leads to addition and combination reactions at high temperatures that in turn may result in undesired coke formation. In order to advance the asphaltenes processing, it is important to evaluate the nature of the radicals present in asphaltenes and causing the changes.

This study was carried out to evaluate to what extent free radicals play a role in asphaltene chemistry. In addition, it was aimed to determine how much of the free radicals present in asphaltenes are persistent. In the current study, the change in free radical concentration of asphaltenes was tracked for 456 hours under air and nitrogen purges. It was observed that the concentration of the free radicals decreases in both cases. The reason for the persistency of the free radicals was investigated to identify whether it is due to caging or steric effects. According to the results of the current study, the reason for the free radical persistency in asphaltenes is mostly due to the steric effects. It was observed that with addition of 1,2-dihydronaphthalene the hydrogen transfer per gram of asphaltenes was 100 times larger than the amount of free radicals present.

Different probe molecules were reacted with asphaltenes at $250\ °\mathrm{C}, 4$ MPa, to evaluate the steric requirements and behavior of the free radicals. It was found out that asphaltenes are capable of reacting with sterically hindered compound having three phenyl rings and complex geometry, such as 1,2-diphenylethenylbenzene in the presence of solvent to give 1,1,2-triphenylethane 0.03±0.01(mg/ml). Moreover, steric requirements of asphaltenes were dominant during their reactions with α-Methyl styrene, 2,4,6-trimethylstyrene, E-stilbene. It was shown that upon reaction of probe molecules with higher amount of asphaltenes, formation of addition products and combination products is inhibited. 1,1-diphenylethylene was found to be effective hydrogen acceptor for asphaltene chemistry evaluation that did not lead to formation of any addition or combination products.

Keywords: asphaltenes, persistent free radicals, steric requirements, hydrogen abstraction, hydrogen acceptor

ACKNOWLEDGEMENT

The first person I would like to thank is my supervisor, Dr. Arno de Klerk, for providing me with such a valuable opportunity and for his guidance throughout my master program. He was always willing to help whenever I had questions. Dr. Arno Moreover, I am very thankful to Dr. Arno for his patience, support, encouragement and understanding, whenever I was panicking. I am also thankful to Dr. Muhammad Siddiquee for his valuable advice and comments.

Next, I would like to thank my mother and sisters for their immense support and unconditional love.

I am also thankful to Isa for his help.

I would also like to thank my research group. Special thanks to Cloribel Santiago Flores, Annapurna Sri Sowmya Turuga, Natalia Montoya Sanchez, Nuvaid Ahad, Tudor Apan, Giselle Uzcategui Barrios. Also, I am thankful to Adriana Rivolta and Sahil Sood for their uplifting attitude and messages.

Lastly, I would like to thank NEXEN for sponsoring this project.

TABLE OF CONTENTS

LIST OF TABLES

LIST OF FIGURES

List of Symbols / Abbreviations

CASRN- Chemical Abstracts Services Registry Number

ASTM-American Society for Testing and Materials

DHN-1,2-dihydronaphthalene

THN-1,2,3,4-tetrahydronaphthalene

N-naphthalene

DHA-9,10-dihydroanthracene

DPE-1,1-diphenylethylene

ES- E-stilbene

TPE- triphenylethylene

TMS-2,4,6-trimethylstyrene

AMS- α-Methylstyrene

SATP- Standard Ambient Temperature, Pressure

Chapter 1 – Introduction

1.1 Background

With the dramatic growth of world population, the demand for the energy sources also increases. The oil has long been the most prevalent energy source for most of the countries. However, there limited reserves of conventional oil left. Consequently, more attention is drawn to the unconventional types of oil. Being the most widespread unconventional oil resource, oil sands gains popularity as an alternative energy source. Canada has one of the largest oil-sands reserves in the world. In 2018, the number for the Canadian Oil sands reserves was around 164 billion barrels (Oil Sands Magazine, 2019). It contains bitumen that has wide range of usage after being subjected to upgrading process.

Bitumen is a viscous compound with a density of (ρ) >1000 kg/m^3 at 15.6 °C (5–10 °API), and dynamic viscosity of (μ) >10^5 mPa·s (cP) at 24 °C. It has to meet pipeline specification in order to be transported. The Canadian pipeline specifications include limits such as kinematic viscosity (ν) < 350 cSt at 7.5 °C, and density (ρ) < 940 kg/m^3 (>19 °API) (Gray, 2015; Banerjee, 2012; Strausz and Lown., 2003).

Dilution and upgrading are most common strategies performed to meet the pipeline specifications.

Dilution is performed by blending bitumen with gas condensate, naphtha, kerosene, and lighter crude oils (Hart, 2014). However, the amount of diluent required to meet the pipeline specifications is very high, in the range of 20–60 v/v % depending on the bitumen type and the diluent. The most commonly used diluents are natural gas condensate and naphtha, but due to limited availability in Canada, the cost of using diluent is quite high, and it has been argued that upgrading should be preferred over dilution as a more cost-effective process (Banerjee, 2012).

Further upgrading of the bitumen involves reactions to modify the structure of molecules present in bitumen, mainly by thermal cracking. This process usually comprises the breaking of large hydrocarbon molecules into smaller ones. The conversion of the molecules during thermal cracking occurs via homolytic bond dissociation which lead to further radical formation. Thus, chemical and free radical reactions at elevated temperatures take place, leading to addition and combination reactions (Gray, 2015). Free radicals significantly affect the properties of the bitumen products. In addition, it has been studied that free radicals are responsible for coke formation (Zachariah et al., 2013). High molecular weight compounds are obtained as a result of combination and addition reactions, and they can give rise to problems in downstream processes.

Free radical reactions play important role in all thermal heavy oil and bitumen upgrading processes. The importance of free radicals is highlighted, since this investigation deals with free radicals.

1.2 Industrial context

One approach to upgrading of bitumen to enable pipeline transport is to upgrade the bitumen only to the point where it meets specifications. This approach is called "partial upgrading", because the extent of upgrading is less than found in existing bitumen upgraders, such as described in (Gray, 2015).

A simplified diagram of a partial upgrading process is shown in Figure 1.1. This is the partial upgrading process design of CNOOC International Ltd., the BituMax™ process.

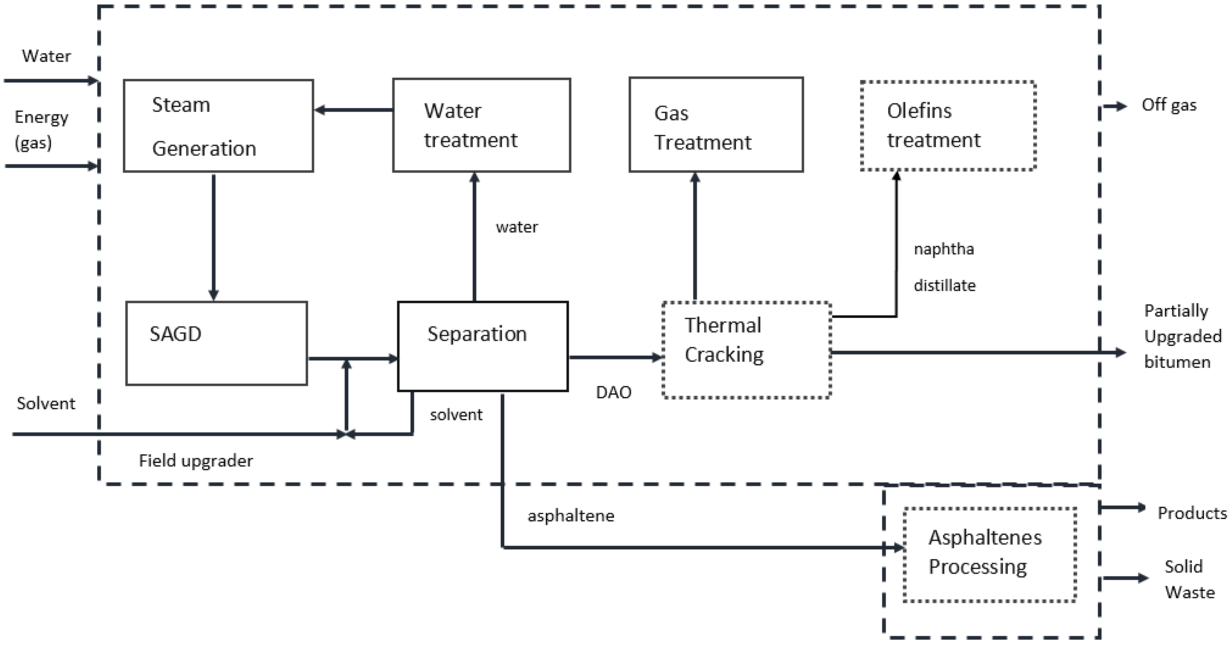

Figure 1. 1. Flow diagram for the BituMax™ partial upgrading process

The first step of this process is a separation step. Solvent deasphalting is performed to separate bitumen into two fractions before the upgrading: deasphalted oil (DAO) and asphaltene fractions.

Deasphalted oil (DAO) is the lighter fraction of bitumen, which is obtained after separation of asphaltenes from bitumen. DAO is further subjected to thermal cracking.

Being the heaviest and most complex fraction of the bitumen, asphaltenes constitutes up to 20% of the bitumen (Strausz and Lown., 2003). Due to its very high asphaltene content, bitumen may give rise to problems while being processed. These mainly include fouling of the utilities, precipitation during transportation, and coke formation in refineries (Ancheyta, 2016). Even though hydroprocessing can be used to avoid coke formation, however it incurs high hydrogen cost that make the process inviable (Ancheyta and Speight, 2007).

In order to minimize the harmful effects of asphaltenes, solvent deasphalting (SDA) process is performed (Figure 1.1). Although asphaltenes may cause serious issues during transportation and processing, however it is not desirable to remove all the asphaltenes from the bitumen. Removal of all the asphaltenes results in a significant reduction of the valuable product from the partial upgrading process. Therefore, depending on the goal, specific operating conditions and solvent can be used to remove the only desired amount of asphaltenes (Mitchell and Speight, 1973; Speight, 2014). This is the approach taken in the BituMax™ process, where the first step is a partial solvent deasphalting. Nevertheless, the asphaltenes that are removed from the bitumen affects overall process cost. Some additional discussion on asphaltenes is useful to place the investigation into context.

Although asphaltenes are the least valuable fraction of the bitumen, they still can find their applicability in different areas such that asphaltenes can be used as coating material for the road pavement. Additionally, asphaltenes can be use as the raw material for the thermal cracking process in order to get lighter and more valuable products (Sheu and Mullins, 1995).

Asphaltene does not have a certain molecular structure and definite physical properties. Asphaltenes are defined as a solubility class that consist of a large range of different molecules (Gray, 2015; Acevedo et al., 2007; Redelius, 2009). Asphaltenes are very complex compounds and their exact compositions and molecular structures are not yet known which make them difficult to study. There exist many challenges for the investigation of the asphaltene structure using conventional methods due to its low solubility as well as high boiling point and complex geometry of the polycyclic aromatic compounds comprising it. It was shown that asphaltenes possess both donor and acceptor properties depending on the site (Naghizada, 2017).

The asphaltenes have a very high free radical concentration that is estimated to be in a range of 0.8×10^{18} to 2.0×10^{20} spins/g (Strausz and Lown, 2003). Since majority of these radicals are persistent free radicals their concentration does not significantly change over time. Carbon free radicals are very reactive and not long-lived radicals, therefore over time their concentration drops considerably. However, the radicals that are not very reactive and have a long lifespan can readily be detected by commonly used spectroscopic techniques. These types of radicals are defined as the persistent free radicals (Hicks, 2007). This is pointed out, because the present study investigated persistent free radicals.

Persistent free radicals significantly affect the nature of the product and have a huge effect on defining free radicals' reactions pathway (Dellinger et al., 2007; DeTar, 1967; Fischer, 1986). The main cause for the properties of the persistent free radicals are their steric effects (Griller and Ingold, 1976; Hicks, 2007; Hicks 2011). Free radicals can be primary, secondary, and tertiary. The tertiary free radicals are the most commonly encountered persistent free radicals in asphaltenes.

Further understanding of the persistent free radicals' nature and behavior would give insight to the asphaltenes reactivity, the pathways of free radicals' reactions and prevention of the high yield coke formation. In addition, it will help to evaluate its impact on the processes involving free radicals, such as the BituMax™ process shown in Figure 1.1.

Evaluation of the origin of free radicals' persistency and their steric requirement for reactions were considered important to advance understanding of the reactions of asphaltenes.

1.3 Objective of this study

The primary objective was to investigate the steric requirements for reactions of persistent free radicals in asphaltenes, and the importance of asphaltenes' steric demand in hydrogenation by hydrogen transfer. Related to this objective, it was necessary to quantify the amount of persistent free radicals in asphaltenes and have some measure of their stability.

1.4 Scope of work

The approach that was taken was to make use of selected probe molecules, with different geometry and properties, to perform hydrogen transfer reactions in asphaltenes. The reasoning was that if the origin of persistent free radicals can be explained by steric protection of the free radical, then there should be a difference in reactivity between probe molecules with different steric requirements.

The work that was performed in this study was organized into the following chapters:

Chapter 2 represents literature review regarding the free radicals and their role in asphaltenes as well as their effect on upgrading

Chapter 3 describes determination of free radical stability over the range of time and investigation of free radicals regeneration phenomena by using donor compound.

Chapter 4 analyzing of **s**teric requirements of asphaltenes, investigated by employing various probe molecules with different geometry and properties.

Chapter 5 Synthesis of the probe molecule similar in properties to the probe molecules available.

Chapter 6 Conclusions and recommendations for future work.

This study forms part of a larger research program under the NSERC / Nexen-CNOOC Inc. Industrial Research Chair in Field Upgrading and Asphaltenes Processing. The results from this work is of value to asphaltenes processing, as well as to the thermal conversion process that was shown in Figure 1.1. The work presented in this study is fundamental in nature and did not pursue any of the indicated applications.

1.5 References

Acevedo, S., Castro, A., Negrin, J.G., Fernández, A., Escobar, G., Piscitelli, V., Delolme, F. and Dessalces, G., 2007. Relations between asphaltene structures and their physical and chemical properties: The rosary-type structure. *Energy & Fuels*, *21*(4), pp.2165-2175.

Ancheyta, J. and Speight, J.G., 2007. *Hydroprocessing of heavy oils and residua*. CRC Press.

Ancheyta, J., 2016. *Deactivation of heavy oil hydroprocessing catalysts: fundamentals and modeling*. John Wiley & Sons.

Banerjee, D.K., 2012. *Oil sands, heavy oil & bitumen: from recovery to refinery*. PennWell Books.

Dellinger, B., Lomnicki, S., Khachatryan, L., Maskos, Z., Hall, R.W., Adounkpe, J., McFerrin, C. and Truong, H., 2007. Formation and stabilization of persistent free radicals. *Proceedings of the Combustion Institute*, *31*(1), pp.521-528.

DeTar, D.F., 1967. Theoretical study of the elementary steps involved in the reaction of benzoyl peroxide with benzene. *Journal of the American Chemical Society*, *89*(16), pp.4058-4068.

Fischer, H., 1986. Unusual selectivities of radical reactions by internal suppression of fast modes. *Journal of the American Chemical Society*, *108*(14), pp.3925-3927.

Gray, M.R., 2015. *Upgrading oilsands bitumen and heavy oil*. University of Alberta.

Griller, D. and Ingold, K.U., 1976. Persistent carbon-centered radicals. *Accounts of Chemical Research*, *9*(1), pp.13-19.

Hart, A., 2014. A review of technologies for transporting heavy crude oil and bitumen via pipelines. *Journal of Petroleum Exploration and Production Technology*, *4*(3), pp.327-336.

Hicks, R. ed., 2011. *Stable radicals: fundamentals and applied aspects of odd-electron compounds*. John Wiley & Sons.

Hicks, R.G., 2007. What's new in stable radical chemistry? *Organic & biomolecular chemistry*, *5*(9), pp.1321-1338.

Mitchell, D.L. and Speight, J.G., 1973. The solubility of asphaltenes in hydrocarbon solvents. *Fuel*, *52*(2), pp.149-152.

Naghizada, N., 2017. Uncatalyzed hydrogen transfer during 100-250° C conversion of asphaltenes. M.Sc. Thesis, University of Alberta: Edmonton, Alberta, Canada.

Oil Sands Magazine. (2019). *World | Oil Sands Magazine*. (online) Available at: https://www.oilsandsmagazine.com/energy-statistics/world#reserves (Accessed 1 Sep. 2019).

Redelius, P., 2009. Asphaltenes in bitumen, what they are and what they are not. *Road Materials and Pavement Design*, *10*(sup1), pp.25-43.

Sheu, E.Y. and Mullins, O.C., 1995. *Fundamentals and applications*. New York: Plenum Press.

Speight, J.G., 2014. *The chemistry and technology of petroleum*. CRC Press.

Strausz, O.P. and Lown, E.M., 2003. *The chemistry of Alberta oil sands, bitumens and heavy oils* (pp. 588-592). Calgary, Alberta, Canada: Alberta Energy Research Institute.

Zachariah, A., Wang, L., Yang, S., Prasad, V. and de Klerk, A., 2013. Suppression of coke formation during bitumen pyrolysis. *Energy & Fuels*, *27*(6), pp.3061-3070.

Chapter 2 – Literature review

2.1 Canada's Oil Sands potential

The increasing energy demand of the world was pointed out in Chapter 1, as well as the oil reserves in Canada. Of relevance to this study is the change in oil supply. The longstanding dominance of conventional oil as a ubiquitous energy source, is eroded by the ever-increasing energy demand of the world (Campbell and Laherrère, 1998; Owen et al., 2010). As a result, unconventional oil sources draw more attention and more research is performed as a promising alternative to the conventional oil. This is pointed out, because this study uses asphaltenes derived from oil sands bitumen as raw material.

Oil sands bitumen is one of the most well-studied and abundant sources of unconventional oil. In addition, having the largest reserves of bitumen in the world, Canada holds the third place, after Venezuela and Saudi Arabia, in total oil reserves in the world. The majority of the oils sands reserves of Canada is located in the province of Alberta (Canadian Association of Petroleum Producers, 2019).

Unlike conventional oil that primarily consists of hydrocarbons and can readily be extracted because of its fluid nature at reservoir conditions, the oil sand is an unconventional oil deposit and consists of a mixture of quartz/clay particles, minerals, metals, water, and bitumen that is immobile at reservoir conditions.

The bitumen content in the oil sands of Alberta varies with the types of deposit and is at most 15 wt%. The oil sands deposits are classified in terms of its bitumen content, which can be divided into three main classes (Banerjee, 2012):

- Low-grade oil sands with bitumen content of 6–8 wt%
- Medium-grade oil sands with bitumen content of 8–10 wt%
- Rich oil sands with bitumen content of >10 wt%

The location of the oil sands as well as the weight percent of the bitumen in oil sands define the viability of the extraction process. The thickness of the oil sands reserves must be over 3 m and the bitumen content must be at least 7 wt% (also known as the cut-off ratio) in order to establish a profitable extraction process (Masliyah et al., 2011).

There is consequently a difference between reserves and recoverable reserves. The Alberta oil sands reserves are estimated to accommodate over 1.7 trillion barrels of bitumen out of which 170 billion barrels are recoverable by the current technology (Richard, 2014; Isaacs, 2005).

Since at least 15 wt% of the bitumen can be classified as *n*-pentane insoluble asphaltenes (see Section 2.2), the recoverable amount of asphaltenes is around 25 billion barrels. This makes this study that investigates persistent free radicals in asphaltenes relevant not only in Canadian context, but also in global context.

2.2 Bitumen and its fractions

Bitumen is a black, dense, viscous mixture of hydrocarbons that also contains heteroatoms, such as nitrogen, oxygen, sulfur. It is defined as a petroleum with density higher than 1000 kg/m^3 and viscosity over 10^4 $\mathrm{mPa.s}$ (Strausz and Lown, 2003). One of analyses used for the characterization of bitumen is SARA (Saturates, Aromatics, Resins, and Asphaltenes) analysis. This analysis is highlighted, because it separated the bitumen based on solubility and the separation of the asphaltenes is analogous to the separation step in the BituMax™ partial upgrading process shown as Figure 1.1 in Chapter 1.

Bitumen has a high asphaltene content, usually about 15-20 wt% *n*-pentane insoluble material (Strausz and Lown, 2003). In order to reduce the viscosity and density, a low asphaltenes content is desirable, which is also considered to be less valuable fraction of the bitumen.

The ultimate goal of removing asphaltenes from the bitumen is to increase the value of the product, thus DAO is itself an upgraded product and can be upgraded further by undergoing chemical reactions and separations (Gray, 2015). DAO contains more light fractions, higher H/C ratio, lower amount of heteroatoms (Shin et al., 2014; Turuga, 2017; Strausz and Lown, 2003) and lower amount of free radicals, than asphaltene fraction (Oliviero Rossi et al., 2018; Tannous and de Klerk, 2019).

Yet, as was pointed out in Chapter 1, removing the asphaltenes from the bitumen results in a yield loss. Ideally, the asphaltenes should be processed to also produce more valuable products.

At moderate temperature and pressure, bitumen and asphaltenes contain free radicals measured to be in the order of 10^{17}-10^{18} spins/g (Khulbe et al., 1992; Payan and de Klerk, 2018; Strausz and Lown, 2003).

2.3 Genesis of free radicals in bitumen

Radical formation may be initiated at about 150 °C for some compounds (Lalevée and Fouassier, 2012). However, the commonly held conception of the initiation process is that free radical initiation mainly occurs at higher temperatures during thermal cracking. Cracking happens at elevated temperatures, typically at temperatures over 350°C (Buch et al., 2003; Zou and Liu, 1994). Free radicals and initiation reactions are discussed further in Section 2.5 and 2.8

Since radicals are already present in bitumen in large amounts, no energy is necessary for the radical initiation process, although at elevated temperatures, an accelerated radical initiation will occur.

Chang et al. (2000) discussed the following pathways regarding the free radicals' origin in coals and bitumen:

- According to the first statement, free radicals were developed during the diagenesis of organic matter. Diagenesis includes biological, physical, chemical changes of organic matter without significant effect of heating. Therefore, during diagenesis hydrocarbons were formed at temperatures less than 60 °C (Melezhik et al., 2012).
- Radicals that originated as the result of the thermal reactions during the catagenesis and metamorphism. Metamorphism refers to alteration of aggregation, texture, or chemical of mineral matter. During catagenesis, however, hydrocarbons were formed at higher temperatures 150-200 °C (Melezhik et al., 2012). In the catagenesis phase, bitumen was formed as a result of thermal degradation (cracking) of kerogen (insoluble organic fraction in the sedimentary matter) (Waples, 1981; Durand, 1980).
- Radicals could have been produced as the result of radiation by radioactive content of mineral matter.

Radicals could also be formed in bitumen as a result of its recovery method from the oil sands deposits. There are two main methods that are widely used to recover oil sands; mining and in situ subsurface recovery.

Mining of oil sands is feasible for the deposits with depth of up to 30 m (Gray, 2015). Surface mining recovers up to 90% of bitumen present in the oil sand (Banerjee, 2012), typically through hot water extraction. However, only 20% of the oil sands deposits are located in the depths favorable for mining operations (Morimoto et al., 2010).

In situ methods, such as steam-assisted gravity drainage (SAGD), are better suited for the recovery of deep deposits. In situ methods recovers less than 80% of the bitumen in the oil sands (Banerjee, 2012). Of relevance to the present discussion, is the impact of temperature on the bitumen during in situ recovery.

SAGD is a thermal in situ recovery method of the bitumen, which involves drilling of two parallel horizontal wells. During the process high pressure steam is introduced into the oil sands through the steam injection well. The steam well transfers the heat through convection and conduction to the oil sands. As a result, viscosity and density of bitumen decreases significantly and under the gravity it flows to the second well (production well), located 3-5 m below the steam well. The bitumen is pumped to the surface and sent to the plants for further treatment (Gray, 2015). The steam temperature during SAGD operation is about 250 °C, as a result oil heats up to 200 °C at the chamber edge (Czarnecki et al., 2013), which can cause the initiation of radicals by thermolysis.

2.4 Asphaltenes

Being the heaviest fraction of the bitumen, the asphaltenes is a solubility class that is insoluble in paraffinic solvents and soluble in toluene (Mullins et al., 2007; Wang et al., 2015). The asphaltenes fraction is mostly aromatic and is the most polar fraction of the bitumen, therefore it is readily soluble in toluene (Alimohammadi et al., 2019). The properties of the asphaltenes are also affected by the concentration of persistent free radicals.

Due to their very complex structure, the study of asphaltene properties poses many challenges. There is no single asphaltenes molecular formula, because it is usually a mixture of many different large organic species. However, there are certain model structures that have been developed in order to assess the properties of the asphaltenes.

The structure of asphaltenes is represented in literature by two different models: archipelago and continental (also known as island). Figure 2.1 illustrates the archipelago and continental models by providing two representative structures. The continental model describes asphaltenes as a mixture of molecules with large fused rings with various functional groups and heteroatoms, and periphery consisting of aliphatic chains. The archipelago model describes asphaltenes as a mixture of molecules with more than one fused rings joined by being attached to alkyl branches (Kuznicki et al., 2008, Greenfield, 2011; Schulze et al., 2016; Strausz et al., 1992).

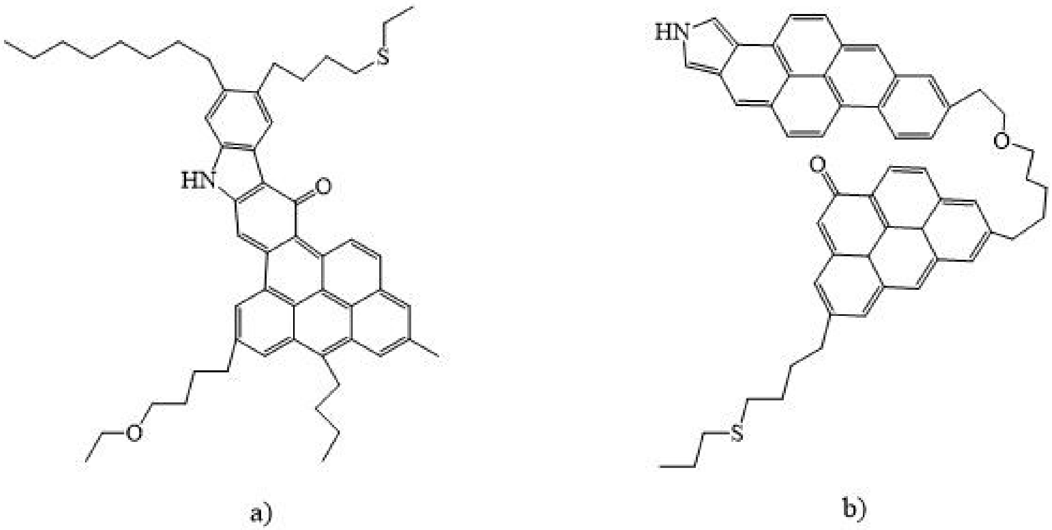

Figure 2. 1. Representation of two most common models of petroleum asphaltenes, a) continental model and b) archipelago model. Reproduced from Kuznicki et al., (2008).

A generic asphaltene molecule is large and contain many atoms of different species that results in a high molecular weight that is estimated to be in the range of 500-1000 g/mol (Groenzin and Mullins, 1999; Badre et al., 2006; Pomerantz et al., 2015; Hortal et al., 2006). Depending on the measurement technique employed, higher molecular weights are sometimes reported.

Since asphaltenes are a mixture of molecules and not a specific species, they do not have a single defined set of physical properties, such as melting point and boiling point (Kopsch, 1994). These properties have a range of values. The properties of the asphaltenes are also affected by the method in which they were obtained, since they are a solubility class and not a chemical class.

Under normal conditions, asphaltenes are solid and shiny particles that resemble glass shards. Above 140 °C the industrially recovered asphaltenes used in this study liquefied, or “melted”, but the temperature above which the asphaltenes are liquid, is also dependent on the fraction that was precipitated. For example, Gray et al. (2004) has reported that the *n*-heptane insoluble asphaltenes extracted form Athabasca bitumen has a “melting” range of 224–294 °C.

The asphaltenes contain mainly material that would be classified as vacuum residue based on boiling point. Performed laboratory experiments reveal that the boiling point of asphaltenes may exceed 727 °C (1000 K) (Desgranges and Delhommelle, 2017).

As mentioned in chapter 1, asphaltenes have a high free radical concentration that ranges between 0.8×10^{18} to 2.0×10^{20} spins/g (Strausz and Lown, 2003). The free radicals in petroleum asphaltenes, like the free radicals found in coals, are mainly divided into three classes: C-free radicals, O-free radicals, and N-free radicals. Reference is made to coal, because most of the electron spin resonance (ESR) spectroscopy of complex mixtures were initially developed for coal. ESR is also used in this investigation to determine the nature and amount of free radicals in asphaltenes.

According to the ESR studies of Petrakis and Grandy (1978), the g-value for carbon centered free radicals in coals are in the range of 2.0025-2.0029, for oxygen-centered free radicals it ranges from 2.0008 to 2.00469 and is about 2.0031 for nitrogen containing radicals. Bersohn and Baird (1966) also provided similar values for the above-mentioned radical classes.

According to the petroleum literature, mostly carbon-centered organic free radicals, as well as vanadyl ion is observed in the ESR analysis of the asphaltenes. The g-value for free radicals in asphaltenes ranges between 2.0028-2.0034 (Guedes et al., 2003). Asphaltenes have a high radical content, both due to organic radicals and vanadyl ions VO^{2+} that are contained in paramagnetic vanadyl-porphyrin-pyrene complexes (Yen et al., 1962; Gafurov et al., 2019).

Depending on the heteroatom content and the nature of the radicals, the g-value of asphaltenes may vary. For example, the g-value for benzosemiquinones is approximately 2.004 and nitroxide radicals have a g-value of around 2.006. Vanadyl ion has a g-value of approximately 1.96 (Eaton et al., 2010). Of importance to this study is that the ESR spectrum of the vanadyl ion does not overlap with that of the organic radicals. It is therefore possible to quantify the organic radicals independently from the paramagnetic vanadyl ions.

2.4.1 Oxidation of asphaltenes (aging)

The asphaltenes free radical content can be changed by air oxidation over time. This type of air oxidation is called aging, or in mined oil sands deposits it is called weathering. It was reported in numerous papers that asphaltenes are undergoing aging during the storage and mainly undergo oxidation at low temperatures, following some reaction patterns of coals (Siddiqui and Ali, 1999; Babu and Cormack, 1983; Jia et al., 2004; Kudynska and Buckmaster, 1966; Wang et al., 2003, Siddiquee and de Klerk, 2014). The most common ways that oxidation is accelerated are by thermal and photochemical means.

The initiation steps in oxidation that lead to free radical formation are shown below:

$$\mathrm{RH} \rightarrow \mathrm{R}^{\bullet} + \mathrm{H}^{\bullet} \qquad \text{Eq. 2.1}$$

$$\mathrm{R}^{\bullet} + \mathrm{O}_2 \rightarrow \mathrm{ROO}^{\bullet} \qquad \text{Eq. 2.2}$$

$$\mathrm{ROO}^{\bullet} + \mathrm{RH} \rightarrow \mathrm{R}^{\bullet} + \mathrm{ROOH} \qquad \text{Eq. 2.3}$$

Compounds with aliphatic chains, and particularly aliphatic chains with double bonds, are subject to chain growth during oxidation. When applied to asphaltenes, chain growth reactions might cause precipitation, lead to coke formation, and can affect transport and downstream processes.

In this study, the presence of air could not be excluded during storage and analysis due to infrastructure limitations. The impact of oxidation on the free radical content of the asphaltenes was therefore evaluated experimentally (see Chapter 3).

2.5 Free radicals

A radical is a molecule with an unpaired electron that possesses a paramagnetic nature. In other words, a radical is a chemical element that lacks one electron to complete its valence shell (Togo, 2004; Fox and Whitesell 2004), or that has distributed the electrons in its valence shell in such a way that one electron is unpaired, e.g. diatomic oxygen ($O^{\bullet}\text{–}O^{\bullet}$).

Carbon free radicals can be primary, secondary, and tertiary depending on the groups attached to the radical carbon atom. In Figure 2.2, the right image is a primary alkyl free radical and is the least stable of three. It is attached to only one carbon (Me = methyl) and has two H-atoms, hence primary. The middle image represents the secondary alkyl free radical which is has only one H-atom and is attached to two additional carbon atoms. The left image is a tertiary alkyl free radical. Being the most stable of all, tertiary free radical has a more evenly distributed electron cloud around the atoms that makes it the most stable (Ali, 2016). The stabilization of the free radicals decreases in the following order: tertiary radicals > secondary radicals > primary radicals (Kossiakoff and Rice, 1943).

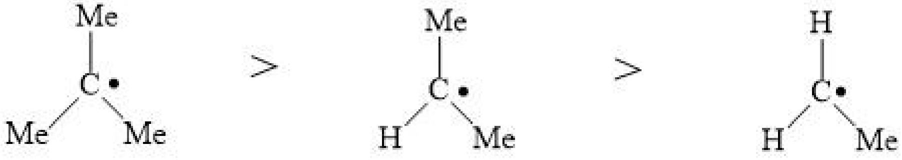

Figure 2. 2. The relative stability of the above mentioned three alkyl free radicals is in the order of tertiary > secondary > primary.

As the electrons get closer to the nucleus, they fall into a lower energy state. Hence, *s*-orbitals possess the lowest energy state in an atom. The *p*-orbitals are farther apart from the nucleus; therefore, they have higher energy. There exists a modified state of orbitals that fall between these two extremes. These hybridized orbitals form from the combination of *s*- and *p*-orbitals. The more *p*-orbitals involved in the formation of hybridized orbitals the higher its energy becomes. In the light of that, the order of the energy for hybridized orbitals (HO) can be shown as; $p > sp^3 > sp^2 > sp > s$. (Fox and Whitesell, 2004; Hademenos, 1999.)

However, the more the *s*-character involved in the bonding the stronger the bond becomes between two HOs, as the *s*-orbital is closer to the nucleus and its electrons are more tightly bounded to the nucleus. The stability of hybridized bonds increases in order of $sp^3 < sp^2 < sp$, as illustrated in Figure 2.3, due to the increased electron affinity of the attached carbon atom.

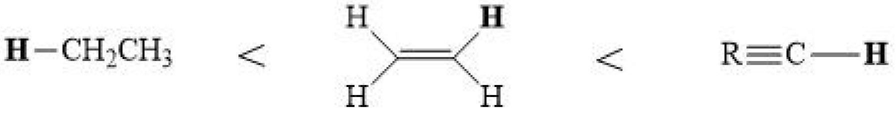

Figure 2. 3. Bond energy is increasing from the left to the right.

There is a decrease in thermodynamic stability of free radicals during the hybridization changes from sp^3 to sp^2 to sp, as the orbital is held closer to the nucleus (Fossey et al., 1995). This is illustrated by Figure 2.4.

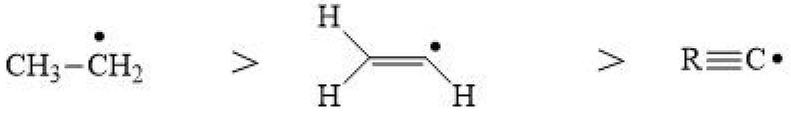

Figure 2. 4. Radical stability decreases from left to right.

The stability of free radicals can further be increased by resonance, when the carbon-centered free radical is next to a double bond, e.g. $(H_2C^{\bullet})-CH = CH_2$. This type of free radical stabilization is important in olefins and alkyl aromatics and is discussed in Section 2.6.1.

2.6 Free radicals stabilization

Organic free radicals are also stabilized by one of the following aspects, or a combination of them: presence of electron-withdrawing or electron-donating groups, delocalization, and steric protection (Griller and Ingold, 1976). Predicting whether electron-withdrawing or electron-donating group is increasing or decreasing the stabilization of the radical is complicated, and it depends on the nature of the compound and the nature of the electron-withdrawing or electron-donating group (Walter, 1966; Janzen, 1969; Poutsma, 2010).

It was necessary to discuss free radical stability, because it is anticipated that free radical stability is a property that affects free radical longevity or persistence.

2.6.1 Resonance Stabilization

Radical resonance occurs when unpaired electron (radical) resonates with the single electron from the π -bond (Figure 2.5).

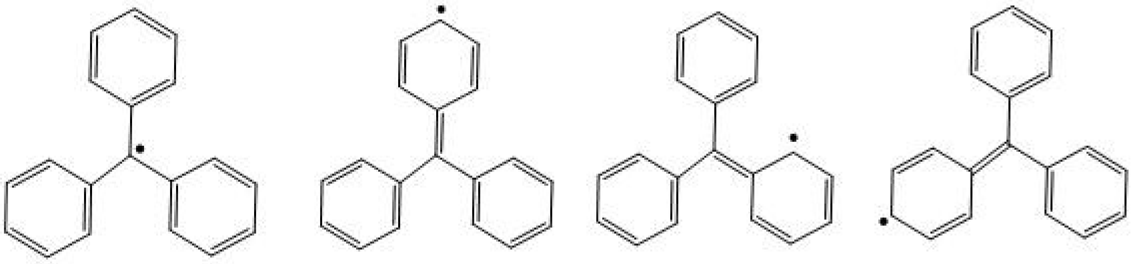

Figure 2. 5. Stabilization of triphenylmethyl radical due to delocalization. Reproduced from Forrester et al., (1968).

In asphaltenes radicals in the aromatic clusters are stabilized through resonance of π-electrons delocalization (Chang et al., 2000). This is illustrated by showing free radicals in polynuclear aromatic structures (Figure 2.6).

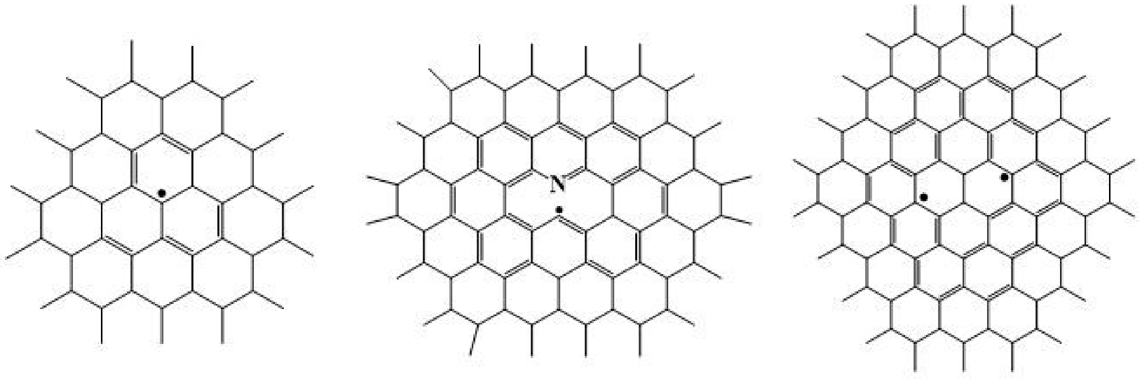

Figure 2. 6. Structures of the type that may be sites of free electrons in petroleum asphaltenes, Reproduced from Chang et al., (2000).

2.6.2 Steric protection

Another factor to provide protection of free radicals against termination reactions is steric hindrance. If the radical center is surrounded by bulk groups, it is sterically protected, and its longevity is increased (Brown and Wang, 2017; Mukherjee and Boudouris, 2017; Moss et al., 2004; Zard, 2003).

For instance, in triphenylmethyl (TPM) radical is stabilized mainly due to steric effects. For resonance stabilization to be dominant all phenyl rings of the compound should be located in the same plane, however, TPM radical is nonplanar. Thus, the electron delocalization in TPM is challenging and radical is stabilized due to shielding provided by phenyl rings (Parsons, 2000).

Steric requirements of the asphaltenes molecules were not covered intensively in the literature. However, it was shown by Carbognani and Rogel (2002), by solvent swelling of asphaltenes, that the asphaltenes possess steric hindrance. Naghizada, (2017) also indicated the possibility of the steric hindrance effects in asphaltenes.

A different form of steric protection is the steric protection provided by the species surrounding the free radical. This type of protection is called caging, because the surrounding species forms a cage around the free radical to restrict access to the free radical.

The caging effect was first mentioned by (Rabinowitch and Wood, 1936). Caging protection of free radicals in asphaltenes is the confinement of the free radical within aromatic compounds making an aggregate that prevents any reactions from happening (Mujica et al., 2000). The structure of asphaltenes, the steric constraints, as well as caging might be viewed as a sort of trapping and provide a reason for the existence of persistent free radicals in asphaltenes (Mujica et al., 2000; Acevedo et al., 1997; Acevedo et al., 2007).

2.7 Persistent free radicals

Bachmann and Wiselogle (1936) brought the notion of persistent free radicals to the attention of the scientific community. In his study, he found out that no self-termination occurred between triphenylmethyl radicals, but it occurred between diphenylmethyl radicals. Hence, he indicated that the triphenylmethyl radical is a persistent free radical and that the diphenylmethyl radical is a transient free radical. Examples of stable free radicals are shown in Figure 2.7.

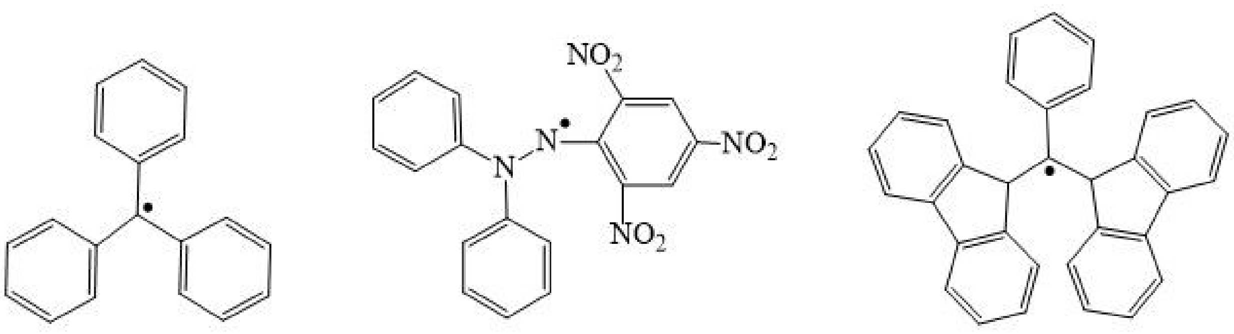

Figure 2. 7. Some examples of the stable free radicals

In general, free radicals can be divided into three categories based on their longevity: transient, stable, and persistent.

Transient free radicals are highly reactive and that is why their steady state concentrations are very low. Brown and Wang (2017) classified transient free radicals as radicals with half-life less than 10^{-3} seconds. Transient free radicals are self-terminating, or readily reacting with the surrounding molecules or radicals and cannot be isolated and observed with conventional spectroscopic methods. Therefore, special types of chemicals are used (also known as spin-trap compounds) in order to interact with transient free radicals via chemical reactions (Gruenwedel and Whitaker, 1986). The process of trapping transient free radicals involves a small amount of diamagnetic compound, the spin-trap, which has a high affinity to the radicals. The reaction of spin-trap and transient free radical results in a product that is a persistent free radical, called the spin-adduct (Perkins, 1980).

The stable free radicals have relatively longer lifetimes and can readily be detected with spectroscopic methods and it can be isolated and employed as a pure substance. Brown and Wang (2017) classified stable free radicals as radicals with half-life more than 10^{-3} seconds. Stable free radicals are reasonable unreactive to the environment, air, and moisture (Hicks, 2007; Griller and Ingold, 1976).

Persistent free radicals, on the other hand, do not self-terminate over geological time. One could therefore say that all persistent free radicals are stable free radicals, but not all stable free radical will be persistent. It was suggested that such level of persistence of radicals and their kinetic stability is provided by steric crowding and not by electronic aspects (Griller and Ingold, 1976; Brown and Wang, 2017).

Steric crowding is an important premise of the present study, which investigated steric effects as potential origin of free radical persistence in asphaltenes in Chapter 4.

2.7.1 Effect of persistent free radicals on the reaction rates.

The change in free Gibbs energy (ΔG) defines the spontaneity of a reaction. When ΔG is negative, a reaction can spontaneously occur. However, Gibbs energy does not define the rate of the reaction that will happen. The rate of a reaction is primarily dominated by its transition state enthalpy ($\Delta H^{\ddagger}$). The lower the enthalpy, the faster the reaction takes place. Radicals' reactions also occur fast and that is because most of the radicals have low activation energy barrier that makes them very reactive. In the case of persistent free radicals, however, the transition state enthalpy is very high which is attributed to its strained transition state. This feature mainly arises from the bulky substituents that surround the central atom and makes the radical very hindered. Because hindered radicals have high transition state enthalpy, they require high activation energy in order to overcome the energy barrier to react.

Steric nature of a radical says a lot about its reactivity. A radical seeks a molecule that is not very hindered and possesses a double bond, because such a molecule will have a low transition state energy that does not require much activation energy to react (Parsons, 2000). Effects of steric hindrance are also discussed in the Sections 2.9.3 and 2.10.2.

2.8 Free radical reactions: Initiation

The generation of a radical can occur through several routes. The following sub-subsections explain the possible radical initiation routes, namely, homolysis, redox reactions and electrochemical reactions.

2.8.1 Homolysis

Homolysis results in formation of two radicals via different routes of initiation. Activation energy for the homolysis process is provided by one of the following ways (Lalevée and Fouassier, 2012):

a) Heating - the most widely used method
b) Light absorption - useful for compounds bearing a suitable chromophore
c) Radiolysis (X-ray, γ irradiation).

The bond breaking due to heating is called thermolysis. Homolysis with light absorption takes place by shedding light on a chemical bond at room temperature, particularly, ultraviolet light is very effective for this purpose. Radiolysis is the bond cleavage method with radiation. Using radiation, an electron of the compound is ejected from the compound that results in a radical cation, which further decomposes into a cation and a radical. Equations 2.4 and 2.5 show an illustration of radiolysis process (Lalevée and Fouassier, 2012).

$$\mathrm{H_2O} \overset{\Upsilon}{\rightarrow} \mathrm{e^-_{aq}, HO^\bullet, H^\bullet} \tag*{Eq. 2.4}$$

$$\mathrm{H_2O^{\bullet+} + H_2O \rightarrow H_3O^+ + OH^\bullet} \tag*{Eq. 2.5}$$

2.8.2 Redox processes

Redox processes are another way of obtaining free radicals via reduction and oxidation reactions. The following equations (Eq. 2.6 and 2.7) demonstrate the free radical generation process though reduction and oxidation processes (Lalevée and Fouassier, 2012).

$$\mathrm{R - X + e^- \rightarrow R - X^\bullet + e^- \rightarrow R^\bullet + X^+} \tag*{Eq. 2.6}$$

$$\mathrm{R-X \rightarrow R-X^{\bullet} + e^{-} \rightarrow R^{\bullet} + X^{+}} \qquad \text{Eq. 2.7}$$

The reduction process (Eq. 2.6) occurs when there is a reagent in the medium that can readily provide an electron. In order that electron to be accepted by the radical precursor, it must have a functional group that has high electron affinity, such as peroxides and halides. In the oxidation case (Eq. 2.7), with the loss of an electron, the original compound splits into a cation and a free radical. For oxidation purposes, strong oxidizing agents are used, such as metal salts that can withdraw an electron from the precursor compound (Lalevée and Fouassier, 2012).

Unlike homolysis, only one radical is being generated per reaction via redox generation route instead of two.

2.8.3 Electrochemical Methods

With the electrochemical method, an electron is being subtracted (Eq. 2.8) from an anion and as a result, a radical is generated. Electrochemical initiation may also happen through reduction, in which an electron is added to a cation to generate a free radical (Eq. 2.9). The reactions below illustrate the free radical formation with electron transfer (Lalevée and Fouassier, 2012).

$$\mathrm{R^{-} - e^{-} \rightarrow R^{\bullet}} \qquad \text{Eq. 2.8}$$

$$\mathrm{R^{+} + e^{-} \rightarrow R^{\bullet}} \qquad \text{Eq. 2.9}$$

2.9 Free radical reactions: Propagation

2.9.1 Hydrogen Atom Abstraction or Hydrogen Atom Transfer (HAT)

Hydrogen abstraction involves abstraction of the hydrogen by the radical from the substrate in a bimolecular compound. The following reaction describes this phenomenon (Lai et al., 2012; Speight, 2019). The major reason for a reaction to proceed is the formation of the stronger σ bond in the product ($R' - H$) than the one in the reactant (H-R), and a more stable radical $R^{\bullet}$(Parsons, 2000).

$$\mathrm{R'^{\bullet} + H-R \rightarrow R'-H + R^{\bullet}} \qquad \text{Eq. 2.10}$$

2.9.2 β-scission (Fragmentation reaction)

β-scission, or radical fragmentation, is the reaction involving bond breakage to produce olefin and a smaller alkyl radical from the bigger radical. It is called β-scission as the C-C bond is in the β-position to the radical center (Figure 2.8) (Gray, 2015).

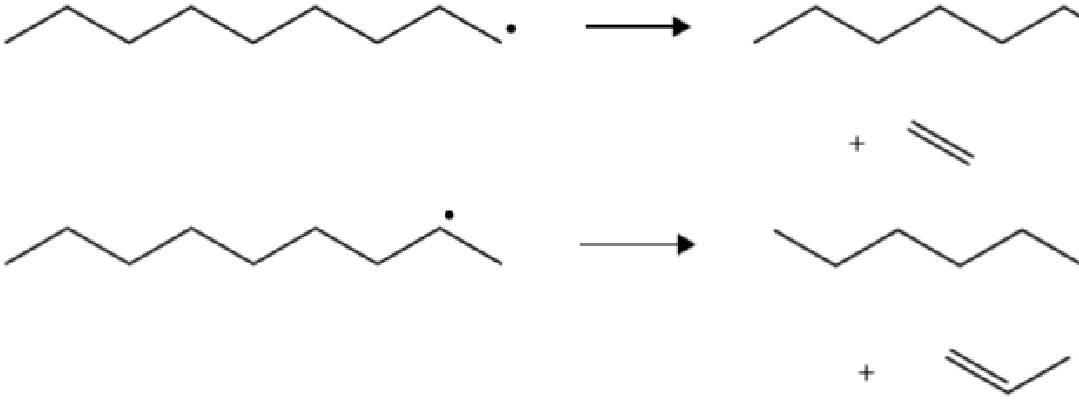

Figure 2. 8. Radical formation via β-scission (Gray, 2015)

In case of cycloalkane (naphthene) radical, the β-scission may result in variety of products depending on the radical position (Figure 2.9).

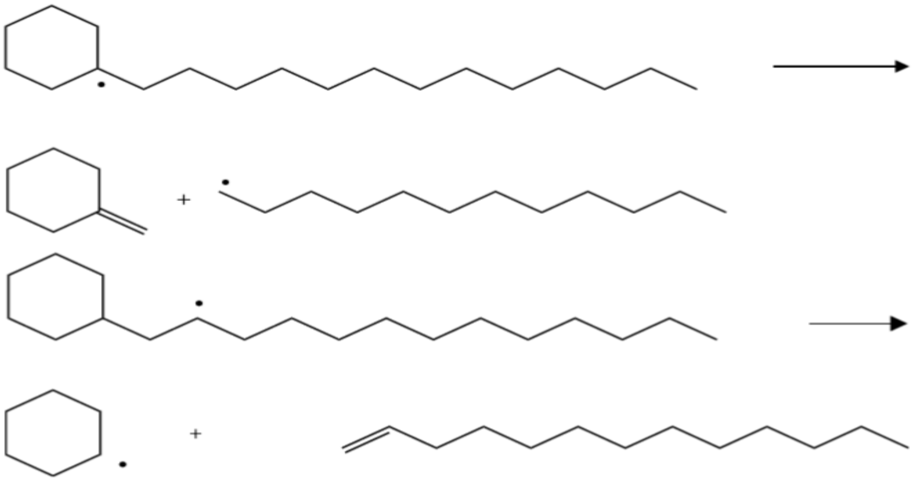

Figure 2. 9. β–scission of substituted cycloalkane radicals (Gray, 2015)

The rate of β-scission increases in the order of radical stability: methyl < ethyl < iso-propyl < *tert*-butyl (Eberhardt, 2000). The β-scission usually takes place along with H-abstraction to stabilize the new free radical that was formed.

Radical fragmentation reactions are mainly endothermic and do not take place spontaneously normal conditions. The reason is that in order for a reaction to occur spontaneously it should have a negative Gibbs energy ($\Delta G = \Delta H - T \cdot \Delta S$). For an endothermic reaction enthalpy (ΔH) of the reaction is negative and since the compound splits into two compounds then entropy (ΔS) increases (Nonhebel et al., 1979; Fossey et al., 1995; Perchyonok, 2011). The prime reason for a fragmentation reaction to take place is the entropy increase as a single radical forms two radicals (Parsons, 2000).

2.9.3 Radical addition reactions

An unsaturated organic molecule is an important source of addition reactions. Therefore, alkenes and alkynes can readily undergo addition reactions. Based on the following reactions, a new radical is generated when an alkene molecule reacts with a radical and converts the existing double bond into a single bond (Nonhebel et al., 1979). In addition, during the reaction, the π-bond of the unsaturated molecule is replaced with a σ bond. The driving force for the reaction is the formation of stronger σ bond from the relatively weak π bond. During the addition reactions radical tends to attack the end of the *π* bond that is less hindered with substituents, which is why the product (a) in Equation 2.11 is formed at a higher rate than the product (b) (Parsons, 2000).

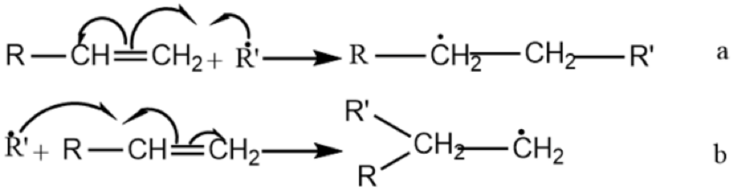

Eq. 2.11

Addition reactions are exothermic (Ouellette and Rawn, 2015).

2.10 Free radical reactions: Termination

2.10.1 Radical recombination

Homocoupling reaction is the combination of the same radicals, while as heterocoupling is the combination of two different radicals resulting in the formation of a single compound (Parsons, 2000).

Radical recombination involves the addition of two free radical species. This type of termination are discussed in Section 2.11 and shown in Equations 2.15 and 2.16.

2.10.2 Radical disproportionation

According to Speight (2019), disproportionation reactions usually happens at temperature range of 450–530 °C and pressure of 20 bars. However, the reaction chemistry of molecules such as dihydronaphthalene suggest that disproportionation may take place at lower temperature if the free radical concentration is high enough (Payan and de Klerk, 2018).

Based on thermodynamic considerations, disproportionation are favored at low temperatures as they are predominantly exothermic (Van Boekel, 2008).

Only if the propagating molecule has a hydrogen atom at the β -position then disproportionation of organic radicals may take place (Parsons, 2000; Denisov et al., 2005; Matyjaszewski and Davis, 2003). Radical disproportionation is depicted in Equation 2.12 (Parsons, 2000):

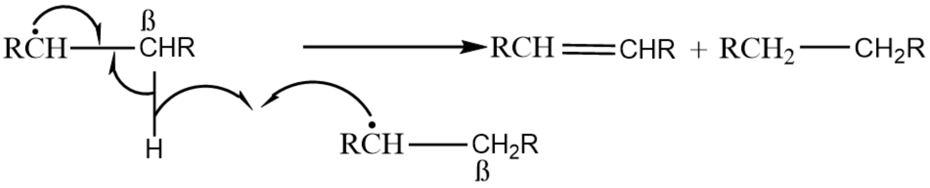

Eq. 2.12

Disproportionation reactions involve an acceptor and a donor where the hydrogen atom is abstracted by the acceptor compound and then the donor compound undergoes further reactions that forms a double bond. During radical disproportionation reactions one molecule functions as an acceptor and another one as the donor (Kelley and Klein, 1974; Benson, 1985). Disproportionation reaction involving two radicals can also be viewed as redox reaction, where one of the compounds is oxidized and the second compound is reduced (Eberhardt, 2000). Steric requirements play role in the radical disproportionation reactions (Fischer, 2001; Kelley and Klein, 1974; Rüchardt et al., 1997). If the radical is sterically crowded by the substituents the disproportionation reactions occur at a higher rate than the combination reactions (Parsons, 2000).

2.11 Reactions leading to free radical termination

Free radical stability affects free radical chain termination reactions. The cross-reaction of transient and persistent free radicals is a potential way to probe the origin of free radical persistence. A simple explanation of this phenomenon is provided below.

Reactions in Equations 2.13-2.16 describe a generic free radical cross-reaction where T represents transient radicals and P represents persistent radicals (Fischer, 2001).

$$\mathrm{Source} \rightarrow \mathrm{T}^{\bullet} \qquad \text{Eq. 2.13}$$

$$\mathrm{Source} \rightarrow \mathrm{P}^{\bullet} \qquad \text{Eq. 2.14}$$

$$\mathrm{T}^{\bullet} + \mathrm{P}^{\bullet} \rightarrow \mathrm{T} - \mathrm{P} \qquad \text{Eq. 2.15}$$

$$\mathrm{T}^{\bullet} + \mathrm{T}^{\bullet} \rightarrow \mathrm{T} - \mathrm{T} \qquad \text{Eq. 2.16}$$

For this example, the same source of feed causes the generation of two different types of radicals, transient radicals (Eq. 2.13) and persistent radicals (Eq. 2.14). Subsequently, the two types of radicals interact and form either a cross-reaction product (Eq. 2.15), or the product of only transient radical termination (Eq. 2.16). Experimentally it was found that the dominant product is the cross-reaction product, T–P. When transient (T) and persistent (P) radicals are formed at the same rate, after a time, reaction route (Eq. 2.15) to produce T–P outweighs reaction route (Eq. 2.16) to produce T–T due to excess concentration buildup of persistent radicals (Fischer, 2001).

Transient radicals (T) self-terminate via reaction route (Eq. 2.16) and whereas persistent radicals do not self-terminate and only disappear via cross-reaction mechanism. Since transient radicals are self-terminating, initially they disappear faster, and persistent radicals’ concentration remains in excess. Due to relative increase in persistent radical concentration, reaction rate of (Eq. 2.15) increases. These reactions never fully reach termination and both transient and persistent radical concentrations diminish over time. Consequently, cross-reaction product T–P is obtained as the main product (Fischer, 2001).

There are a few possible scenarios with the above-mentioned mechanism that may also occur (Fischer, 2001):

First, if both radicals are formed at the same rate then cross-reaction product is the dominant. Second, if the transient radical (T) further is converted by propagation into another transient radical (T′), cross-reaction between the second transient radical (T′) and the persistent radical (P) will be dominant. Additionally, if this happens to lead to a propagation reaction, the persistent radical (P) will forms another persistent radical (P′) and then cross-reaction between the transient radical (T) and the second persistent radical becomes more selective (P′-T). Third, due to self-termination of transient radicals, the concentration of persistent radicals (P, P′) will surpass concentration of transient radicals (T, T′).

The use of reagents that could form transient free radicals to probe the nature of persistent free radicals in asphaltenes was of interest in this study. Different reactions were used in Chapters 3 and 4 that employed these principles.

2.12 Conclusion

Understanding the role of steric requirements in the radical stability is necessary in order to evaluate their importance in free radicals' reactions. Asphaltenes have complex structure and high molecular weight, which makes using traditional analyzing methods difficult to perform. However, employing probe molecules with asphaltenes as described in Section 2.11, it is possible to perform their examination using conventional analyzing techniques that can give us insight about the reaction and their requirements in the asphaltenes. In this respect the present investigation will build on the foundation laid by the hydrogen transfer studies of Naghizada et al. (2017) and Payan and de Klerk (2018). However, the objective of the present investigation is different and focused on the origin of persistent free radical stability as outlined in Section 2.6.2 and 2.7.

2.13 References

Acevedo, S., Castro, A., Negrin, J.G., Fernández, A., Escobar, G., Piscitelli, V., Delolme, F. and Dessalces, G., 2007. Relations between asphaltene structures and their physical and chemical properties: The rosary-type structure. *Energy & fuels*, *21*(4), pp.2165-2175.

Acevedo, S., Escobar, G., Ranaudo, M.A., Pinate, J., Amorín, A., Díaz, M. and Silva, P., 1997. Observations about the structure and dispersion of petroleum asphaltenes aggregates obtained from dialysis fractionation and characterization. *Energy & Fuels*, *11*(4), pp.774-778.

Ali, H. (2016). *Reaction Mechanism in Organic Chemistry*. 1st ed. S. Chand, p.111.

Alimohammadi, S., Zendehboudi, S. and James, L., 2019. A comprehensive review of asphaltene deposition in petroleum reservoirs: Theory, challenges, and tips. *Fuel*, *252*, pp.753-791.

Babu, D.R. and Cormack, D.E., 1983. Low temperature oxidation of Athabasca bitumen. *The Canadian Journal of Chemical Engineering*, *61*(4), pp.575-580.

Bachmann, W.E. and Wiselogle, F.Y., 1936. The relative stability of pentaarylethanes. iii. 1 the reversible dissociation of pentaarylethanes. *The Journal of Organic Chemistry*, *1*(4), pp.354-382.

Badre, S., Goncalves, C.C., Norinaga, K., Gustavson, G. and Mullins, O.C., 2006. Molecular size and weight of asphaltene and asphaltene solubility fractions from coals, crude oils and bitumen. *Fuel*, *85*(1), pp.1-11.

Banerjee, D.K., 2012. *Oil sands, heavy oil & bitumen: from recovery to refinery*. PennWell Books.

Benson, S.W., 1985. Disproportionation of free radicals. *The Journal of Physical Chemistry*, *89*(20), pp.4366-4369.

Bersohn, M. and Baird, J.C., 1966. Introduction to electron paramagnetic resonance.

Brown, R.C. and Wang, K., 2017. *Fast Pyrolysis of Biomass: Advances in Science and Technology* (Vol. 50). Royal Society of Chemistry.

Buch, L., Groenzin, H., Buenrostro-Gonzalez, E., Andersen, S.I., Lira-Galeana, C. and Mullins, O.C., 2003. Molecular size of asphaltene fractions obtained from residuum hydrotreatment☆. *Fuel*, *82*(9), pp.1075-1084.

Campbell, C.J. and Laherrère, J.H., 1998. The end of cheap oil. *Scientific American*, *278*(3), pp.78-83.

Canadian Association of Petroleum Producers (2019). *Canada's Energy Resources*. (online) Canadian Association of Petroleum Producers. Available at: https://www.capp.ca/canadian-oil-and-natural-gas/canadas-petroleum-resources (Accessed 26 Aug. 2019).

Carbognani, L. and Rogel, E., 2002. Solvent swelling of petroleum asphaltenes. *Energy & fuels*, *16*(6), pp.1348-1358.

Chang, H.L., Wong, G.K., Lin, J.R. and Yen, T.F., 2000. Electron spin resonance study of bituminous substances and asphaltenes. In *Developments in petroleum science* (Vol. 40, pp. 229-280). Elsevier.

Czarnecki, J., Masliyah, J., Xu, Z. and Dobras, M., 2013. Handbook on Theory and Practice of Bitumen Recovery from Athabasca Oil Sands. *Volume II Industrial Practice, Canada: Kingsley Knowledge Publishing*.

Denisov, E.T., Denisova, T.G. and Pokidova, T.S., 2005. *Handbook of free radical initiators*. John Wiley & Sons.

Desgranges, C. and Delhommelle, J., 2017. Coarse-Grained Model and Boiling Point Prediction for Asphaltene Model Compounds via HMC-WL Simulations. *Energy & Fuels*, *31*(10), pp.10699-10705.

Durand, B. ed., 1980. Kerogen: Insoluble organic matter from sedimentary rocks. Editions technip.

Eaton, G.R., Eaton, S.S., Barr, D.P. and Weber, R.T., 2010. *Quantitative Epr*. Springer Science & Business Media.

Eberhardt, M.K., 2000. *Reactive oxygen metabolites: chemistry and medical consequences*. CRC press.

Fischer, H., 2001. The persistent radical effect: a principle for selective radical reactions and living radical polymerizations. *Chemical reviews*, *101*(12), pp.3581-3610.

Forrester, A.R., Hay, J.M. and Thomson, R.H., 1968. Organic chemistry of stable free radicals.

Fossey, J., Lefort, D. and Sorba, J. (1995). *Free radicals in organic chemistry*. Chichester: John Wiley & Sons.

Fox, M. and Whitesell, J. (2004). *Organic chemistry*. Sudbury, Mass.: Jones and Bartlett Publishers

Gafurov, M., Mamin, G., Gracheva, I., Murzakhanov, F., Ganeeva, Y., Yusupova, T. and Orlinskii, S., 2019. High-Field (3.4 T) ENDOR Investigation of Asphaltenes in Native Oil and Vanadyl Complexes by Asphaltene Adsorption on Alumina Surface. *Geofluids*, *2019*.

Gray, M.R., 2015. *Upgrading oilsands bitumen and heavy oil*. University of Alberta.

Gray, M.R., Assenheimer, G., Boddez, L. and McCaffrey, W.C., 2004. Melting and fluid behavior of asphaltene films at 200− 500 C. *Energy & fuels*, *18*(5), pp.1419-1423.

Greenfield, M.L., 2011. Molecular modelling and simulation of asphaltenes and bituminous materials. *International Journal of Pavement Engineering*, *12*(4), pp.325-341.

Griller, D. and Ingold, K.U., 1976. Persistent carbon-centered radicals. *Accounts of Chemical Research*, *9*(1), pp.13-19.

Groenzin, H. and Mullins, O.C., 1999. Asphaltene molecular size and structure. *The Journal of Physical Chemistry A*, *103*(50), pp.11237-11245.

Gruenwedel, D.W. and Whitaker, J.R. eds., 1986. *Food Analysis: Principles and Techniques (In 4 Volumes)*. CRC Press.

Guedes, C.L.B., Di Mauro, E., Antunes, V. and Mangrich, A.S., 2003. Photochemical weathering study of Brazilian petroleum by EPR spectroscopy. *Marine Chemistry*, *84*(1-2), pp.105-112.

Hademenos, G.J., 1999. *Schaum's Outline of Organic Chemistry*. McGraw Hill Professional.

Hicks, R.G., 2007. What's new in stable radical chemistry?. *Organic & biomolecular chemistry*, *5*(9), pp.1321-1338.

Hortal, A.R., Martínez-Haya, B., Lobato, M.D., Pedrosa, J.M. and Lago, S., 2006. On the determination of molecular weight distributions of asphaltenes and their aggregates in laser desorption ionization experiments. *Journal of mass spectrometry*, *41*(7), pp.960-968.

Isaacs, E., 2005. Canadian Oil Sands: development and future outlook. *Alberta Energy Research Institute, Calgary*.

Janzen, E.G., 1969. Substituent effects on electron spin resonance spectra and stability of free radicals. *Accounts of Chemical Research*, *2*(9), pp.279-288.

Jia, N., Moore, R.G., Mehta, S.A., Van Fraassen, K., Ursenbach, M. and Zalewski, E., 2004, January. Compositional changes for Athabasca bitumen in the presence of oxygen under low temperature conditions. In *Canadian International Petroleum Conference*. Petroleum Society of Canada.

Kelley, R.D. and Klein, R., 1974. Cross disproportionation of alkyl radicals. *The Journal of Physical Chemistry*, *78*(16), pp.1586-1595.

Khulbe, K.C., Mann, R.S., Lamarche, G. and Lamarche, A.M., 1992. Electron spin resonance study of the thermal decomposition of solvent extracted Athabasca tar sand bitumen. *Fuel processing technology*, *31*(2), pp.91-103.

Kopsch, H., 1994. On the thermal behavior of petroleum asphaltenes. *Thermochimica acta*, *235*(2), pp.271-275.

Kossiakoff, A. and Rice, F.O., 1943. Thermal decomposition of hydrocarbons, resonance stabilization and isomerization of free radicals1. *Journal of the American Chemical Society*, *65*(4), pp.590-595.

Kudynska, J. and Buckmaster, H.A., 1996. Low-temperature oxidation kinetics of high-volatile bituminous coal studied by dynamic in situ 9 GHz cwepr spectroscopy. *Fuel*, *75*(7), pp.872-878.

Kuznicki, T., Masliyah, J.H. and Bhattacharjee, S., 2008. Molecular dynamics study of model molecules resembling asphaltene-like structures in aqueous organic solvent systems. *Energy & Fuels*, *22*(4), pp.2379-2389.

Lai, W., Li, C., Chen, H. and Shaik, S., 2012. Hydrogen-abstraction reactivity patterns from A to Y: the valence bond way. *Angewandte Chemie International Edition*, *51*(23), pp.5556-5578.

Lalevée, J. and Fouassier, J.P., 2012. Overview of radical initiation. *Encyclopedia of Radicals in Chemistry, Biology and Materials*.

Masliyah, J., Czarnecki, J. and Xu, Z., 2011. Handbook on theory and practice of bitumen recovery from Athabasca oil sands, volume 1: Theoretical basis. *Canada: Kingsley Knowledge Publishing*.

Matyjaszewski, K. and Davis, T.P., 2003. *Handbook of radical polymerization*. John Wiley & Sons.

Melezhik, V., Prave, A.R., Hanski, E.J., Fallick, A.E., Lepland, A., Kump, L.R. and Strauss, H. eds., 2012. *Reading the Archive of Earth's Oxygenation: Volume 3: Global Events and the Fennoscandian Arctic Russia-Drilling Early Earth Project*. Springer Science & Business Media.

Morimoto, M., Sugimoto, Y., Saotome, Y., Sato, S. and Takanohashi, T., 2010. Effect of supercritical water on upgrading reaction of oil sand bitumen. The Journal of Supercritical Fluids, 55(1), pp.223-231.

Moss, R.A., Platz, M. and Jones, M. eds., 2004. *Reactive intermediate chemistry* (p. 1084). Hoboken, NJ: Wiley-Interscience.

Mujica, V., Nieto, P., Puerta, L. and Acevedo, S., 2000. Caging of molecules by asphaltenes. A model for free radical preservation in crude oils. *Energy & fuels*, *14*(3), pp.632-639.

Mukherjee, S. and Boudouris, B.W., 2017. *Organic Radical Polymers: New Avenues in Organic Electronics*. New York: Springer.

Mullins, O.C., Sheu, E.Y., Hammami, A. and Marshall, A.G., 2007. *Asphaltenes, heavy oils, and petroleomics*. Springer Science & Business Media.

Naghizada, N., 2017. Uncatalyzed hydrogen transfer during 100-250° C conversion of asphaltenes. M.Sc. Thesis, University of Alberta: Edmonton, Alberta, Canada.

Naghizada, N., Prado, G.H. and de Klerk, A., 2017. Uncatalyzed hydrogen transfer during 100–250 °C conversion of asphaltenes. *Energy & Fuels*, *31*(7), pp.6800-6811.

Nonhebel, D.C., Tedder, J.M. and Walton, J.C., 1979. *Radicals*. CUP Archive.

Oliviero Rossi, C., Caputo, P., Ashimova, S., Fabozzi, A., D'Errico, G. and Angelico, R., 2018. Effects of natural antioxidant agents on the bitumen aging process: An epr and rheological investigation. *Applied Sciences*, *8*(8), p.1405.

Ouellette, R.J. and Rawn, J.D., 2015. *Organic Chemistry Study Guide: Key Concepts, Problems, and Solutions*. Elsevier.

Owen, N.A., Inderwildi, O.R. and King, D.A., 2010. The status of conventional world oil reserves—Hype or cause for concern?. *Energy policy*, *38*(8), pp.4743-4749.

Parsons, A.F., 2000. An introduction to free radical chemistry. Wiley-Blackwell.

Payan, F. and de Klerk, A., 2018. Hydrogen Transfer in Asphaltenes and Bitumen at 250° C. *Energy & fuels*, *32*(9), pp.9340-9348.

Perchyonok, V.T., 2011. Radical reactions in aqueous media. *Encyclopedia of Inorganic and Bioinorganic Chemistry*, pp.1-22.

Perkins, M.J., 1980. Spin trapping. In *Advances in physical organic chemistry* (Vol. 17, pp. 1-64). Academic Press.

Petrakis, L. and Grandy, D.W., 1978. Electron spin resonance spectrometric study of free radicals in coals. *Analytical Chemistry*, *50*(2), pp.303-308.

Pomerantz, A.E., Wu, Q., Mullins, O.C. and Zare, R.N., 2015. Laser-based mass spectrometric assessment of asphaltene molecular weight, molecular architecture, and nanoaggregate number. *Energy & Fuels*, *29*(5), pp.2833-2842.

Poutsma, M.L., 2010. The radical stabilization energy of a substituted carbon-centered free radical depends on both the functionality of the substituent and the ordinality of the radical. *The Journal of organic chemistry*, *76*(1), pp.270-276.

Rabinowitch, E. and Wood, W.C., 1936. The collison mechanism and the primary photochemical process in solutions. *Transactions of the Faraday Society*, *32*, pp.1381-1387.

Richard, S., 2014. A more sustainable way to win oil from oil sands. *Journal of Sustainable Energy Engineering*, *1*(4), pp.286-298.

Rüchardt, C.; Gerst, M.; Ebenhoch, J. Uncatalyzed Transfer Hydrogenation and Transfer Hydrogenolysis: Two Novel Types of Hydrogen-Transfer Reactions. *Angewandte Chemie International Edition in English* 1997*, 36*, 1406-1430.

Schulze, M., Scherer, A., Hampel, F., Stryker, J.M. and Tykwinski, R.R., 2016. Synthesis and Aggregation Behavior of Chiral Naphthoquinoline Petroporphyrin Asphaltene Model Compounds. *Chemistry–A European Journal*, *22*(10), pp.3378-3386.

Shin, S., Lee, J.M., Hwang, J.W., Jung, H.W., Nho, N.S. and Lee, K.B., 2014. Physical and rheological properties of deasphalted oil produced from solvent deasphalting. *Chemical Engineering Journal*, *257*, pp.242-247.

Siddiquee, M.N. and de Klerk, A., 2014. Hydrocarbon addition reactions during low-temperature autoxidation of oilsands bitumen. *Energy & Fuels*, *28*(11), pp.6848-6859.

Siddiqui, M.N. and Ali, M.F., 1999. Studies on the aging behavior of the Arabian asphalts. *Fuel*, *78*(9), pp.1005-1015.

Speight, J.G., 2019. Handbook of Petrochemical Processes. CRC Press.

Strausz, O.P. and Lown, E.M., 2003. *The chemistry of Alberta oil sands, bitumens and heavy oils* (pp. 588-592). Calgary, Alberta, Canada: Alberta Energy Research Institute.

Strausz, O.P., Mojelsky, T.W. and Lown, E.M., 1992. The molecular structure of asphaltene: an unfolding story. *Fuel*, *71*(12), pp.1355-1363.

Tannous, J.H. and de Klerk, A., 2019. Quantification of the Free Radical Content of Oilsands Bitumen Fractions. *Energy & Fuels*.

Togo, H., 2004. *Advanced free radical reactions for organic synthesis*. Elsevier.

Turuga, A.S.S., 2017. Effect of Solvent Deasphalting Process on the Properties of Deasphalted Oil and Asphaltenes from Bitumen. M.Sc. Thesis, University of Alberta: Edmonton, Alberta, Canada.

Van Boekel, M.A., 2008. *Kinetic modeling of reactions in foods*. CRC press.

Walter, R.I., 1966. Substituent effects on the properties of stable aromatic free radicals. The criterion for non-hammett behavior1. *Journal of the American Chemical Society*, *88*(9), pp.1923-1930.

Wang, H., Dlugogorski, B.Z. and Kennedy, E.M., 2003. Coal oxidation at low temperatures: oxygen consumption, oxidation products, reaction mechanism and kinetic modelling. *Progress in energy and combustion science*, *29*(6), pp.487-513.

Wang, P., Dong, Z.J., Tan, Y.Q. and Liu, Z.Y., 2015. Investigating the interactions of the saturate, aromatic, resin, and asphaltene four fractions in asphalt binders by molecular simulations. *Energy & Fuels*, *29*(1), pp.112-121.

Waples, D.W., 1981. Organic geochemistry for exploration geologists. Burgess Pub. Co..

Yen, T.F., Erdman, J.G. and Saraceno, A.J., 1962. Investigation of the Nature of Free Radicals in Petroleum Asphaltenes and Related Substances by Electron Spin Resonance. *Analytical Chemistry*, *34*(6), pp.694-700.

Zard, S.Z., 2003. *Radical reactions in organic synthesis* (No. 7). Oxford University Press on Demand.

Zou, R. and Liu, L., 1994. Role of Asphaltenes in Petroleum Cracking and Refining. In *Developments in Petroleum Science*(Vol. 40, pp. 339-363). Elsevier.

Chapter 3 – Behavior and amount of free radicals in asphaltenes

3.1 Introduction

The BituMax™ partial upgrading process (shown in Figure 1.1 in Chapter 1) employs a solvent deasphalting step. Unlike laboratory precipitation of asphaltenes, where high solvent-to-bitumen ratio can be used, practically the amount of solvent must be limited. This means that the asphaltenes separation is less rigorous. To make this study as relevant as practical to the BituMax™ process, the material used were industrially precipitated asphaltenes from the solvent deasphalting (SDA) unit in Nexen Long Lake Upgrader.

As mentioned in previous chapters, the asphaltenes contain a high amount of free radicals at standard conditions (Strausz and Lown 2003; Schultz and Selucky 1981; Niizuma, et al., 1977). The first step in this study was to quantify the amount of free radicals present in the asphaltenes. The change in concentration of persistent free radicals in asphaltenes during storage time under different conditions was also evaluated. These experiments established the baseline for the study.

The next step was to evaluate the potential contribution of "caging" to the persistence of free radicals, as was discussed in Chapter 2. In caging the free radical is protected from reaction by the surrounding molecules that create a barrier for mass transport. In bitumen, which is a very viscous fluid, explaining free radical persistence in terms of caging appears plausible. In the case of asphaltenes, which are solids after precipitation, the same would hold true. Thus, if the persistence of the free radical species is due to caging, then the persistent free radical species should become accessible for reaction as mass transport becomes less limiting.

The change in persistent free radical concentration in the asphaltenes with decrease of mass transport limitation was explored. The approach taken was to add different amounts of a reactive solvent to the asphaltenes, thereby diluting the asphaltenes and reducing the viscosity. The reactive solvent that was selected was 1,2-dihydronaphthalene, which is capable of reactions both as hydrogen donor and as hydrogen acceptor.

3.2 Experimental procedure

3.2.1 Materials

The industrially precipitated asphaltenes from the solvent deasphalting (SDA) unit in Nexen Long Lake Upgrader was characterized. These asphaltenes were industrially precipitated using *n*-pentane, but due to the low solvent-to-bitumen ratio employed in the industrial process, the asphaltenes still contain around some *n*-pentane soluble material.

Elemental Analysis of industrial asphaltenes was performed in the Analytical laboratory of the Department of Chemistry at University of Alberta by Thermo Flash 2000 CHNS analyzer. Oxygen amount (wt%) was calculated by subtracting the sum of the other four contents (C, H, N, and S) from the 100%. The analyses were performed twice for the same batch of sample and the results are presented in Table 3.1.

Table 3. 1. Elemental analysis of the industrially precipitated asphaltenes

Name	x	s
Carbon (wt%)	81.88	0.13
Hydrogen (wt%)	7.92	0
Nitrogen (wt%)	1.11	0
Sulfur (wt%)	7.29	0.03
Oxygen (wt%)	1.89	0.11

x = average value; s = standard deviation

Quantification of the free radical content of the asphaltenes is presented as part of the results of this study. The other chemicals and materials that were employed in the experimental work are listed in Table 3.2.

Table 3. 2. Materials employed in the experiments

Chemical compound name	Formula	Purity %[a]	CASRN[b]	Supplier
toluene	C_7H_8	99.9	108-88-3	Fischer Chemical
methanol	CH_3OH	99.9	67-56-1	Fischer Chemical
1,2-dihydronaphthalene	$C_{10}H_{10}$	98	447-53-0	Aldrich
1,2,3,4-tetrahydronaphthalene	$C_{10}H_{12}$	99	19-64-2	Sigma-Aldrich
naphthalene	$C_{10}H_8$	99	91-20-3	Aldrich
2,2-diphenyl-1-(2,4,6-trinitrophenyl)hydrazyl	$C_{18}H_{12}N_5O_6$	NA	1898-66-4	Sigma-Aldrich
α-methylnaphthalene	$C_{11}H_{10}$	96	90-12-0	Alfa Aesar

[a] - This is the purity of the material guaranteed by the supplier; material was not further purified.

[b]- CASRN = Chemical Abstracts Services Registry Number

3.2.2 Equipment and procedures

3.2.2.1 Asphaltene behavior over the range of time under nitrogen and air

Asphaltenes were dissolved in toluene and two cases were considered. In the first case, the tubes were purged with nitrogen. For that purpose, tubes were covered with 3 layers of parafilm, 2 holes were made and then nitrogen was inserted through one of them and the residue air was removed from the second hole. Tubes were purged with 10 ml of nitrogen and air accordingly. This is illustrated by Figure 3.1.

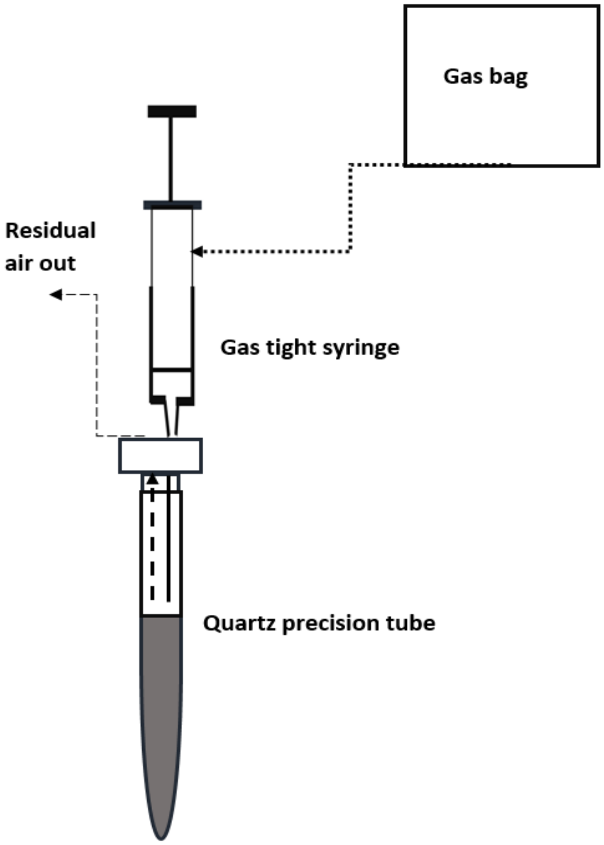

Figure 3. 1. Setup for accurate quantification of free radicals

Afterwards, the tube was covered with the cap and sealed with the parafilm layer, in order to avoid the penetration of air over time. Tubes were kept in the dark compartment.

For better and homogeneous radical redistribution before analysis by electron spin resonance (ESR) spectroscopy, the tubes were placed into the beaker with distilled water, which was placed into a Branson 2800 ultrasonic bath that was also filled with distilled water. The measurements were taken at 0 and 456 hours after the sample filling.

3.2.2.2 Asphaltenes behavior with the addition of 1,2-dihydronaphthalene

The reactions were carried out with different ratios of 1,2-dihydronaphthalene (DHN) and the asphaltenes. The mixture of asphaltenes were added into the vial and the 1,2-dihydronaphthalene was homogenized using the ultrasonic bath for 15 minutes. The reactions were carried out for 1 hour at 250 °C and 4 MPa initial N_2 pressure using the reaction assemble described below.

(Naghizada, 2017) noted that reactor walls could affect the hydrogen transfer rate. As this study was quantitative the reactions were carried in the vial. The operation pressure of the reactions was kept above the vapor pressure of compounds to maintain a liquid phase reaction (Yaws et al., 2009). These reaction conditions were similar to those previously employed (Payan and de Klerk 2018).

DHN: Asphaltenes were added 500±10 mg at the 1:1 (wt/wt) ratio reaction. Using Mettler Toledo XP 1203S, with maximum 1210g and readability of 1 mg, using Eppendorf Research Plus pipette of 20-200 µl (#119628 A).

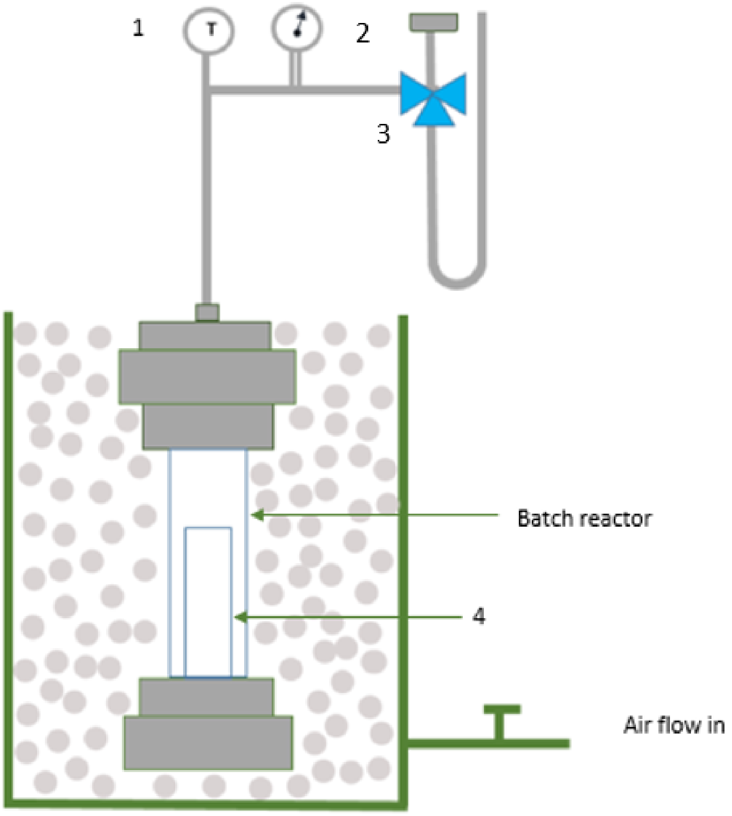

Figure 3. 2. Schematic of the micro-batch reactor placed in the fluidized sand bath.
1) Temperature monitor inside the reactor 2) Pressure gauge 3) 3-way valve 4) glass vial

Reaction assembly (Figure 3.2): All the experiments were carried out in batch micro-reactors from Swagelok, with dimensions as follows: 8.6 cm length; 2.54cm diameter, equipped with the pressure gauge, thermocouple; and three-way valve. Reactors were placed into sand baths purchased from Omega (model FSB – 3). Thermocouple was installed to measure the temperature inside the reactor and was controlled with Omron control system.

No solvent was used to recover the mixtures after reaction from the micro-batch reactor. The recovered material was subsequently extracted with a solvent. Methanol was employed as the extraction solvent to recover unreacted DHN and the reaction products from the conversion of DHN from the asphaltenes. The extracted material was stirred for 30 minutes at 250 rpm with a magnetic stirrer in the fume hood. The converted asphaltenes were obtained by filtration of the methanol extract of the reaction mixture. The converted asphaltenes were dried in the Thermoscientific vacuum oven at 80 °C and 61 kPa absolute pressure.

3.2.2.3 Reaction between DPPH and 1,2-dihydronaphthalene

DPPH and DHN were mixed together in toluene, with 0.5wt% each in around 8.7 g of toluene, to investigate their possible reactivity at ambient conditions. The mixture was homogenized by using the ultrasonic bath for 10 minutes and left for approximately 5 minutes to dry the tubes before analysis. Later, the mixture was inserted into the quartz precision tubes (Wilmad-LabGlass) for the ESR measurements. The samples were analyzed twice, 72 hours apart, to see the impact of time on the free radical concentration.

3.2.3 Analyses

3.2.3.1 Electron spin resonance

Electron spin resonance (ESR) spectroscopy was performed using Active Spectrum Micro ESR equipment. For quantification of free radicals concentration 5 mm thin wall quartz precision tubes from Wilmad-LabGlass were used for the measurements.

Spectra were obtained under the following settings: Microwave power was set to be 15 mW in order to avoid the saturation effect of the signal from free-radicals, frequency set to 9.7 Ghz. Start sweep field: 3200; end sweep field: 3600G. Number of points: 2400. Sweep time: 113 s. Number of sweeps: 7. Digital gain: 12 dB. Sweep delay: 30 s.

The quantification of free radicals was performed by comparison of the double integrated value of the ESR signal first derivative with the DPPH calibration curve (Figure 3.3), as it had the highest value of the regression coefficient: (R^2=0.998) in the range of interest. The calibration was performed using 2,2-Diphenyl-1-picrylhydrazyl (DPPH) (g-factor 2.0036) (Eaton et al., 2010).

Three data points were used to plot the calibration curve to obtain the linear equation, as the double integration of the samples fell within the range of the calibration curve.

The ESR spectra are recorded as the first derivative spectra and each spectrum is represented as a function of intensity versus the g-factor. Double integration was performed to get the area under the absorption plot and thus to quantify the free radicals concentration.

For experimental measurements approximately 20 mg of compound was dissolved in 162 mg of toluene to obtain a solution of 11 wt%. Samples were weighed using a high precision MT XS 105 scale purchased from Mettler Toledo, with maximum capacity of 120 g and readability of 0.01 mg. All the measurements were performed twice. All the measurements were performed at room temperature.

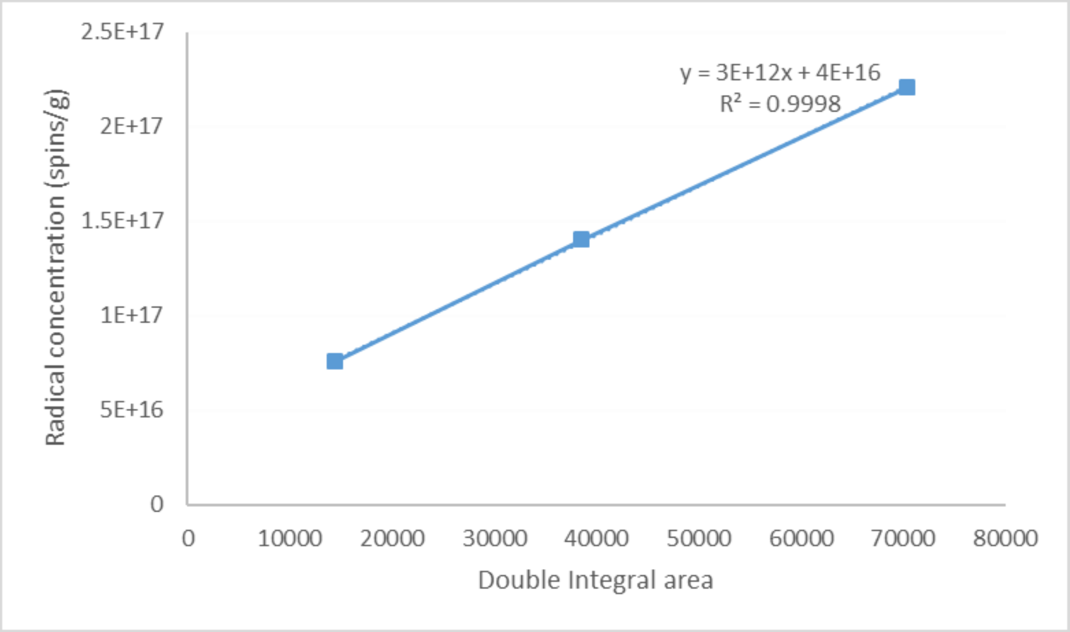

Figure 3. 3. Calibration curve built using DPPH at different concentrations diluted in toluene.

3.2.3.2 Gas chromatography coupled with mass spectrometry

Gas chromatography coupled with mass spectrometer (GC-MS) was used to determine compounds. NIST library was used by the software for identifying the molecules based on their electron impact mass spectrum. Bruker Scion 450 –GC was used with capillary column, ZB-5 column (30 m x 0.25 mm x 0.25 μm), using Helium as a mobile phase with 1 ml/min flow. Split ratio of 50/1. The analyses were performed in the Mass Spectrometry Facility of the Department of Chemistry at University of Alberta by SCION 456-GC-TQ (Triple Quadrupole).

The program was altered for the front peaks (lighter compounds) and heavy compounds. For the front peaks the method was as following: injector temperature was set at 200°C. Oven temperature set at 50°C which was raised to 320°C, temperature was increased at the rate of 25°C /min and hold at 320°C was 5.2 minutes. For the latest peaks the method used had the following parameters: injector temperature 275°C, oven temperature set at 50°C which was raised to 250°C at the rate of 25°C /min , then the temperature was raised from 250°C to 320°C at the rate of 5°C /min and hold for 10 minutes at 320°C.

3.2.3.3 Gas chromatography coupled with flame ionization detector

Quantification of the products was performed using gas chromatography with flame ionization detector (GC-FID) using a 7890 A Agilent GC system, equipped with the column (VF-200 ms) having the following dimensions: 30 m x 0.25 mm x 0.25 µm. Injector temperature: 200°C. Split ratio 100:1. Nitrogen was used as a carrier gas with the flow rate 0.5 ml/min. The oven temperature was 45°C for 0 min and increased from 45°C to 320°C with 5°C /min and temperature was kept at 320 °C for 10 min. The samples were prepared using methanol as solvent.

Response factor of Internal Standard toluene (ISTD) was calculated according to the formula of (Dietz, 1967; Katritzky et al., 1994):

$$\mathrm{RF} = \frac{\mathrm{A_{comp}} \times \mathrm{M_{(ISTD)}}}{\mathrm{A_{(ISTD)}} \times \mathrm{M_{comp}}} \qquad \text{Eq. 3.1}$$

Where RF is response factor, A_{comp} = Area of the compound, A_{ISTD} = Area of the internal standard, M_{ISTD}= mass of the Internal standard, M_{comp} = mass of the compound. Response factor is the ratio of peaks to the masses and depends on the nature of hydrocarbons.

Once the RF of ISTD is known (RF_{ISTD}=0.93) the mass of the compound is determined by the following formula.

$$\mathrm{M_{comp}} = \frac{\mathrm{A_{comp}} \times \mathrm{M_{(ISTD)}}}{\mathrm{A_{(ISTD)}} \times \mathrm{RF}} \qquad \text{Eq. 3.2}$$

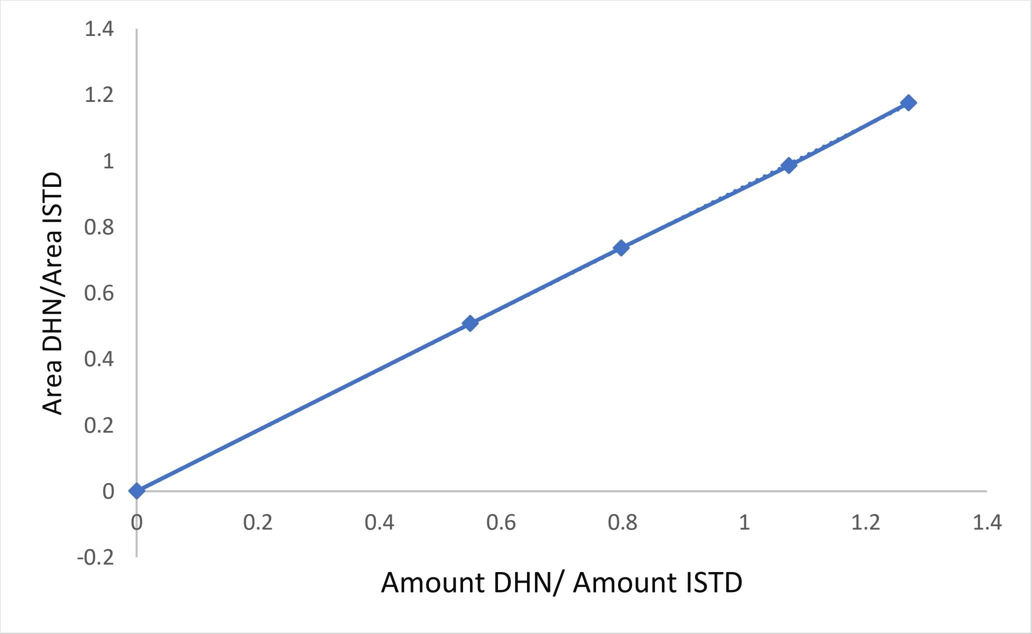

Figure 3. 4. Calibration curve for 1,2-dihydronaphthalene obtained by GC-FID using α-methylnaphthalene as an internal standard. Regression coefficient: R2=0.999; Linear equation: $y = 0.92x - 9\times10^{-5}$. Retention Time of 1,2-dihydronaphthalene: 15.074 minutes.

Calibration of the compounds was performed for an accurate quantification of the results. One of the calibration curves is shown for illustratative purposes in Figure 3.4. The other calibration curves are reported in the Appendix A.

3.3 Results

3.3.1 Change in radical concentration of asphaltenes over time and with N_2/air

In the introduction to this chapter it was explained that it was necessary to establish as baseline for this study.

The free radical content was determined under nitrogen and air atmosphere, and the storage stability of solutions of asphaltenes was evaluated over a time period of 456 h (19 days) under both nitrogen and air. The results of the ESR quantification are presented in Table 3.3.

Table 3. 3. Free radical concentration of the asphaltenes after being purged with air and nitrogen. Experiments were performed in duplicates.

Gas purged	Time (hours)	Radical concentration (spins/g)		g-factor	
		x	s	x	s
Air purged	0	2.4E+18	2.4E+17	2.002	-[a]
	456	2.3E+18	2.2E+17	2.002	0.001
N_2 purged	0	2.1E+18	2.0E+17	2.002	-[a]
	456	2.0E+18	2.5E+17	2.002	-[a]

[a] -No significant deviation was observed between the duplicate measurements;

x = average value; s = standard deviation.

The results in Table 3.3 indicated that there was a slight decrease in the free radical content over the period of 456 h. However, the change was within the uncertainty of the measurements.

The atmosphere in which the measurements were performed affected the observed free radical content. The free radical concentration of asphaltenes was greater when the measurement was performed in air, compared to when the sample tube was purged with nitrogen. This might be due to the paramagnetic nature of the air (Montanari et al., 1998).

3.3.2 Change in radical concentration of asphaltenes with the addition of DHN

Dihydronaphthalene (DHN) is a hydrogen donor and a hydrogen acceptor, which could react with the asphaltenes by hydrogen transfer to produce different products shown in Figure 3.5

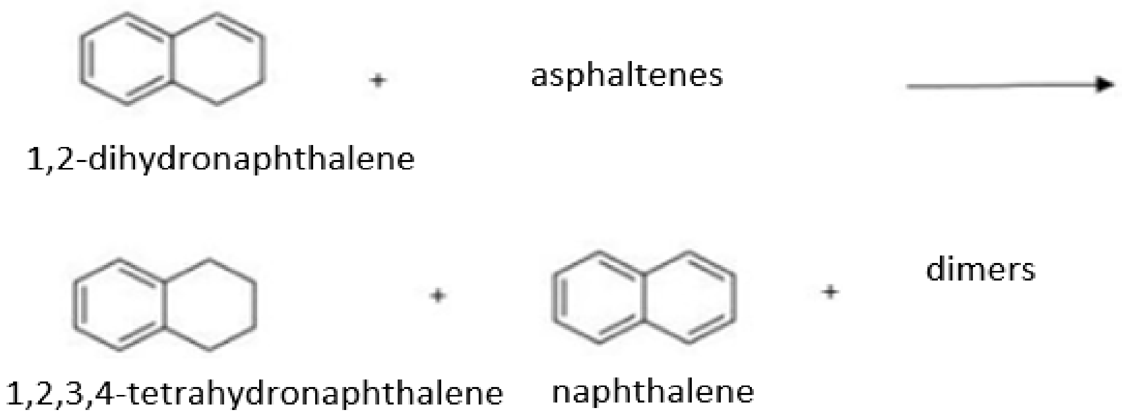

Figure 3. 5. Representation of the reaction products after reacting asphaltenes with 1,2-dihydronaphthalene

Table 3.4 shows the amount of methanol extractable compounds obtained with the addition of three different ratios of DHN and ashpaltenes. Since the procedure involved liquid extraction in methanol, the compounds partitioned between the asphaltenes and methanol phases. Not all of the material was recovered, some remaining in the asphaltenes.

To illustrate the nature of the reaction product, one of the chromatograms that were obtained is shown in Figure 3.6, with the retention time period 9.8–11.2 min magnified in Figure 3.7.

Table 3. 4. Quantification (in mmol) of the products in methanol extracted performed by GC-FID.

DHN: Asphaltenes ratio (wt/wt)		THN	N	DHN	1,2,3,3',4,4'-Hexahydro-1,1'-binaphthalene	1,1',2,2',3,3',4,4'-octahydro-1,1'-Binaphthalene	Unrecovered
1:1[a]	x	0.399	0.538	1.902	0.951	0.175	0.596
	s	0.067	0.0846	0.191	0.096	0.006	0.326
1.6:1[b]	x	0.382	0.606	2.327	-[c]	0.039	2.989
	s	0.054	0.079	0.229	-[c]	0.011	0.324
2.4:1[b]	x	0.748	1.238	4.767	2.384	0.185	2.029
	s	0.126	0.202	0.485	0.243	0.052	0.877

[a]-reactions performed in duplicate; [b]-reactions performed in triplicate; [c]-peaks were too small to be integrated and quantified; x-average value; s-standard deviation value;

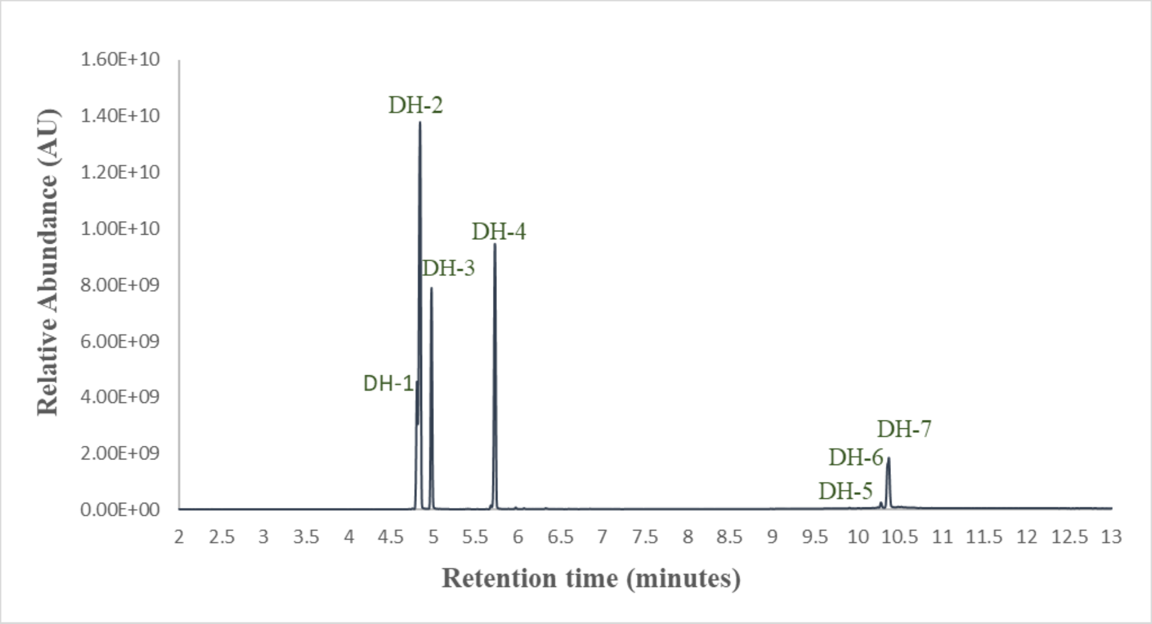

Figure 3. 6. Chromatogram of the products in the methanol extract from the reaction of 1,2-dihydronaphtlalene and asphaltenes conducted at 4MPa initial N_2 pressure and 250°C.

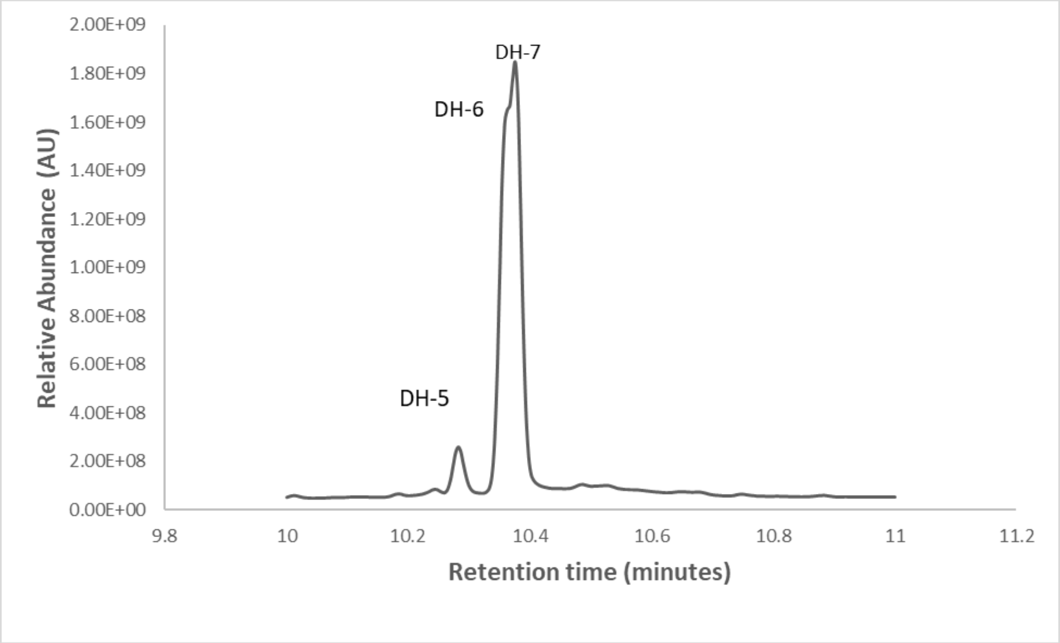

Figure 3. 7. Magnified portion of the chromatogram shown in Figure 3.6, showing the heavy products overlap in the methanol extract.

Products DH-1; DH-2; DH-3; DH-4 were identified using mass spectra and confirmed using commercially obtained authentic compounds. Confidence in the identification is therefore high.

Table 3. 5. Products in methanol extract after 1,2-dihydronaphthalene and asphaltenes reaction at 250 °C and 4 MPa initial N_2 pressure identified using probe molecules.

Symbol	Specification	Product Name	Retention time (minutes)
DH-1	product	1,2,3,4-tetrahydronaphthalene	4.805
DH-2	product	1,2-dihydronaphthalene	4.835
DH-3	product	naphthalene	4.976
DH-4	ISTD [a]	α-methylnaphthalene	5.723

[a] ISTD = Internal standard used for quantification.

The identification of the heavier products, DH-5; DH-6; DH-7 shown in Figure 3.7 was more challenging. Based on the mass spectra it was suspected that these were dimers of DHN, as indicated in Table 3.6.

Table 3. 6. Heavy products identified in methanol extract using GC-MS suggested by NIST library after reaction of asphaltenes with 1,2-dihydronaphthalene

Heavy product name	Symbols	Formula	Retention time (min)	CASRN[a]	Possible structures that are consistent with the mass spectra
1,2,3,3',4,4'-Hexahydro-1,1'-binaphthalene	DH-5	C20H20	11.169	193816-75-0	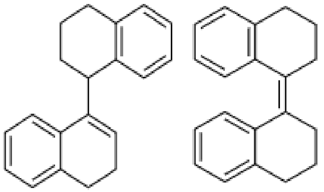
1,1',2,2',3,3',4,4'-octahydro-1,1'-Binaphthalene	DH-6, DH-7	C20H22	11.305	1154-13-8	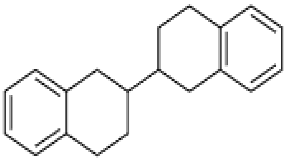

[a] CASRN = Chemical Abstracts Services Registry Number

The mass spectra representing DH-5; DH-6; DH-7 are shown in Figures 3.8–3.10. These are shown because the actual species represented by each is associated with some uncertainty.

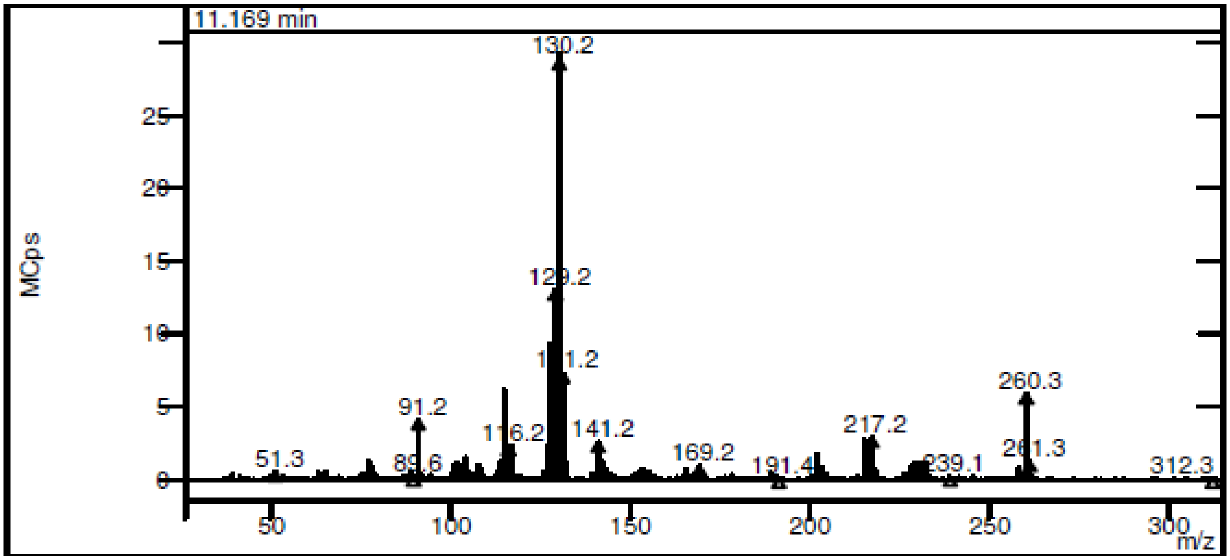

Figure 3. 8. Electron impact mass spectra of heavy product DH-5 in methanol extract at retention time of 11.169 min.

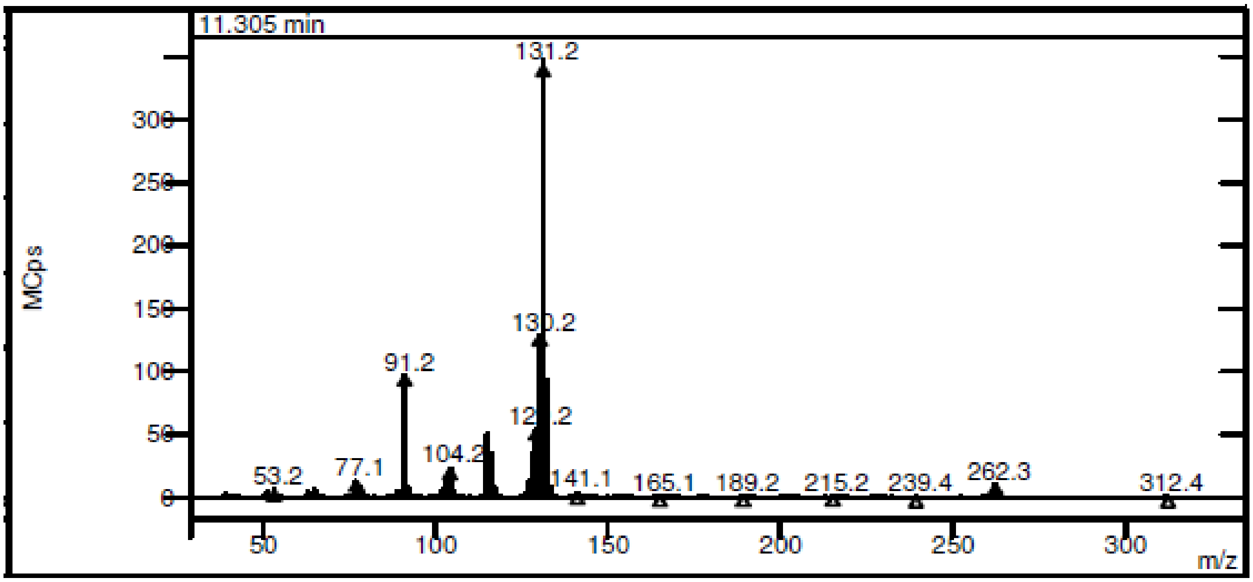

Figure 3. 9. Electron impact mass spectra of heavy product DH-6 in methanol extract at retention time of 11.305 min

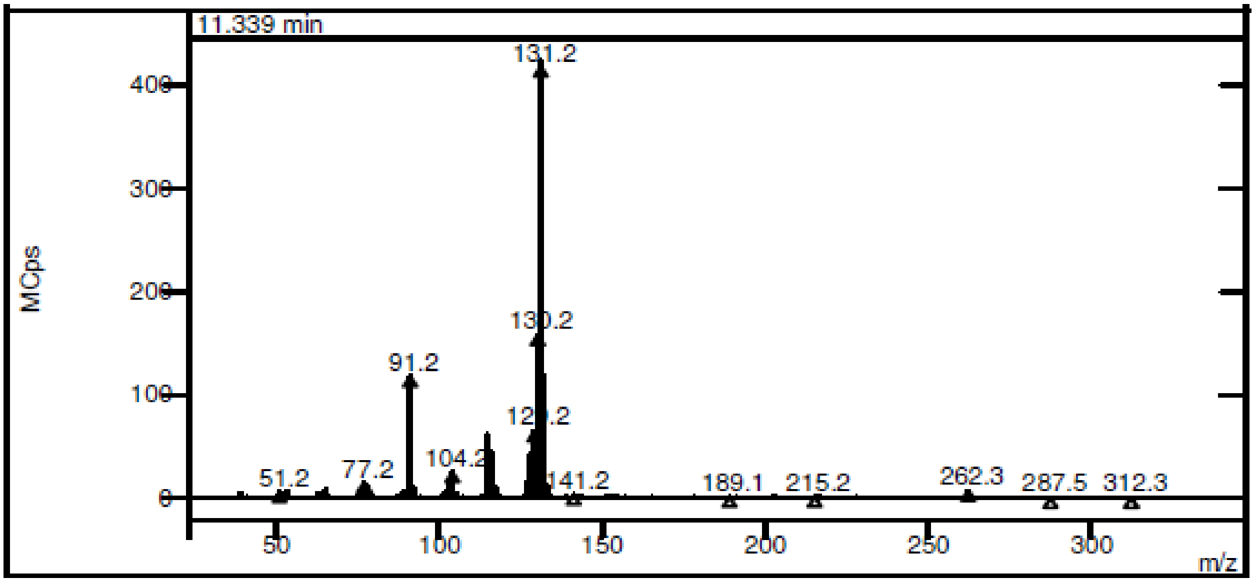

Figure 3. 10. Electron impact mass spectra of heavy product DH-7 in methanol extract at retention time of 11.339 min

As seen in the mass spectra, (Figure 3.8-3.10) the product DH-5 has molecular mass of 260 g/mole, and mass of the products DH-6 and DH-7 is 262 g/mole, which corresponds to the mass of the products' dimers. It was not possible to separate the peaks DH-6 and DH-7 completely (see Figure

3.7). The dimers were identified using suggestions from the NIST library. These products are consistent with the anticipated reaction chemistry (Figure 3.5).

The free radical content of the reaction products was measured by ESR. These results are shown in Figure 3.11.

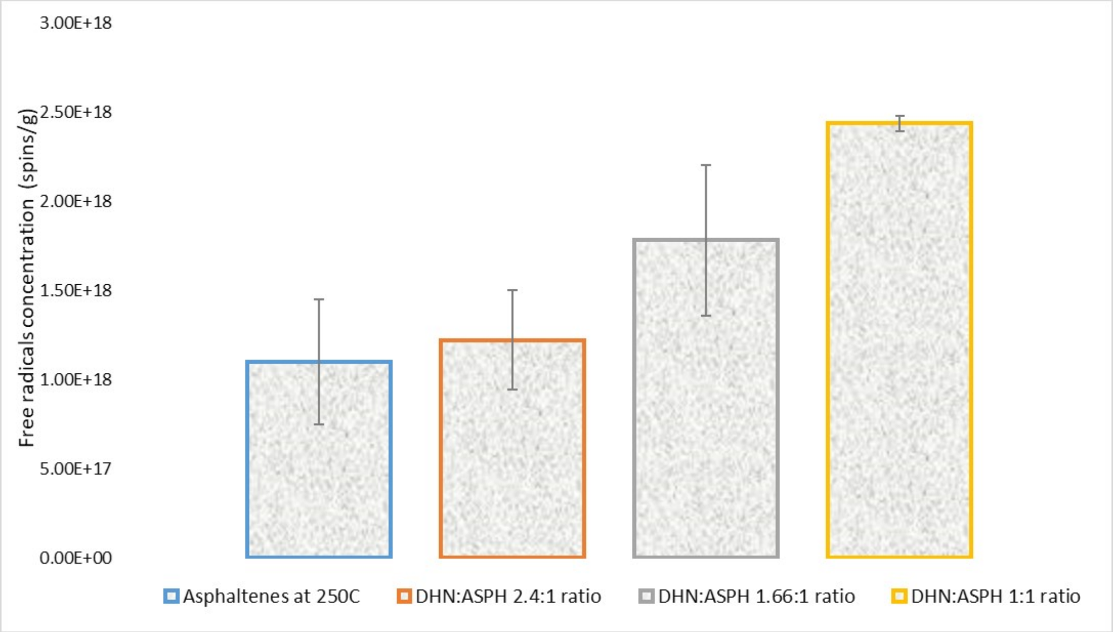

Figure 3. 11. Free radicals concentration of Nexen industrial asphaltenes and mixture of asphaltenes +1,2 dihydronaphthalene at different (wt/wt) ratios after the reaction conditions

As seen from the results (Figure 3.11) the concentration of the free radicals is decreasing as the amount of the DHN compound added is increased. The lowest free radical concentration was recorded for the reaction of asphaltenes on their own, the sample has a lower radical concentration compared to products obtained after the reactions with DHN. This initially appeared incongruous, but it should be pointed out that the results are shown on to total sample mass basis.

The results in Figure 3.11 had to be converted to an asphaltenes only basis. However, to do so it was necessary to determine whether DHN on its own also contributed to the formation of free radicals in the product. Self-initiation of DHN at the reaction conditions was reported before (Payan and de Klerk, 2018). The DHN was therefore exposed to the same reaction conditions as the reactions of the asphaltenes and asphaltenes+DHN and the reaction product was analyzed by electron spin resonance spectroscopy (Figure 3.12).

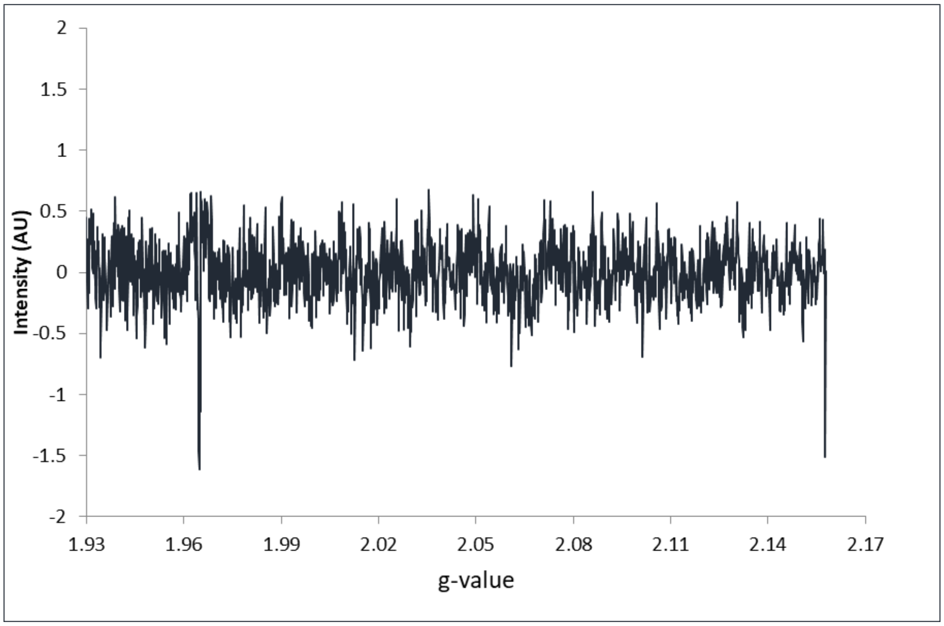

Figure 3. 12. The ESR spectra of 1,2-dihydronaphthalene conversion products at 250 °C, 4MPa N_2 atmosphere

There was no evidence of free radicals in the reaction product from the self-reaction of DHN (Figure 3.12). Recalculating the free radical content of the products shown in Figure 3.11 to be on an asphaltenes basis only, would therefore not compromise the integrity of the results, because the self-reaction products of DHN did not result in a detectable amount of free radicals in the product. The measured values on spins/g basis and recalculated values on spins/g asphaltenes basis, are both shown in Table 3.7.

Table 3. 7. Free radicals concentration of asphaltenes conversion products; and asphaltenes:DHN mixtures at different ratios after reaction at 250 °C. Experiments were conducted in duplicate

Materials	Free radical concentration (spins/g sample)		Free radical concentration (spins/g asphaltenes)
	x	s	
Asphaltenes	1.10E+18	3.5E+17	1.1E+18
DHN:asphaltenes, 1:1 wt/wt	2.44E+18	4.2E+16	4.9E+18
DHN:asphaltenes 1.6:1 wt/wt	1.78E+18	4.2E+17	4.6E+18
DHN:asphaltenes 2.4:1 wt/wt	1.22E+18	2.8E+17	4.1E+18

x = average, s = standard deviation

After reaction at 250°C in the presence of DHN, the free radical content expressed on an asphaltenes basis was around 4 times higher than after reaction of the asphaltenes on its own. The DHN resulted in changes in the free radical concentration in the asphaltenes (Table 3.7), without contributing to the increase in free radical concentration (Figure 3.12).

To better understand hydrogen transfer, a calculation similar to that performed by Payan and de Klerk (2018) was made for the results shown in Table 3.5. The results are shown in Figure 3.13.

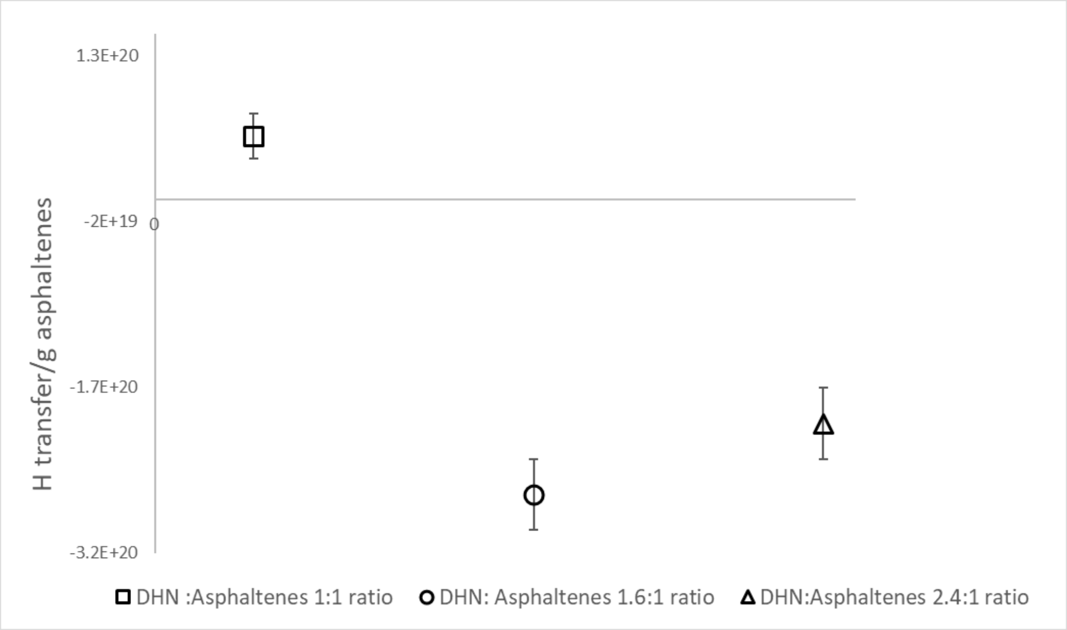

Figure 3. 13. Hydrogen atoms transferred/g asphaltenes after the reaction of asphaltene with 1,2-dihydronaphthalene at different (wt/wt) ratios 250 °C, 4MPa, based on the GC-FID results of MeOH extract.

As seen from the graph, the amount of hydrogen transferred to asphaltenes is increasing as the amount of the DHN molecule increases in the medium. However, after adding 1,2-dihydronaphthalene to asphaltenes in 2.4:1 (wt/wt) ratio the hydrogen transfer decreases compared to the reaction mixture of 1.6:1(wt/wt) ratio. The negative values of the amount of hydrogen transferred means asphaltenes were acting mainly as hydrogen acceptors.

3.3.3 Reaction between DPPH and 1,2-dihydronaphthalene

However, it was of interest if the hydrogen transfer of 1,2–dihydronaphthalene happens at the standard ambient temperature, pressure (SATP) conditions in the presence of the initiator, such as asphaltene. As it was noted (Naghizada et al, 2017) that asphaltenes are pretty unreactive at temperatures below 150°C. It was anticipated that the reaction will proceed slowly if asphaltenes would be employed as a radical source to demonstrate the changes by ESR, moreover, due to high deviation it would be difficult to evaluate the change in the radicals, thus, it was decided to employ the 2,2-Diphenyl-1-(2,4,6-trinitrophenyl) hydrazyl as the stable radical.

For that purpose, the 2,2-diphenyl-1-(2,4,6-trinitrophenyl) hydrazyl and 1,2-dihydronaphthalene were mixed 1:1 (wt/wt) ratio and the change in radical concentration was tracked. The decrease in organic free radical concentration was observed over time (Figure 3.14).

It was of interest to observe the change in free radical concentration. It was expected to see a decrease in radical concentration as the termination reactions by hydrogen transfer to DPPH could take place.

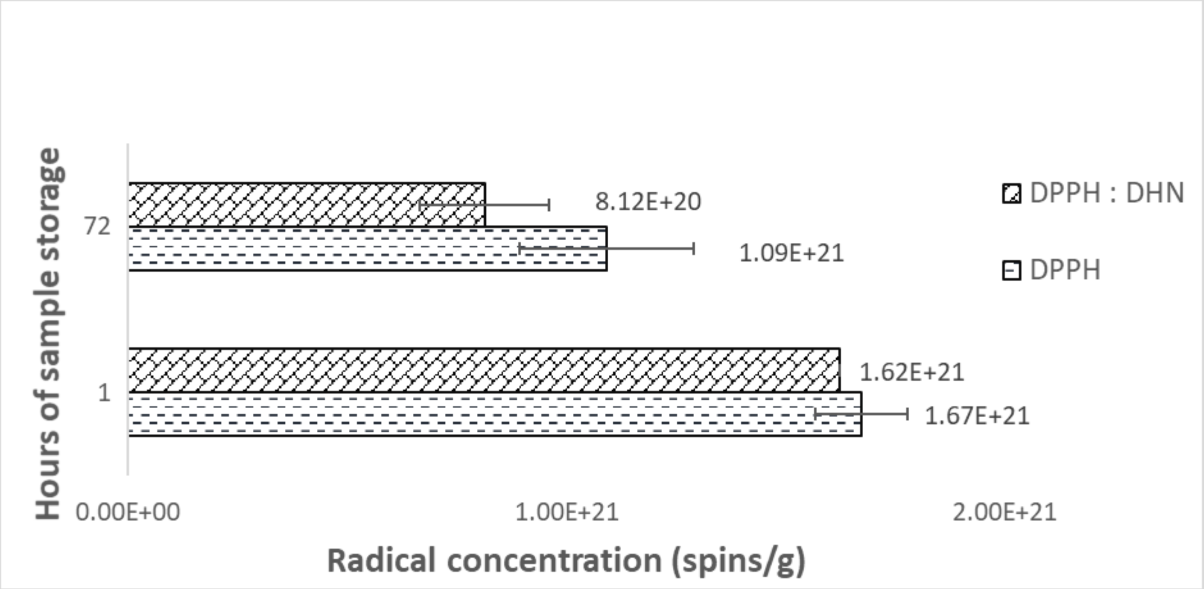

Figure 3. 14. Radical concentration of DPPH samples over the time; DPPH:DHN 1:1 (wt/wt) ratio; at 1 and 72 hours of sample storage. Experiments were conducted in duplicate.

Though the color change of the sample was not observed, it was ascribed to the low reactivity of the compounds at SATP conditions. It is shown that the radical concentration is decreasing more noticeably when 1,2–dihydronaphthalene was added. However, results might not be conclusive, as there was a deviation in the quantification of the radical concentration using the ESR.

To evaluate the precision of consecutive measurements, the DPPH concentration was measured consecutively at 0.013 wt % concentration for 3 times in a row. The average value obtained was 1.6E+21 spins/g and the standard deviation was 8.3E+19, i.e. a relative standard deviation of 5%.

3.4 Discussion

3.4.1 Nature of free radicals

The g-factor (also known as Lande factor) corresponds to the magnetic field of resonance position in the spectrum. The condition of the unpair electron is the primary factor affecting the g-factor, in case of asphaltenes it depends on the properties of the mixture of the free radicals and their orbital characteristics. Another parameter affecting the value of g-factor is the heteroatom content of the mixture (Oliviero et al., 2018; Montanari et al., 1998). The value of g-factor is directly proportional with the quantity of heteroatoms present in the system (Scotti and Montanari, 1998). The g-value of 2.0025 is in the agreement with Petrakis et al., 1978 values reported for the coals, corresponds to the carbon-centred π-radicals with 5-7 rings (Petrakis and Grandy, 1978). The g-factor for asphaltenes in the current study was found to be close to those of aromatic systems (Yen et al., 1962).

3.4.2 Free radicals decay over the range of time

As mentioned in chapter 2, it was reported in numerous papers that asphaltenes are undergoing aging-oxidation during the storage (Siddiqui and Ali, 1999; Babu and Cormack, 1983; Jia et al., 2004; Kudynska and Buckmaster, 1966; Wang et al., 2003; Siddiquee and de Klerk, 2014; Zhang et al., 2011). Decrease in free radicals concentration was also observed by Zhang et al.,(2010) and Montanari et al., (1998).

As shown in Table 3.3, the radical concentration is greater in the case when asphaltene is purged with air which might be due to the paramagnetic nature of the air (Montanari et al., 1998) rather than aging-oxidation. Also, it is seen that the radical concentration of asphaltenes decreases in a greater rate when purged with nitrogen gas which is assumed to happen due to the difference in the diffusion rates of the gases (Schmidt, 1945). One should therefore distinguish the impact of air (oxygen) atmosphere on analysis and changes caused by oxidation on storage.

Oxidation is a surface reaction, so depending on the surface area of contact the rate of oxidation changes accordingly. Hydroperoxides (ROOH) or peroxygens ($ROO^{\bullet}$) are formed as a result of oxygenation of free radicals (Kudynska 1996). As radicals are already present in asphaltenes, as shown in the numerous references (Strausz and Lown, 2003; Schultz and Selucky, 1981; Niizuma et al., 1977; Scotti and Montanari, 1998) and current work, there is no need for an initiation step to produce free radicals during free radical reactions.

The sequence of oxidation reactions for oxidation-aging can therefore start with the organic free radical species already formed:

$$\mathrm{R^{\bullet} + O_2 \rightarrow ROO^{\bullet}} \qquad \text{Eq 3.3.}$$

The activation energy for the above reaction is 0 (Siddiquee 2016).

$$\mathrm{ROO^{\bullet} + RH \rightarrow ROOH + R^{\bullet}} \qquad \text{Eq. 3.4}$$

$$\mathrm{R^{\bullet} + R^{\bullet} \rightarrow R_2} \qquad \text{Eq. 3.5}$$

The termination reactions are assumed to have 0 activation energy, since activation energies of most combination (termination) reactions is zero (Matyjaszewski and Davis, 2003; Flagan and Seinfeld, 2012). The radical reactions and combination reactions lead to polymerization reactions that occur slowly even at room temperatures (Molton et al., 1978).

From the reaction sequence (Eq. 3.3 to 3.4), it can be seen that there is chain propagation, but not chain branching, i.e. the number of reagent radicals remain the same. Oxidation-aging in the absence of hydroperoxide decomposition would lead to a decrease (Eq. 3.5) in free radical concentration over time. However, this decrease is analogous to termination in the absence of oxidation, although the reacting species and rates might be different.

3.4.3 Free radical behavior of asphaltenes with addition of DHN compound

As was explained in the introduction, one of the explanations for persistence of free radicals in asphaltenes that was noted, was free radical caging. It was argued that if free radical persistence if due to caging, then the persistent free radical species should become accessible for reaction as mass transport becomes less limiting. Mass transport in asphaltenes can be improved by the addition of a solvent to increase fluidity.

In this study a reactive solvent that was added, which would not only decrease mass transport resistance by increasing fluidity but could also react with the asphaltenes free radicals liberated from cages. It was anticipated that this would lead to a decrease in the persistent free radical content.

As was seen in the Table 3.7 and Figure 3.11, the free radicals concentration increased with addition of the solvent DHN. It was shown by Payan and de Klerk (2018) that self-initiation of DHN occurs at reaction conditions (250°C), thus it was expected that DHN could generate radicals as a result of conversion. Figure 3.12 shows it was not possible to observe free radicals in DHN after reaction, as the concentration of free radicals was too low to be observed by ESR. The free radicals produced by DHN self-reaction were therefore transient free radicals and there was no measurable persistent free radical content.

The observed increase in free radical content after reaction of the asphaltenes with DHN (Table 3.7 and Figure 3.11) was due to asphaltenes derived products.

Asphaltenes on their own was reactive if the temperature was increased to 250°C, with the persistent free radical content decreasing from 2.4E+18 spins/g (Table 3.3) to 1.1E+18 spins/g (Table 3.7). Using an argument based on caging, the increase in asphaltenes temperature was sufficient to increase fluidity to the extent that caging was disrupted and termination-type free radical reactions could occur, analogous to shown in eq. 3.6.

The addition of DHN would have caused a further decrease in fluidity at 250°C. However, in case of the asphaltenes: DHN reaction the free radicals concentration was higher in the reaction product, 4.1E+18 to 4.9E+18 spins/g asphaltenes (Table 3.7), than in the asphaltenes feed, 2.4E+18 spins/g (Table 3.3).

The persistent free radicals in asphaltenes were reactive and it was possible to increase their concentration through reaction with DHN. Since the reaction product was more fluid and the free radicals persisted after reaction and at a higher concentration than in the reaction product from asphaltenes alone, it seems unlikely that the origin of free radical persistence in asphaltenes can be attributed to caging. The reaction product of asphaltenes with DHN would be less prone to caging than the reaction product of asphaltenes on its own. Yet, the concentration of free radicals that persisted after reaction of asphaltenes with DHN, which was more fluid, was about four times higher than that of asphaltenes, which was less fluid.

3.4.4 Extent of hydrogen transfer in reaction of asphaltenes with addition of DHN

As shown in Figure 3.13, the amount of hydrogen atoms transferred per gram of asphaltenes is approximately 100 times higher than the number of free radicals in asphaltenes in Figure 3.11.

This could be because of the regeneration of the free radicals that occurs and new radicals that are formed during the reaction with DHN compound. This also is not conclusive as conversion of DHN itself occurs simultaneously. Moreover, when DHN to asphaltene ratio is 1.6:1 (wt/wt) the hydrogen transfer is higher than in the case when the ratio is 2.4:1 (wt/wt). This implies that the available site in the asphaltenes are limited, which is consistent with Naghizada's (2017) work. In his study, he demonstrated that with an increase in asphaltene weight ratio in the asphaltene-acceptor reaction mixture the concentration of the main hydrogenated product (cumene) also increased. However, due to challenges in extraction of mixture, it is not possible to say it conclusively, as the mass of unrecovered compounds is difficult to evaluate.

From the previous studies, it was suspected that asphaltene radicals might regenerate without termination. As seen from the Figure 3.14 there was some indication that radical concentration decreases with the addition of the DHN compound. However, as mentioned earlier, it was also observed that asphaltene has less radicals after the reaction conditions than the asphaltene and 1,2–dihydronaphthalene mixture.

3.4.5 Hydrogen tunneling effect

The comparatively low temperature at which DHN self-initiates requires some discussion. One of the potential reasons noted in literature is the tunneling effect of hydrogen.

During hydrogen transfer reactions a lower energy barrier might be experienced that is significantly lower than the calculated Arrhenius activation energy. This phenomenon is known as the tunneling effect, which may lower the theoretical activation energy by 10 to 20 percent. Based on the uncertainty principle of the quantum physics, when the momentum of a particle is assessed with a high accuracy, the uncertainty of its position increases. After a time, a particle may occur at either side of the energy barrier without reaching the peak of the energy barrier (Caldin and Gold, 2013; Trotman-Dickenson, 1965).

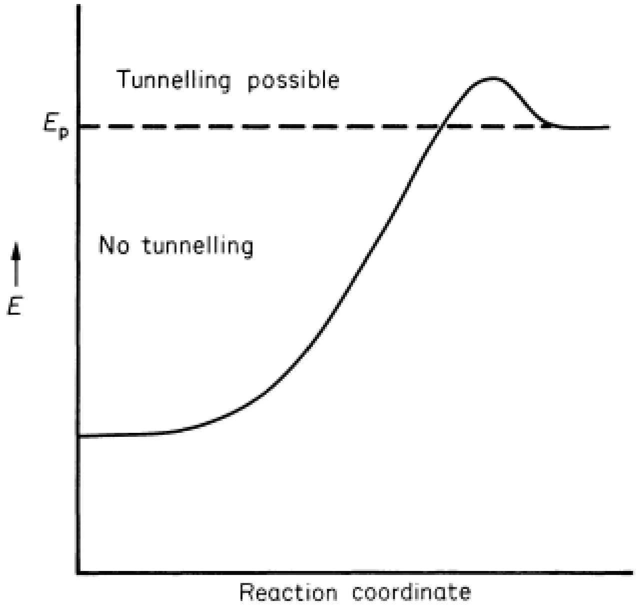

Figure 3. 15. Representation of the tunneling effect (Caldin and Gold, 2013)

3.4.6 Reaction between DPPH and 1,2-dihydronaphthalene

In previous studies, it was shown that DPPH ESR absorption decreases over time when dissolved in toluene and stored in dark (Yordanov and Christova,1994; Slangen 1970).

As shown in Figure 3.14., the radical concentration of DPPH and DHN mixture decreased in faster rate than the case that DPPH is stored separately. Reaction between DHN and DPPH is thermodinamically unfavorable, as the bond dissociation energy of DHN (80-86.4 kcal/mole) is higher than that of DPPH (79.6 kcal/mole) (Luo, 2002; Mahoney et al., 1973). However it could be kinetically favorable.

3.5 Conclusions

The change in persistent free radical concentration in the asphaltenes with decrease of mass transport limitation was investigated. Key findings were:

- Free radicals concentration decreased over time with both nitrogen and oxygen purges. The results revealed that the decrease was greater in case of nitrogen purging.
- The origin of a higher free radical content when measurements were conducted in an air atmosphere was not due to oxidation-aging.

- DHN undergoes self-initiation and conversion at 250°C. The resulting product from DHN self-conversion appears to have no persistent free radicals, no radicals were detected using ESR in the product from DHN self-reaction at the reaction conditions.
- It seems unlikely that the origin of free radical persistence in asphaltenes can be attributed to caging. The persistent free radical content of asphaltenes after conversion in the presence of DHN was higher than conversion on its own. The potential for caging in the former case was less than in the latter case, which is inconsistent with an explanation of persistence of free radicals based on caging.
- Adding a hydrogen donor doesn't always ensure the decrease in free radicals' concentration.
- It was revealed that the number for hydrogen transfer is about 100 times larger than the amount of free radicals present.

3.6 References

Babu, D.R. and Cormack, D.E., 1983. Low temperature oxidation of Athabasca bitumen. *The Canadian Journal of Chemical Engineering*, *61*(4), pp.575-580.

Caldin, E.F. and Gold, V., 2013. *Proton-transfer reactions*. Springer.

Dietz, W.A., 1967. Response factors for gas chromatographic analyses. *Journal of Chromatographic Science*, *5*(2), pp.68-71.

Eaton, G. R., Eaton, S. S., Barr, D. P., & Weber, R. T. (2010). *Quantitative Epr*. Springer Science & Business Media.

Flagan, R. C., & Seinfeld, J. H. (2012). *Fundamentals of air pollution engineering*. Courier Corporation.

Jia, N., Moore, R.G., Mehta, S.A., Van Fraassen, K., Ursenbach, M. and Zalewski, E., 2004, January. Compositional changes for Athabasca bitumen in the presence of oxygen under low temperature conditions. In *Canadian International Petroleum Conference*. Petroleum Society of Canada.

Katritzky, A.R., Ignatchenko, E.S., Barcock, R.A., Lobanov, V.S. and Karelson, M., 1994. Prediction of gas chromatographic retention times and response factors using a general qualitative structure-property relationships treatment. *Analytical Chemistry*, *66*(11), pp.1799-1807.

Kudynska, J. and Buckmaster, H.A., 1996. Low-temperature oxidation kinetics of high-volatile bituminous coal studied by dynamic in situ 9 GHz CWEPR spectroscopy. *Fuel*, *75*(7), pp.872-878.

Luo, Y. R. (2002). *Handbook of bond dissociation energies in organic compounds*. CRC press.

Mahoney, L.R., Mendenhall, G.D. and Ingold, K.U., 1973. Calorimetric and equilibrium studies on some stable nitroxide and iminoxy radicals. Approximate oxygen-hydrogen bond dissociation energies in hydroxylamines and oximes. *Journal of the American Chemical Society*, *95*(26), pp.8610-8614.

Matyjaszewski, K., & Davis, T. P. (2003). *Handbook of radical polymerization*. John Wiley & Sons.

Molton, P.M., Demmitt, T.F., Donovan, J.M. and Miller, R.K., 1978. Mechanism of conversion of cellulose wastes to liquid fuels in alkaline solution. In: D.L. Klass (Ed.), Energy from Biomass and Wastes III. Institute of Gas Technology, Chicago, IL, p. 293.

Montanari, L., Clericuzio, M., Del Piero, G., & Scotti, R. (1998). Asphaltene radicals and their interaction with molecular oxygen: An EPR probe of their molecular characteristics and tendency to aggregate. *Applied Magnetic Resonance*, *14*(1), 81-100.

Naghizada, N., 2017. *Uncatalyzed hydrogen transfer during 100-250 C conversion of asphaltenes*. M.Sc. Thesis, University of Alberta: Edmonton, Alberta, Canada.

Naghizada, N., Prado, G.H. and de Klerk, A., 2017. Uncatalyzed hydrogen transfer during 100–250 C conversion of asphaltenes. *Energy & fuels*, *31*(7), pp.6800-6811.

Niizuma, S., Steele, C.T., Gunning, H.E. and Strausz, O.P., 1977. Electron spin resonance study of free radicals in Athabasca asphaltene. *Fuel*, *56*(3), pp.249-256.

Oliviero Rossi, C., Caputo, P., Ashimova, S., Fabozzi, A., D'Errico, G., & Angelico, R. (2018). Effects of natural antioxidant agents on the bitumen aging process: An epr and rheological investigation. *Applied Sciences*, *8*(8), 1405.

Payan, F. and de Klerk, A., 2018. Hydrogen Transfer in Asphaltenes and Bitumen at 250° C. *Energy & fuels*, *32*(9), pp.9340-9348.

Petrakis, L., & Grandy, D. W. (1978). Electron spin resonance spectrometric study of free radicals in coals. *Analytical Chemistry*, *50*(2), 303-308.

Schmidt, L. D. (1945). Changes in coal during storage. *Chemistry of coal utilization*, *18*, 627-676.

Schultz, K.F. and Selucky, M.L., 1981. Esr measurements on asphaltene and resin fractions from various separation methods. *Fuel*, *60*(10), pp.951-956.

Scotti, R. and Montanari, L., 1998. Molecular structure and intermolecular interaction of asphaltenes by FT-IR, NMR, EPR. In *Structures and dynamics of asphaltenes* (pp. 79-113). Springer, Boston, MA.

Siddiquee, M. N., de Klerk, A., & Nazemifard, N. (2016). Application of microfluidics to control product selectivity during non-catalytic oxidation of naphthenic-aromatic hydrocarbons. *Reaction Chemistry & Engineering*, *1*(4), 418-435.

Siddiquee, M.N. and de Klerk, A., 2014. Hydrocarbon addition reactions during low-temperature autoxidation of oilsands bitumen. *Energy & Fuels*, *28*(11), pp.6848-6859.

Siddiqui, M.N. and Ali, M.F., 1999. Studies on the aging behavior of the Arabian asphalts. *Fuel*, *78*(9), pp.1005-1015.

Slangen, H.J.M., 1970. Determination of the spin concentration by electron spin resonance. *Journal of Physics E: Scientific Instruments*, *3*(10), p.775.

Strausz, O.P. and Lown, E.M., 2003. *The chemistry of Alberta oil sands, bitumens and heavy oils* (pp. 588-592). Calgary, Alberta, Canada: Alberta Energy Research Institute.

Trotman-Dickenson, A.F., 1965. The abstraction of hydrogen atoms by free radicals. *Advances in free radical chemistry*, *1*, pp.1-38.

Wang, H., Dlugogorski, B.Z. and Kennedy, E.M., 2003. Coal oxidation at low temperatures: oxygen consumption, oxidation products, reaction mechanism and kinetic modelling. *Progress in energy and combustion science*, *29*(6), pp.487-513.

Yaws, C.L., Narasimhan, P. and Gabbula, C., 2009. *Yaws' Handbook of Antoine Coefficients for Vapor Pressure (2nd Electronic Edition)*. New York: Knovel.

Yen, T.F., Erdman, J.G. and Saraceno, A.J., 1962. Investigation of the Nature of Free Radicals in Petroleum Asphaltenes and Related Substances by Electron Spin Resonance. *Analytical Chemistry*, *34*(6), pp.694-700.

Yordanov, N. D., & Christova, A. (1994). DPPH as a primary standard for quantitative EPR spectrometry. *Applied Magnetic Resonance*, *6*(1-2), 341-345.

Zhang, N., Zhao, S., Sun, X., Xu, Z. and Xu, C., 2010. Storage stability of the visbreaking product from Venezuela heavy oil. *Energy & Fuels*, *24*(7), pp.3970-3976.

Zhang, Q., Sun, H.H. and Geng, J.G., 2011. Chemical Effects of Environmental Factors on Asphalt Aging. In *Advanced Materials Research* (Vol. 243, pp. 1067-1071). Trans Tech Publications.

Chapter 4 – Investigation of asphaltenes' steric requirements

4.1 Introduction

One possible reason for free radical persistence in asphaltenes, is that the free radical position is difficult to access due to the structure of the radical species. Such a situation would arise if the radical center is surrounded by groups that are bulky in structure and make it difficult for any other species to approach and interact with the radical center. This is the equivalent of intramolecular "caging", because the steric bulk of the groups surrounding the free radical center prevents interaction with other species thereby causing the free radical center to be persistent.

In the previous works by Naghizada et al. (2017) and Payan and de Klerk (2018), it was demonstrated that asphaltenes possess both acceptor and donor properties. In this chapter, steric requirements were explored by employing different probe molecules with different substituents surrounding a styrene core. The styrene core gave all of the probe molecules hydrogen acceptor properties, but by changing the substituents close to the C=C of the styrene core, the bulkiness of the probe molecules was different. Thus, if the free radicals in asphaltenes were sterically protected, only the probe molecules with sterically lean and easy to access C=C groups would be able to interact with the free radicals species in the asphaltenes.

The probe molecules with different steric requirements employed were 1,1-diphenylethylene (DPE), 2,4,6-trimethylstyrene (TMS), E-stilbene (ES), Triphenylethylene (TPE), 1,1,2,2-tetraphenylethylene (1,1,2,2-TPE), and α-methylstyrene (AMS). The structures are shown in Figure 4.1.

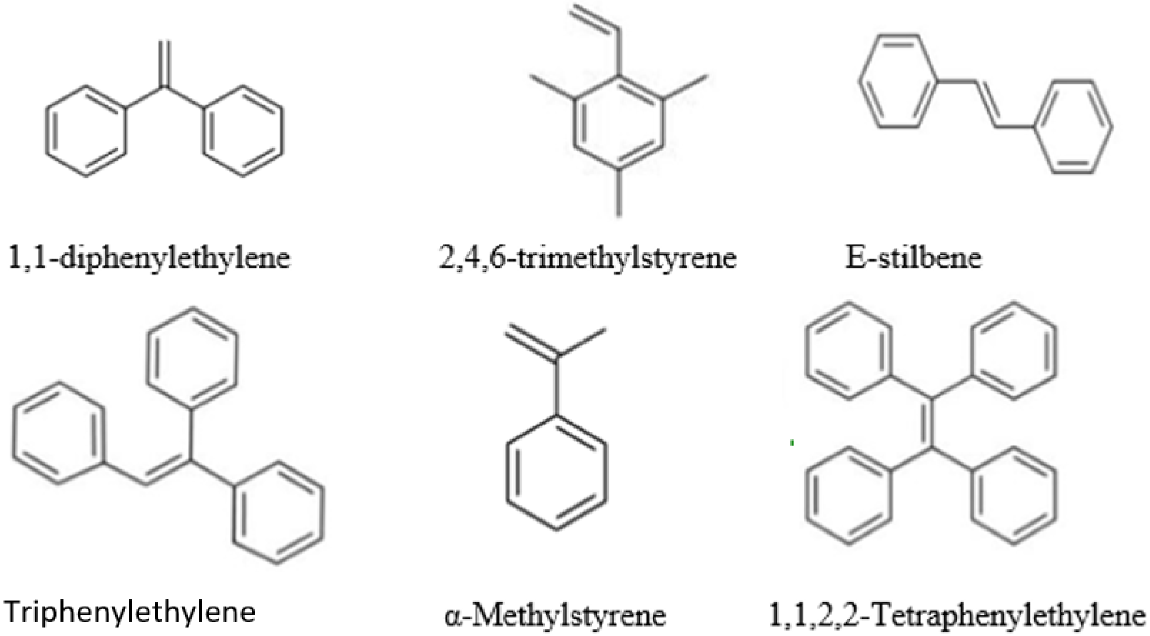

Figure 4. 1. Representation of probe molecules employed in the study

These compounds were selected based on structure and ceiling temperature when known, but the probe molecule selection was also tempered by cost and availability.

The acceptor properties of the type of compounds employed in this study and their thermodynamic properties have been explored by Rüchardt et al., (1997). In their study, acceptor molecules reacted with a donor compound, 9,10-dihydroanthracene (DHA), at 300 °C without catalyst. It was suggested that hydrogen transfer reactions were proceeding at lower temperatures due to the tunneling effect, where energy barrier is less than the predicted Arrhenius activation energy (discussed in Chapter 3). In this study an even lower temperature, 250 °C, was used to improve the selectivity of the probe molecules and reduce side-reactions that would naturally take place at elevated temperature.

4.2 Experimental

4.2.1 Materials

The different probe molecules used in the study, as well as solvents and compounds used to assist with identification of products are reported in Table 4.1. The asphaltenes were the same as described in Chapter 3.

Table 4. 1. Materials used for the reactions in the current study

Chemical compound name	Formula	Purity %[a]	CASRN[b]	Supplier
Triphenylethylene	$C_{20}H_{15}$	98	58-72-0	Alfa Aesar
1,1-diphenylethylene	$C_{14}H_{12}$	98	530-48-3	Alfa Aesar
2,4,6-trimethylstyrene	$C_{11}H_{14}$	95	769-25-5	Sigma-Aldrich
E-stilbene	$C_{14}H_{12}$	96	103-30-0	Sigma-Aldrich
α-Methylstyrene	C_9H_{10}	99	98-83-9	Sigma-Aldrich
1,1,2,2-tetraphenylethylene	$C_{26}H_{20}$	99	632-51-9	Sigma-Aldrich
1,1,2-triphenylethane	$C_{20}H_{18}$	NA	1520-42-9	Sigma-Aldrich
Methanol	CH_3OH	99.9	67-56-1	Fischer Chemical
Cyclohexane	C_6H_{12}	99.5+	110-82-7	Sigma-Aldrich
α-methylnaphthalene	$C_{11}H_{10}$	96	90-12-0	Alfa Aesar
9,10-dihydroanthracene	$C_{14}H_{12}$	97	613-31-0	Sigma-Aldrich
Z-stilbene	$C_{14}H_{12}$	97	645-49-8	Alfa Aesar
Bibenzyl	$C_{14}H_{14}$	99	103-29-7	Acros Organics
Anthracene	$C_{14}H_{10}$	97	120-12-7	Sigma-Aldrich
Methylene chloride	CH_2Cl_2	99.9	75-09-2	Fischer Chemical
Cumene	C_9H_{12}	98	98-82-8	Aldrich

[a] - This is the purity of the material guaranteed by the supplier; material was not further purified.

[b] - CASRN = Chemical Abstracts Services Registry Number

For probe molecules, compounds with lower ceiling temperatures were selected to avoid formation of heavier products at the reaction conditions. It was reported that the ceiling temperature for αphenylstyrene is 107±2 °C (Mathieson 1960), for stilbene it is below 61 °C (Wyman and Altares 1964), and α-methylstyrene is 61 °C (Lin et al. 1997, McCormick 1957). No information on the ceiling temperature of Triphenylethylene polymerization could be found, however, it was selected as the most sterically hindered compound to investigate the steric requirements of asphaltenes. To get more detailed insight into the steric requirements, it was decided synthesize additional compounds, such as hex-1-en-2-ylbenzene, on which more detailed information is provided in Chapter 5.

4.2.2 Equipment and procedure

4.2.2.1 Establishing pressure requirements

It was necessary to ensure that the probe molecules were present in the liquid phase at the reaction temperature of 250 °C. It was therefore necessary to maintain the reaction pressure above the vapor pressure of the compounds used. The vapor pressure of each compound under reaction conditions was considered and calculated employing Antoine equation (Eq 4.1) to verify that all the compounds are in the liquid state at reaction conditions (Yaws, 2009).

The vapor pressures of the compounds were estimated according to:

$$\log_{10} P = A - \frac{B}{T+C} \qquad \text{Eq. 4.1}$$

where A, B, C are Antoine's coefficients and T stands for the temperature in °C and P stands for pressure in mm Hg. The Antoine coefficients are presented in Table 4.2 and were used to calculate the vapor pressure of the compounds at 250 °C, which is presented in the same table.

Table 4. 2. Antoine coefficients and the calculated pressure at 250 °C

Compound	A	B	C	Vapor pressure (MPa)
E-stilbene (ES)	7.15	2030.21	169.30	0.03
1,1-diphenylethylene (DPE)	7.14	1973.74	186.35	0.06
Triphenylethylene (TPE)	7.35	2553.77	175.95	0.00
2,4,6-trimethylstyrene (TMS)	7.15	1737.97	197.96	0.25
α-methylstyrene (AMS)	7.13	1641.01	220.78	0.59
1,1,2,2-tetraphenylethylene	7.32	2818.91	140.8	0.00

A pressure of 4 MPa was selected, which is similar to that used in previously by Naghizada et al. (2017) and Payan and de Klerk (2018) was well above the vapor pressure of the compounds.

According to Sánchez-Lemus et al. (2016) with the increase in the boiling point of the heavy oil cuts the vapor pressure decreases. Considering asphaltenes are the heaviest distillation cut, therefore the vapor pressure was assumed to be significantly below the 4 MPa operating pressure selected for the reaction.

4.2.2.2 Phase of reaction mixture

Although the temperature of reaction was selected beforehand, 250 °C, based on considerations explained in the introduction, it was necessary for all compounds to be in the liquid phase at the reaction temperature. It was known from previous work that the industrial asphaltenes used in this study liquefy below 150 °C. However, some of the probe molecules were solids. It was necessary to check the melting point temperature to confirm that those probe molecules will be liquid at the reaction temperature.

E-stilbene and Triphenylethylene have melting points of 120-125 °C and 68-73 °C respectively (Mathai 1960; Peña–López et al. 2013; Amini and Etemadi 2013; Wu et al. 2015; Ru et al. 2018). The melting point of the donor compound 9,10-dihydroanthracene (DHA) was 109-118 °C (Kuimov et al. 2018; Smith et al. 2017). 1,1,2,2-Tetraphenylethylene had the highest melting point, which was in the range 213-225.2 °C (Jin et al. 2018; Pelletier et al. 2012).

4.2.2.3 Procedure followed for reactions of probe molecules and asphaltenes

The reactions were performed in micro-batch reactors at 250 °C and 4 MPa initial N_2 pressure and were conducted for an hour of reaction time.

All the Experiments were carried out in micro-batch reactors with glass vial insert. The micro-batch reactors were manufactured from Swagelok fittings, with dimensions as follows: 7.6 cm length; 1.9 cm diameter, equipped with the pressure gauge, and three-way valve as described in Chapter 3. All the experiments were performed in duplicate.

Probe molecules and asphaltenes were placed in the 11 ml glass vial in order to reduce interaction with the reactor walls that could affect the reaction rate. For each experiment with asphaltenes and probe molecule, 0.5±0.02 g of asphaltenes and 0.5±0.02 g of probe molecule was inserted into the glass vial (1:1 wt ratio). For experiments that included DHA, 0.25±0.02 g of asphaltenes, 0.5±0.02 g of probe molecule, and 0.25±0.02 g of DHA was inserted into the glass vial (1:2:1 wt ratio). The mixture of asphaltene and liquid probe molecules was homogenized using Branson 2800 ultrasound bath for 15 min. Reaction mixture with solid compounds were mixed manually until the uniform distribution of compounds was obtained.

Measurements were performed using a Mettler Toledo XP 1203S balance, with maximum capacity of 1210 g and readability of 1 mg. The liquid probe molecules were dispense using an Eppendorf Research Plus pipette of 20-200 µl (#119628 A).

Before each run, the reactors were leak-tested and pressurized with N_2 up to 2 MPa pressure for three times in order to remove the residual atmospheric oxygen from the reactor. Then the reactor was pressurized to 4 MPa with N_2 before reaction. The pressurized micro-batch reactors were placed in a preheated fluidized sand bath heater (Omega). The reactors were heated up and temperature was measured using thermocouple. The experiments that were performed are summarized in Table 4.3.

Table 4. 3. Experiments denotation for the ease of description

Experiment Carried out at 250 °C, 4MPa N_2	Probe molecule [a]	Weight based ratio		
		Asphaltenes	Probe molecule	DHA
Experiment 1	DPE	1	1	-
Experiment 2	DPE	1	2	1
Experiment 3	DPE	-	1	1
Experiment 4	ES	1	1	-
Experiment 5	ES	1	2	1
Experiment 6	ES	-	1	1
Experiment 7	TPE	1	1	-
Experiment 8	TPE	1	2	1
Experiment 9	TPE	-	1	1
Experiment 10	AMS	1	1	-
Experiment 11	AMS	1	2	1
Experiment 12	AMS	-	1	1
Experiment 13	TMS	1	1	-
Experiment 14	TMS	1	2	1
Experiment 15	TMS	-	1	1
Experiment 16 [b]	1,1,2,2-TPE	1	1	-

[a] -DPE = 1,1-diphenylethylene; ES = E-stilbene; TPE = Triphenylethylene; AMS = α-methylstyrene; TMS = 2,4,6-trimethylstyrene; 1,1,2,2-TPE = 1,1,2,2-tetraphenylethylene.

[b] -The reason for only a single experiment with 1,1,2,2-tetraphenylethylene is that no reaction was observed.

After the reaction period of 1 h, reactors were left in the fumehood to cool to the ambient temperature. Recovery of the product from the vial was carried out with 2 ml methylene chloride. The methylene chloride was evaporated using Heidolph Hei-VAP rotary evaporator at 27 °C, 70 rpm, and 650 mbar absolute pressure.

Since it was not possible to analyze the reaction products of the probe molecules in the presence of the asphaltenes, the reaction products were obtained by methanol extraction. The probe molecules and reaction products were extracted with 100 ml of methanol (density 0.78906 g/ml), measured using 100 ml volumetric flask. The extraction mixture was stirred using heating plate at 250 rpm for 30 minutes. An internal standard (ISTD) was added to each methanol extract before it was analyzed. Only a small sample of the whole methanol-extract was taken and filtered through a syringe filter before it was analyzed by gas chromatography. Additional information is provided in Appendix B.

In addition to the experiments in Table 4.3, control experiments were performed. All the probe molecules were reacted at 250 °C and 4 MPa to confirm that they do not decompose under the reaction conditions. Control reactions were performed with 0.5±0.02 g of the probe molecule.

For material balance purposes the weight of the reactor assembly was monitored at different stages of the procedure. The weight of the empty reactor assembly, as well as reactor weight after the reaction was measured using MS 6001 S scale, with maximum capacity of 6200 g, and readability of 100 mg.

4.2.2.4 Hydrogenation of probe molecules

To increase confidence in the identification of products, where practical use was made of authentic compounds. For example, the hydrogen transfer product of α-methylstyrene is cumene and to support the identification of cumene by gas chromatography with mass spectrometry (GC-MS), cumene was purchased as an authentic compound (Table 4.1). This was not possible for the anticipated products from hydrogen transfer of all compounds. In selected cases, the hydrogenated product was prepared from the olefin.

Hydrogenation of 1,1-diphenylethylene and 2,4,6-trimethylstyrene was performed. A smaller reactor was used for this purpose in order not to consume much hydrogen gas. For the hydrogenation reaction, 319 mg of compound, 17 mg of catalyst 10% Pd/C catalyst (Aldrich Chemistry, #205699), dehydrated ethanol 199 mg were all added to the glass vial. The procedure was based on data on analogous types of hydrogenation from literature (Brown et al. 1938; Kooyman 1955; Nakamula et al. 2008; Akchurin et al. 2016). Reactions were performed in duplicate.

Reactor was leak tested, pressurized with nitrogen for 3 times in order to remove all the residual oxygen left in the reactor. After a successful leak test, reactors were pressurized to 400 kPa hydrogen (H_2) pressure and left in the fumehood at room temperature for 18 hours away from all heating sources.

All the Experiments were carried out in micro-batch reactors with glass vial insert as described in Chapter 3. Quantification of the hydrogenation products was performed at the same conditions as of the reactions of interest. Thus, accounting for the response factor corresponding to the concentration of the extracted products.

4.2.3 Analyses

4.2.3.1 Gas chromatography coupled with mass spectrometry

Gas chromatography coupled with mass spectrometer (GC-MS) was used to determine compounds. The equipment used was an Agilent 7820A coupled with Agilent 5977E mass selective detector. Separation was performed on an HP-5 column (30 m x 0.25 mm x 0.25 μm) using helium as a carrier mobile gas at constant flow of 0.5 ml/min. The temperature program started at 45 °C and temperature was increased by 5 °C/min up to 320 °C with hold time of 10 minutes, split ratio: 100/1.

For E-stilbene reaction products, the method with same parameters was used, however for better determination the oven temperature was increased by only 2 °C/min to improve separation, due to overlap of Z-stilbene and bibenzyl signals.

The NIST library was used by the software for identifying the molecules based on their electron impact mass spectrum.

4.2.3.2 Gas chromatography coupled with flame ionization detector

The method used was the same as described in Chapter 3. The internal standard used for quantification was not the same as in Chapter 3.

The calibration curves were obtained for the GC-FID. α-Methylnaphthalene was used as internal standard for triphenylethylene, 1,1-diphenylethylene, E-stilbene, bibenzyl, and Z-stilbene. Cyclohexane was used as an internal standard for α-methylstyrene, cumene, and 2,4,6-trimethylstyrene. The calibration curves are shown in Appendix B.2.

Different concentrations of probe molecules were added for each level of calibration, to 100 ml volumetric flask, keeping concentration of internal standard (ISTD) being relatively the same for each probe molecule throughout the calibration. Methanol was used as a solvent, each sample was filled in to the 100 ml. All samples were mixed for 30 minutes at 250 rpm. Each sample was injected three times, to obtain the average value.

4.2.3.3 Simulated Distillation

The boiling point distribution of the reaction products from the experiments with asphaltenes and probe molecules in 1:1 mixtures were evaluated by Simulated Distillation (SimDis) following the standard test method ASTM D7169 – 11.

The equipment used for this analysis was an Agilent 7890B high temperature gas chromatograph (GC) with flame ionization detector (FID). The column employed is DB-HT-SIMDIS with the following dimensions: 5 m × 0.53 mm × 0.15 μm. Samples were prepared by dilution in CS_2 (≥99%, Fischer Chemical) to 0.7-0.8 wt%.

Polywax 655 and reference material 5010 were used for the calibration.

The samples in these analyses did not elute completely, which implies that there is material in the sample with a higher equivalent normal boiling point temperature than 720 °C. Analyses were performed in duplicate.

4.3 Results

4.3.1 Quantification of reaction products

When doing experiments with probe molecules and asphaltenes there are two experimental challenges that must be addressed. The first challenge that of GC-FID response factors. This challenge is not directly related to reactions with asphaltenes but depends on the nature of the probe molecules. The second challenge is extraction and partitioning. In order to recover the reaction products after reaction with asphaltenes to be analyzed by GC-FID, they need to be extracted using a solvent that is insoluble in asphaltenes and will remain a separate phase, while at the same time can dissolve the probe molecules and their reaction products.

4.3.1.1 Calibration of the probe molecules for quantification

The GC-FID response factors were determined relative to the internal standard added to the methanol extracted product. These relative response factors could then be used when analyzing the methanol extract of the reaction products to quantify the unknown amount of probe molecules in the reaction product.

The principle is as follows. When the area response of the GC-FID for the probe molecule relative to the internal standard is known, then it is possible to calculate the concentration of an unknown amount of the probe molecule in a methanol extract. By adding a known amount of internal standard (as described in the experimental section), the peak area of the unknown amount of probe molecule after reaction can be related to the peak area of the known amount of internal standard in the chromatogram.

The relative GC-FID response factors for probe molecules and their hydrogenated products were not known and had to be determined experimentally.

As the study is quantitative, it was decided to start from quantifying the probe molecules and possibly the available products using calibration curves. Calibration of the probe molecules was performed for accurate quantification of reaction products. Accurate and reliable quantification of reaction products was achieved via calibration of probe molecules.

The regression factor for most of the calibration curves in Appendix B built according to the data in Tables 4.4 to 4.8 was around $R^2= 0.999$.

Table 4. 4. Calibration data obtained by GC-FID for AMS

	Levels		
	1	2	3
AMS			
Concentration (mg/ml)	1.0	2.0	3.0
Amount AMS/Amount ISTD	1.0	2.1	3.0
Area AMS/Area ISTD	1.2	2.8	3.9
Cumene			
Concentration (mg/ml)	0.4	1.0	1.7
Amount Cumene/Amount ISTD	0.4	1.0	1.7
Area Cumene/Area ISTD	0.5	1.4	2.2
ISTD			
Concentration (mg/ml)	1.0	1.0	1.0

Table 4. 5. Calibration data obtained by GC-FID for DPE

	Levels			
	1	2	3	4
DPE				
Concentration (mg/ml)	2.1	3.1	4.0	5.0
Amount DPE/Amount ISTD	1.07	1.52	2.05	2.57
Area DPE/Area ISTD	1.12	1.63	2.22	2.77
ISTD				
Concentration (mg/ml)	1.9	2.0	2.0	2.0

Table 4. 6. Calibration data obtained by GC-FID for TMS

	Levels		
	1	2	3
TMS			
Concentration (mg/ml)	1.0	1.8	2.2
Amount TMS/Amount ISTD	0.99	1.75	2.24
Area TMS/Area ISTD	0.98	1.90	2.41
ISTD			
Concentration (mg/ml)	1.0	1.0	1.0

Table 4. 7. Calibration data obtained by GC-FID for TPE

	Levels		
	1	2	3
TPE			
Concentration (mg/ml)	2.0	4.0	5.0
Amount TPE/Amount ISTD	1.03	2.01	2.53
Area TPE/Area ISTD	1.37	2.70	3.21
ISTD			
Concentration (mg/ml)	2.0	2.0	2.0

Table 4. 8. Calibration data obtained by GC-FID for E-stilbene

	Levels			
	1	2	3	4
E-stilbene				
Concentration (mg/ml)	1.6	2.1	2.6	5.0
Amount E-stilbene/Amount ISTD	0.79	1.09	1.32	2.57
Area E-stilbene/Area ISTD	0.82	1.15	1.41	2.67
Z-stilbene				
Concentration (mg/ml)	0.5	1.1	1.5	2.1
Amount Z-stilbene/Amount ISTD	0.25	0.56	0.78	1.09
Area Z-stilbene/Area ISTD	0.24	0.57	0.83	1.18
Bibenzyl				
Concentration (mg/ml)	1.0	1.4	1.8	-
Amount Bibenzyl/Amount ISTD	0.47	0.74	0.93	-
Area Bibenzyl/Area ISTD	0.49	0.78	0.98	-
ISTD				
Concentration (mg/ml)	2.0	1.9	2.0	2.0

4.3.1.2 Extraction efficiency of the probe molecules

When methanol extraction is performed, a large excess of methanol is used. The reason for this is that the probe molecules and their reaction products will partition between the methanol and asphaltenes phases following liquid-liquid equilibrium. The liquid-liquid equilibrium determines the concentration in each phase, whereas the amount of each phase determines the total amount of material that will be present in each phase. Thus, even if the partition coefficient is poor, when a large excess (>100:1) methanol to asphaltenes is employed, the amount of material that can be extracted is sufficient for analysis.

Control Experiments were performed for adequate quantification of probe molecules. From Figure 4.2, it is evident that the extraction of almost all of probe molecules increases with an increase in the amount of DHA and with a decrease in asphaltene concentration in the mixture.

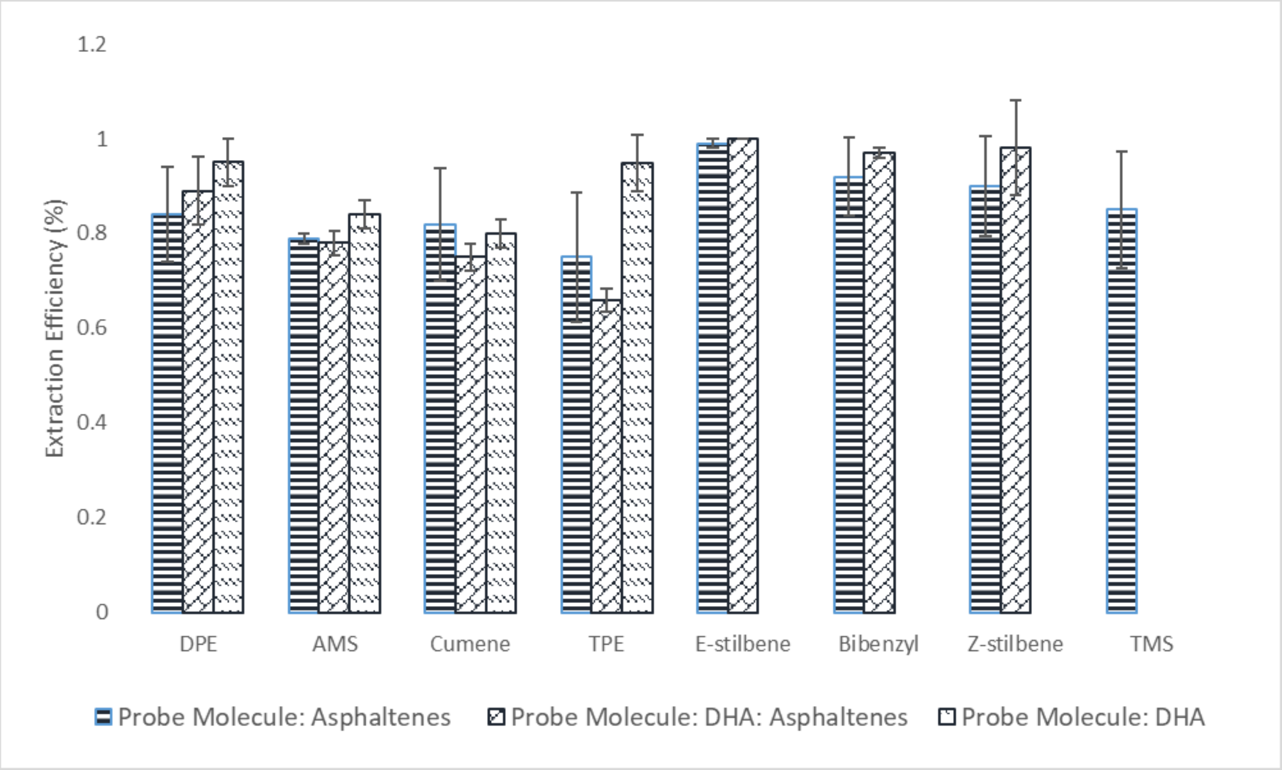

Figure 4. 2. Extraction efficiencies of probe molecules in methanol obtained by GC-FID

Some of the compounds, such as E-stilbene, bibenzyl, TMS were available in limited amount, therefore it was not possible to analyze their extraction efficiencies in all three cases. The quantification was performed based on the data available. The highest standard deviation is observed during TPE: asphaltenes (1:1 wt/wt) extraction. Moreover, TPE probe molecule was the species that was extracted in the lowest amount.

4.3.2 Hydrogenation of the probe molecules

As was explained before, catalytic hydrogenation of some compounds was performed to produce their hydrogenated analogue to assist with identification in the reaction products from reactions with asphaltenes.

Despite the mild hydrogenation conditions, the olefinic products were quantitatively converted to their corresponding paraffinic analogues:

The chromatogram after hydrogenation of 1,1-diphenylethylene to 1,1-diphenylethane is shown in Figure 4.3 and electron impact mass spectrum of 1,1-diphenylethane obtained after the reaction is shown in Figure 4.4.

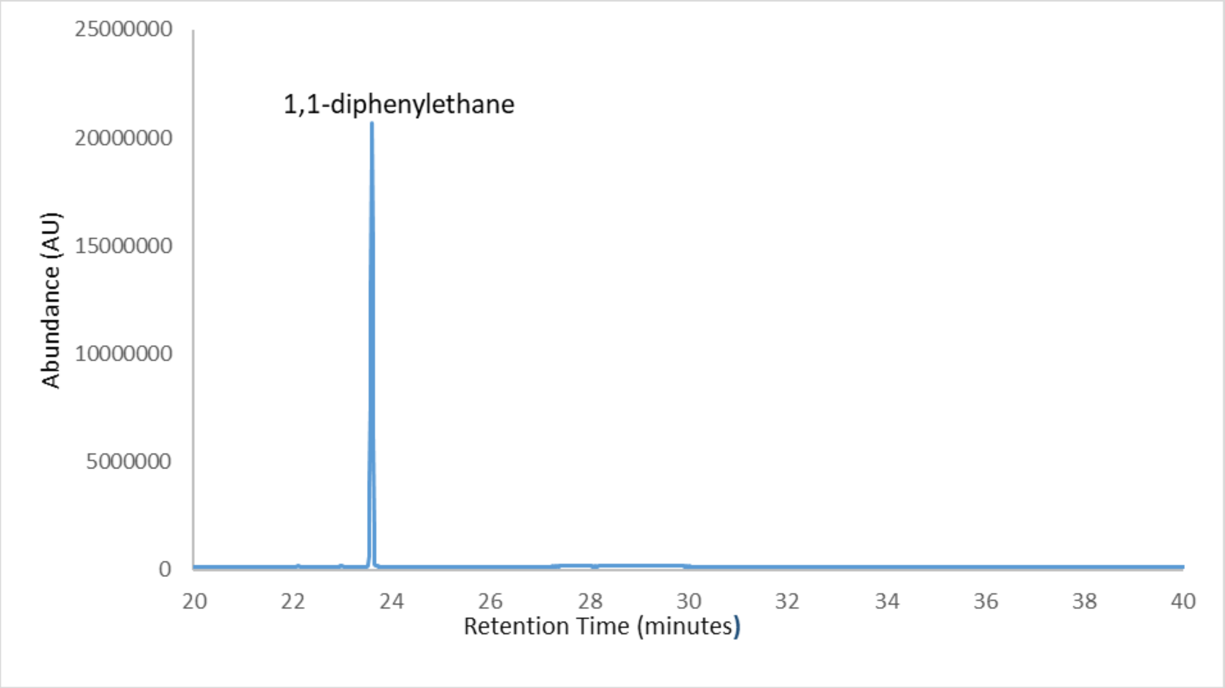

Figure 4. 3. GC-MS chromatogram of 1,1-diphenylethane

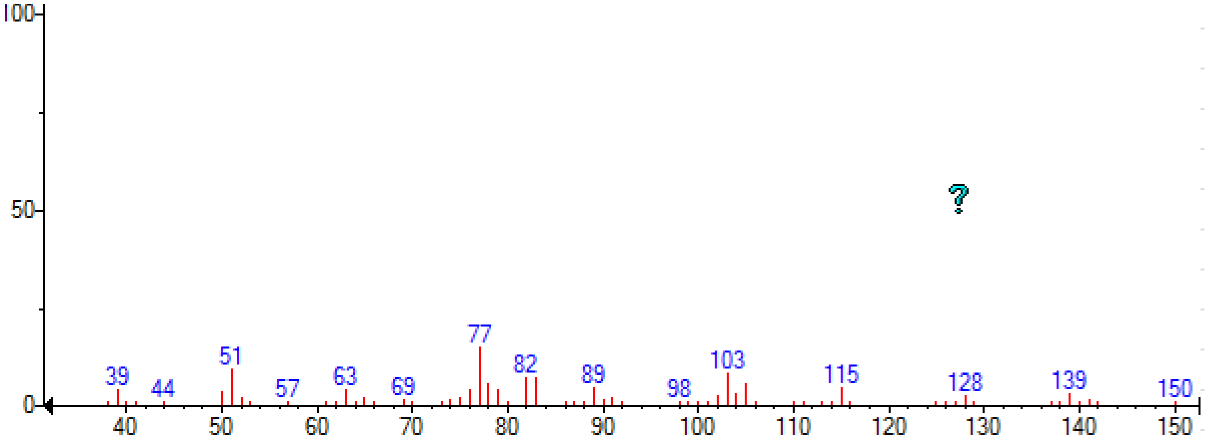

Figure 4. 4. Mass ionization spectrum of 1,1-diphenylethane formed as the result of 1,1-diphenylethylene hydrogenation

The chromatogram after hydrogenation of 2,4,6-trimethylstyene to 1-ethyl-2,4,6-trimethylbenzene is shown in Figure 4.5 and electron impact mass spectrum of 1-ethyl-2,4,6-trimethylbenzene obtained after the reaction is shown in Figure 4.6.

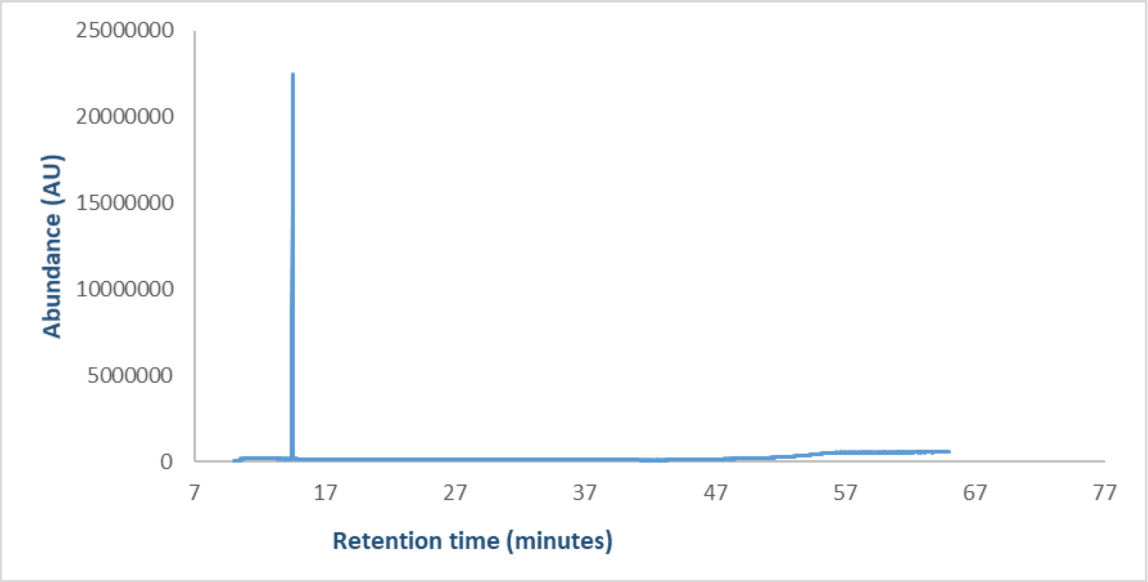

Figure 4. 5. Chromatogram of 1-ethyl-2,4,6-trimethylbenzene

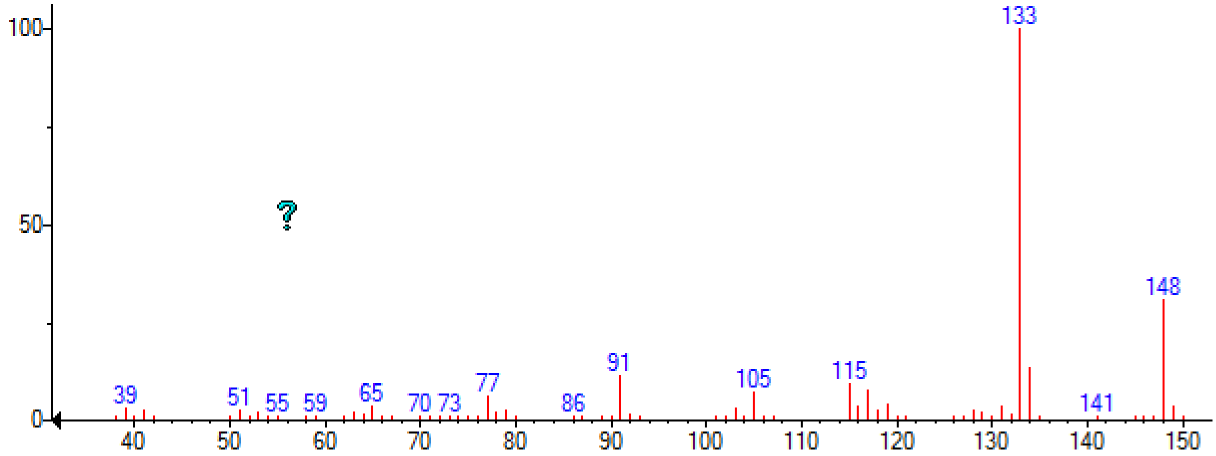

Figure 4. 6. Mass ionization spectrum of 1-ethyl-2,4,6-trimethylbenzene formed as the result of 2,4,6-trimethylstyrene hydrogenation

Based on the mass ionization spectrum in Figure 4.6, the NIST database suggested a match to an analogous compound but with a different configuration of methyl groups. It is difficult to distinguish isomers based on their mass spectra. It appeared unlikely that methyl migration would take place during hydrogenation at room temperature. However, it could not be confirmed due to the absence of an authentic model compound (which was the reason for performing the hydrogenation in the first place).

4.3.3 Reactions of asphaltenes with probe molecules

For each of the probe molecules, three types of experiments were performed. Since it was only the probe molecule that varied, it is useful to discuss the types of experiments first, before presenting the results.

(a) Experiments with a 1:1 mixture of probe molecules and asphaltenes evaluated the ability of the asphaltenes to transfer hydrogen to the probe molecule. All of the probe molecules were hydrogen acceptors. It was speculated that at least some of the persistent free radicals in the asphaltenes were radicals of the type –(HC•)–(CH_2)– that formed part of a larger structure providing resonance or other types of stabilization that discussed in Chapter 2. Such a free radical would be able to transfer hydrogen to the probe molecule, with itself being converted to an olefin –(HC)=(CH)– in the process. Depending on the steric requirements for this reaction, probe molecules with an olefinic group that are easily accessible would be converted to a larger extent than a probe molecule where the olefinic group is less accessible. Hydrogenation is of course not the only possible reaction and the probe molecule can also form an addition product, which is a chain propagation reaction. For this reason, the disappearance of the probe molecule, irrespective of the type of reaction was monitored, as well as conversion to the hydrogenated product.

(b) Experiments with a 1:1 mixture of probe molecule and 9,10-dihydroantracene (DHA) evaluated the ability of the probe molecule to be hydrogenated by a hydrogen donor. It also served as a control reaction, because neither of the reagents contained free radicals. Although the transfer of hydrogen was in principle possible, it required molecule induced homolysis as an initiation step. Thus, when a meaningful conversion of the probe molecule with DHA was observed, the probe molecule was not selective. Differently put, when the probe molecule could be hydrogenated through initiation by molecule induced homolysis, it would be capable of reaction with hydrogen donor groups in asphaltenes that were not associated with persistent free radical species. Conversely, if no or negligible reaction was observed between the probe molecule and DHA, then the probe molecule was very selective.

(c) Experiments with a 2:1:1 mixture of probe molecule, 9,10-dihydroantracene and asphaltenes, provided a ready source of hydrogen transfer to the probe molecule to hydrogenate it after its first hydrogen transfer reaction with the asphaltenes. It also provided a competitive reaction pathway, since free radicals of the type –(HC•)–(CH_2)– can also be hydrogenated by hydrogen transfer from DHA. Overall the reaction system was more complex, but because the literature on DHA is more abundant, the competitive reaction of the probe molecule with DHA provided some comparative information about relative reactivity with DHA as a constant reference.

The results for the reactions with 1,1-diphenylethylene (DPE) as probe molecule are presented in Table 4.9.

The conversion of DPE was calculated from the amount of DPE in the extracted product, after correcting for the extraction efficiency and making use of the appropriate response factor. Due to the different possible reactions, including reactions that would cause DPE to form addition products that could not be extracted in methanol and that had unknown response factors, the conversion was employed in combination with the quantification of the hydrogenated product of the probe molecule to calculate (estimate) the mass of the probe molecule that were present as "unrecovered" product. Quantification of the addition products; unrecovered compounds, were based on the parent reactant probe molecule, due to the absence of samples for calibration. These comments are applicable to all of the results.

Table 4. 9. Product quantification of DPE reactions with asphaltenes and DHA in methanol extract at reaction conditions (250 °C, 4 MPa). Feed ratios are given on weight basis.

Experiments	Initial input of DPE (mg/ml)		1,1-diphenylethane (mg/ml)		Unrecovered products (mg/ml)		Conversion	
	x	s	x	s	x	s	x	s
DPE: asphaltenes 1:1 ratio (Exp. 1)	5.09	0.05	0.369	0.016	3.628	0.373	0.75	0.013
DPE: DHA: asphaltenes 2:1:1 ratio (Exp. 2)	5.06	0.01	2.391	0.05	0.525	0.144	0.576	0.02
DPE: DHA 1:1 ratio (Exp. 3)	5.03	0.04	4.548	0.073	0.28	0.096	0.961	0

As seen from Table 4.9, the amount of 1,1-diphenylethane increased with the addition of donor compound. Since the control reaction (Experiment 3) with DPE and DHA resulted in a high conversion of the DPE, DPE was not a selective probe molecule. The conversion of DPE with asphaltenes would therefore not be indicative of reactions only with persistent free radicals.

The results for the reactions with E-stilbene (ES) as probe molecule are presented in Table 4.10

Table 4. 10. Product quantification of E-stilbene reactions with asphaltenes and DHA in methanol extract at reaction conditions (250 °C, 4 MPa). Feed ratios are given on weight basis.

Experiments	Input E-stilbene (mg/ml)		Bibenzyl (mg/ml)		Unrecovered product (mg/ml)		Conversion	
	x	s	x	s	x	s	x	s
ES: asphaltenes 1:1 ratio (Exp. 4)	5.02	0.02	0.084	0.001	2.115	0.009	0.452	0.003
ES: DHA: asphaltenes 2:1:1 ratio (Exp. 5)	5.06	0.01	0.513	0.053	0.276	0.391	0.169	0.065
ES: DHA 1:1 ratio (Exp. 6)	5.05	0.01	No hydrogen transfer was observed [a]					

[a]-No hydrogen transfer was observed, or the peak was too small to be integrated by GC-FID

According to Table 4.10, no hydrogen transfer was observed during the control experiment with ES and DHA (Experiment 6). This meant that ES was a selective probe molecule for interaction with free radicals in asphaltenes. With addition of DHA compound (Experiment 5) the amount of bibenzyl formation was increased compared to bibenzyl formation during Experiment 4. Moreover, with addition of donor compound decrease in the unrecovered product is observed.

The results for the reactions with triphenylethylene (TPE), as probe molecule are presented in Table 4.11.

Table 4. 11. Product quantification of TPE reactions with asphaltenes and DHA in methanol extract at reaction conditions (250 °C, 4 MPa). Feed ratios are given on weight basis.

Experiments	Input TPE (mg/ml)		1,1,2-triphenylethane (mg/ml)		Unrecovered product (mg/ml)		Conversion	
	x	s	x	s	x	s	x	s
TPE: DHA: asphaltenes 2:1:1 ratio (Exp. 8)	5.02	0.05	0.03	0.01	0.32	0.17	0.07	0.03
TPE: asphaltenes 1:1 ratio (Exp. 7)	5.04	0.02	No hydrogen transfer observed [a]					
TPE: DHA 1:1 ratio (Exp. 9)	5.04	0.01	No hydrogen transfer observed [a]					

[a]-The peaks of the product were too small to be integrated by GC-FID

As depicted in Table 4.11, during TPE:DHA (Experiment 9) and TPE:asphaltenes (Experiment 7) reactions the 1,1,2-triphenylethane was formed in unquantifiable amount. However, during TPE: DHA: asphaltenes (Experiment 8) reaction the mass concentration of 1,1,2-triphenylethane was above 0.03±0.01 (mg/ml).

This was an interesting observation, because it showed that TPE was a selective probe molecule, but it was incapable of reacting with any of the free radicals in asphaltenes. However, when a hydrogen donor was added, the transfer of hydrogen from DHA created new reaction possibilities that resulted in some reaction. Only some of the reaction of TPE can be explained in terms of partially dehydrogenated DHA.

Experiments 10-12, the reactions with α-methylstyrene, are experiments that offered more opportunities for product identification. The results for the reactions with α-methylstyrene (AMS) as probe molecule are presented in Table 4.12.

The control experiment (Experiment 12) indicated that AMS was not a selective probe molecule. The AMS was very reactive and even in the presence of DHA, which is a hydrogen donor, it was prone to form products other than cumene, which is the hydrogenated product.

Nevertheless, it was interesting to see how the asphaltenes and asphaltenes in combination with DHA modified the product selectivity from the reaction with AMS. The results of the more detailed analysis of the reaction products are presented in Figure 4.7 and Table 4.12, Table 4.13, Table 4.14. The quantification of products in Tables 4.12 and 4.13 can be considered semi-quantitative, as product A-5 was not considered during the quantification of the compounds. Quantification of DHA and anthracene was not performed. See the following figures for further information.

Table 4. 12. Product quantification of AMS reactions with asphaltenes and DHA in methanol extract at reaction conditions (250 °C, 4 MPa). Feed ratios are given on weight basis.

Experiments	Initial input Of AMS (mg/ml)		Cumene (mg/ml)		Unrecovered products (mg/ml)		Conversion	
	x	s	x	s	x	s	x	s
AMS: asphaltenes 1:1 ratio (Exp. 10)	5.06	0.10	0.232	0.092	2.977	0.338	0.7	0.04
AMS: DHA: asphaltenes 2:1:1 ratio (Exp. 11)	5.07	0.04	0.763	0.011	2.145	0.011	0.7	0
AMS: DHA 1:1 ratio (Exp. 12)	5.03	0.04	0.309	0.039	0.833	0.312	0.3	0.05

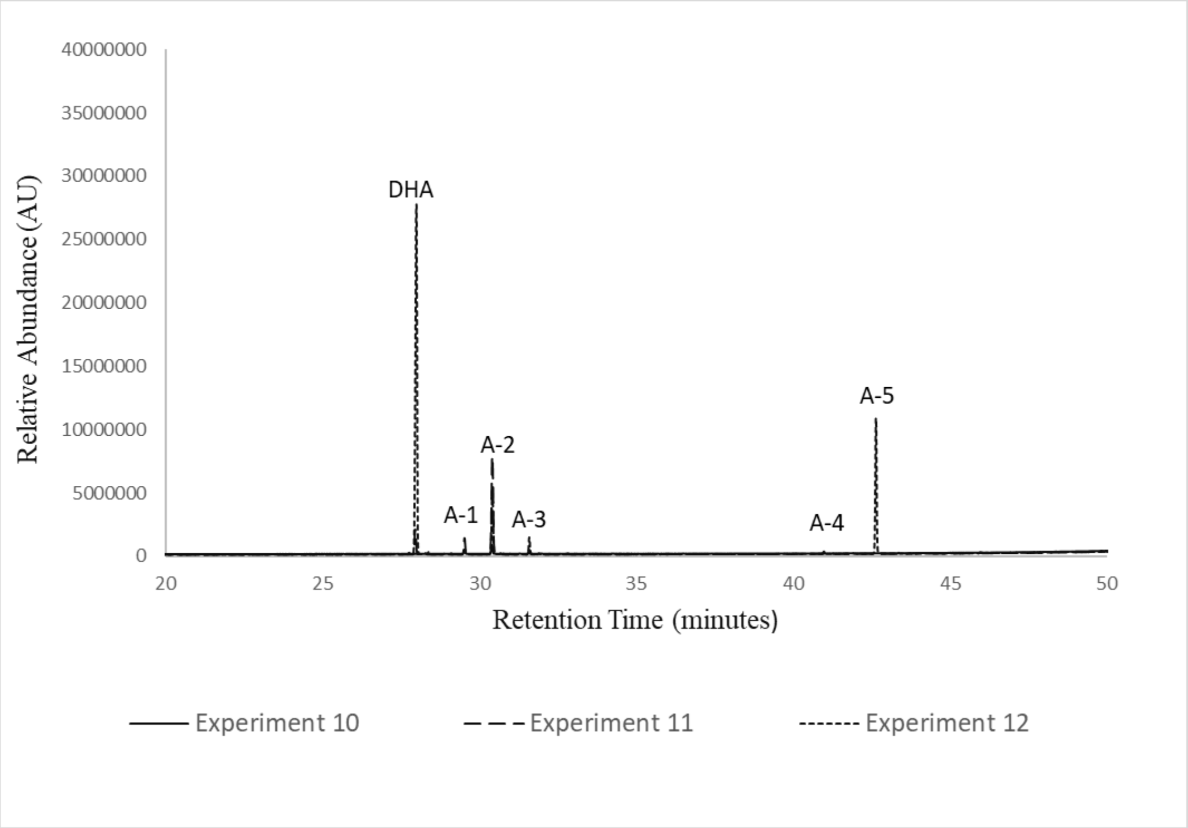

Figure 4. 7. Addition products formed during AMS reactions with asphaltenes and DHA at 250 °C, 4MPa N_2 pressure. Note: At retention time of 30.5 minutes compound A-2 overlaps with anthracene. Ratios are based on mass.

Table 4. 13. Product selectivity, conversion and recovery of AMS reactions with asphaltenes and DHA

Compound name	Selectivity of product (mole based)		Selectivity unrecovered (mole based)		Byproduct selectivity (mole based)	
	x	s	x	s	x	s
A-Methylstyrene			0.85	0.079		
Cumene	0.066	0.028				
(2,3-Dimethylbutane-2,3-diyl)dibenzene					0.062	0.08
(4-methylpent-1-ene-2,4-diyl)dibenzene					0.142	0.18
Hex-1-ene-2,5-diyldibenzene					0.009	0
Experiment 11						
A-Methylstyrene			0.63	0.006		
Cumene	0.222	0.002				
(2,3-Dimethylbutane-2,3-diyl)dibenzene					0.031	0
(4-methylpent-1-ene-2,4-diyl)dibenzene					0.014	0
Hex-1-ene-2,5-diyldibenzene					0.012	0
1,2-diphenylethyne					0.019	0
Experiment 12						
A-Methylstyrene			0.53	0.118		
Cumene	0.205	0.058				
(2,3-Dimethylbutane-2,3-diyl)dibenzene					0.046	0.01
(4-methylpent-1-ene-2,4-diyl)dibenzene					0.015	0
Hex-1-ene-2,5-diyldibenzene					0.151	0.03
1,2-diphenylethyne					0.050	0.01
9-(1-phenylethyl)-9,10-dihydroanthracene					-	

Addition products obtained as a result of reactions involving AMS as probe molecule were observed. As was pointed out already, such reactions took place even in the presence of DHA as hydrogen donor. The addition products A-1 to A-5 in Figures 4.7, were analyzed by GC-MS in an attempt to identify the nature of the addition products. Although mass spectrometry is not useful for the identification of individual isomers, the suggested compounds presented in Table 4.14 provided some indication of the likely compounds to be found.

Table 4. 14. Representation of the products obtained after reactions of Experiment 10; 11; 12 at 250 °C, 4 MPa (N_2) pressure as suggested by NIST database obtained by GC-MS

Heavy Product Name	Symbol	Formula	Retention Time (Minutes)	CASRN	Representation
(2,3-Dimethylbutane-2,3-diyl)dibenzene	A-1	$C_{18}H_{22}$	27.526	1889-67-4	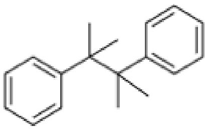
(4-methylpent-1-ene-2,4-diyl)dibenzene	A-2	$C_{18}H_{20}$	28.456	6362-80-7	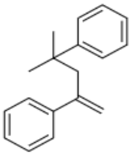
hex-1-ene-2,5-diyldibenzene	A-3	$C_{18}H_{20}$	29.59	32375-29-4	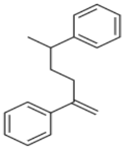
1,2-diphenylethyne	A-4	$C_{14}H_{10}$	38.959	501-65-5	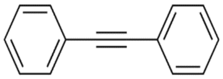
9-(1-phenylethyl)-9,10-dihydroanthracene	A-5	$C_{22}H_{20}$	40.491	95166-74-8	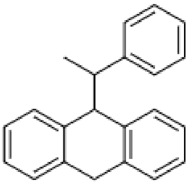

It was possible to observe heavy compound 9-(1-phenylethyl)-9,10-dihydroanthracene as a result of addition reaction between cumene and DHA molecules in the current study. Suggestions by NIST database were employed to describe the addition products and heavy compounds, as it was not possible to confirm them using probe molecules.

For Experiment 10, addition products (2,3-Dimethylbutane-2,3-diyl)dibenzene; (4-methylpent-1-ene-2,4-diyl)dibenzene; hex-1-ene-2,5-diyldibenzene were formed;

For Experiment 11, addition products (2,3-Dimethylbutane-2,3-diyl)dibenzene; (4-methylpent-1-ene-2,4-diyl)dibenzene; hex-1-ene-2,5-diyldibenzene; 1,2-diphenylethyne were formed;

In case of the Experiment 12, addition products such as (2,3-Dimethylbutane-2,3-diyl)dibenzene; (4-methylpent-1-ene-2,4-diyl)dibenzene; hex-1-ene-2,5-diyldibenzene; 1,2-diphenylethyne ; 9-(1-phenylethyl)-9,10-dihydroanthracene were formed.

Experiments 13-15, the reactions with 2,4,6-trimethylstyrene, were also experiments that offered more opportunities for product identification. The results for the reactions with 2,4,6-trimethylstyrene (TMS) as probe molecule are presented in Table 4.15.

Table 4. 15. Product quantification of TMS reactions with asphaltenes and DHA in methanol extract at reaction conditions (250 °C, 4 MPa). Feed ratios are given on weight basis.

Experiments	Initial input Of TMS (mg/ml)		Obtained TMS hydrogenation product (mg/ml)		Unrecovered products (mg/ml)		Conversion	
	x	s	x	s	x	s	x	s
TMS: asphaltenes 1:1 ratio (Exp. 13)	5.09	0.02	0.105	0.057	1.552	1.191	0.337	0.208
TMS: DHA: asphaltenes 2:1:1 ratio (Exp. 14)	4.93	0.03	0.437	0.109	1.025	0.841	0.35	0.151
TMS: DHA 1:1 ratio(Exp. 15)	5.00	0.14	No hydrogen transfer was observed[a]					

[a]-The peaks of the product were too small to be integrated by GC-FID

According to Table 4.15, the TMS molecule could not abstract hydrogen from the DHA (Experiment 15), which made TMS a selective probe molecule. The TMS was capable of reacting with the asphaltenes. With addition of DHA, the amount of the formation of main hydrogenated product increased (Experiment 14) and the formation of unrecovered compounds decreased.

The results of the more detailed analysis of the reaction products are presented in Figure 4.8 and Table 4.16. The quantification of products in Table 4.16 can be considered semi-quantitative, because response factors were not available for all of the products.

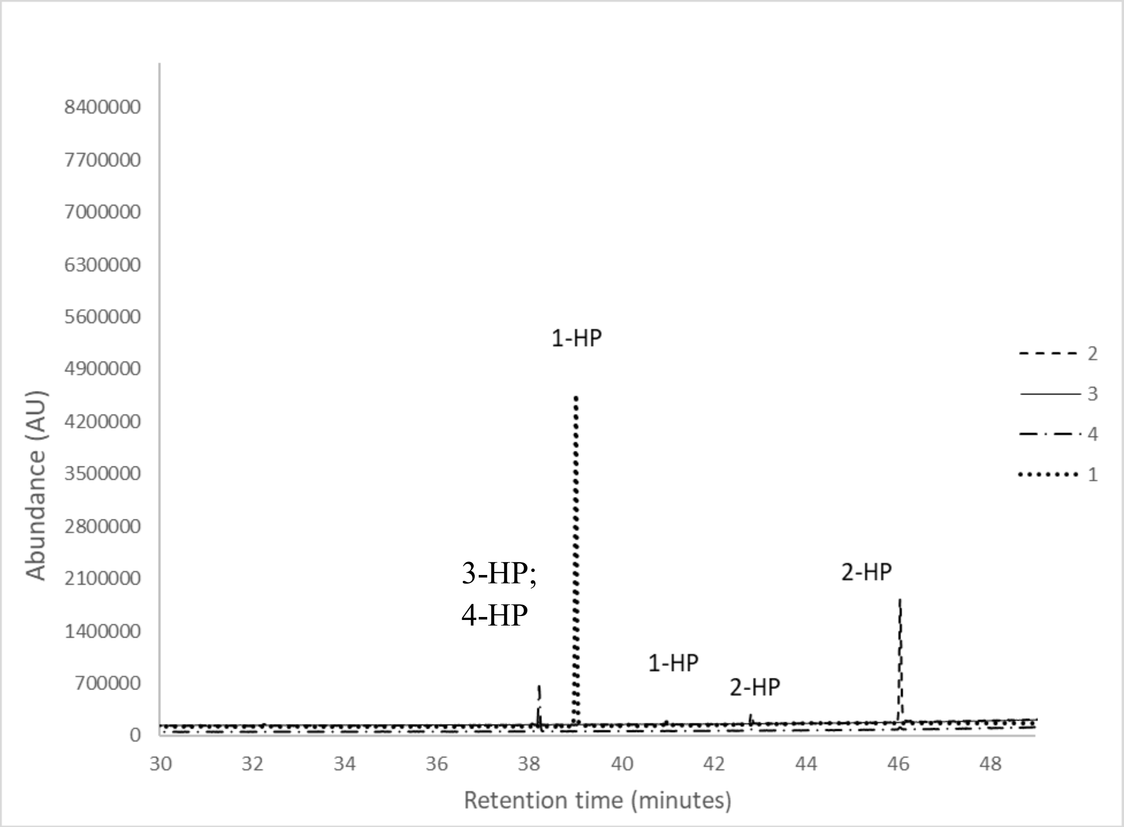

Figure 4. 8. Heavy products formed during TMS reactions with asphaltenes and DHA at 250 °C, 4 MPa N_2 pressure

Table 4. 16. Product selectivity, conversion and recovery of TMS reactions with asphaltenes and DHA

Experiment 13						
Compound name	Selectivity of product (mole based)		Selectivity unrecovered[a] (mole based)		Byproduct selectivity (mole based)	
	x	s	x	s	x	s
2,4,6-trimethylstyrene			0.9	0.2		
2-ethyl-1,3,5-trimethylbenzene	0.852	0.17				
Heavy products[a]					0.1	0.1
Experiment 14						
2,4,6-trimethylstyrene			0.5	0.3		
2-ethyl-1,3,5-trimethylbenzene	0.293	0.18				
Heavy products[a]					0.2	0.1

[a]- Heavy and unrecovered products were quantified based on TMS calibration.

Some additional observations from the results presented in Figure 4.8 to clarify what each of the peaks in the chromatogram represents:

1) 1-HP= TMS conversion products (1-HP-heavy products)
2) 2-HP =products obtained after Experiment 15 (2-HP-heavy products)
3) 3-HP= products obtained after Experiment 13 (3-HP-heavy products)
4) 4-HP =product obtained after Experiment 14 (4-HP-heavy products)

TMS was forming heavier compounds than the 9-(1-phenylethyl)-9,10-dihydroanthracene (suggested by NIST library using the GC-MS) that was eluting at 42.6 minutes using the same method and parameters during reaction with DHA.

From Figure 4.8, it can be seen that as a result of TMS conversion, 1-HP-heavy products were formed, where experiment was performed once. During Experiment 15, 2-HP-heavy products were formed as a result of polymerisation. After Experiment 13, 3-HP-heavy products were formed. In the case of Experiment 14, 4-HP-heavy products were formed. It was difficult to identify the compounds using GC-MS, however it was possible to observe the trend of heavy compounds formation.

The results for the reactions with 1,1,2,2-tetraphenylethylene (1,1,2,2-TPE) as probe molecule are presented in Table 4.17.

Table 4. 17. Product quantification of 1,1,2,2-tetraphenylethylene reactions with asphaltenes in methanol extract at reaction conditions (250 °C, 4MPa). Feed ratios are given on weight basis.

Experiments	Initial input Of 1,1,2,2-TPE (mg/ml)		Cumene (mg/ml)	Unrecovered products (mg/ml)	Conversion
	x	s			
1,1,2,2-TPE: asphaltenes 1:1 ratio (Exp. 16)	5.03	0.01	No hydrogen transfer was observed		

No reaction was observed in the experiments with 1,1,2,2-tetraphenylethylene and asphaltenes and therefore no further experiments were conducted.

4.3.4 Simulated distillation of reaction products

To obtain an indication of heavier product formation, the reaction products, simulated distillation was performed on the reaction products. Simulated distillation makes use of high temperature gas chromatography to approximate the distillation profile of oil samples. The simulated distillation profiles are shown in Figure 4.9.

The data shown in Figure 4.9 was repeated in Figure 4.10, but with points shown to indicate the boiling point of different compounds that were identified in the reaction products. The normal boiling points of those compounds that were obtained from literature are listed in Table 4.18 with the source references mentioned below the table.

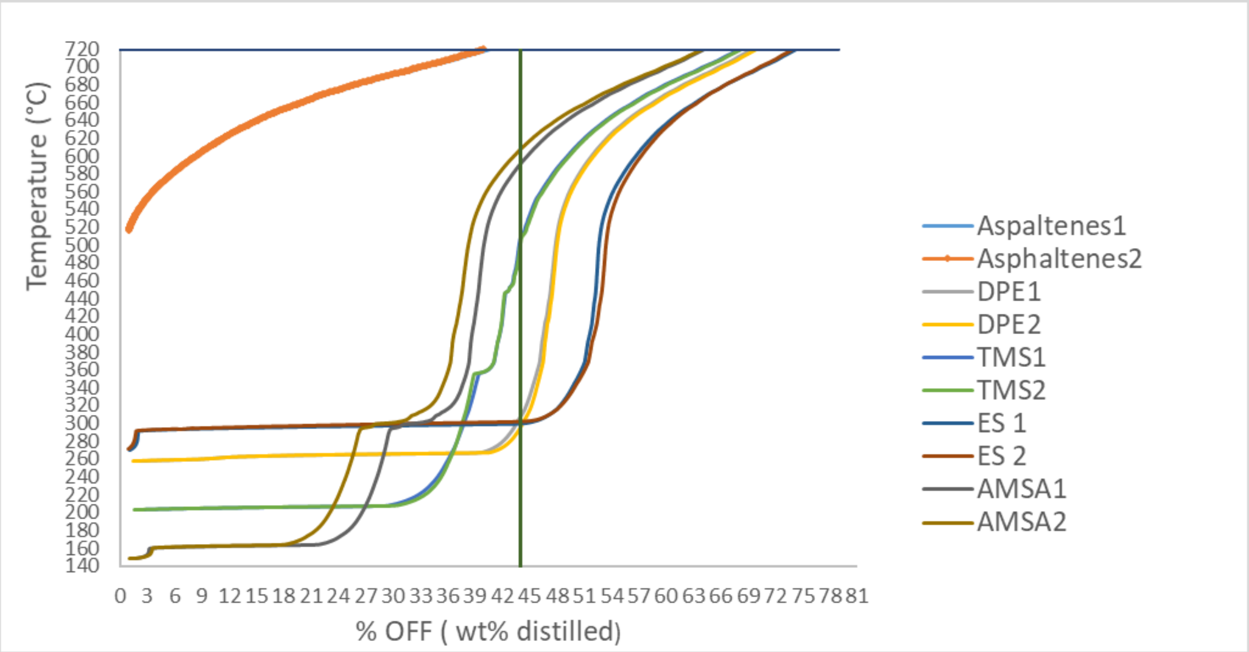

Figure 4. 9. Boiling curves obtained by simulated distillation for reactions of probe molecule with asphaltenes in 1:1 mixture. All analyses were performed in duplicate. The abbreviations used to identify the reactions: Asphaltenes - Asphaltenes converion ; DPE - Experiment 1; ES – Experiment 4; AMS - Experiment 10; TMS -Experiment 13 . Note: the number in front of each symbol stands for the indication of Experiment number.

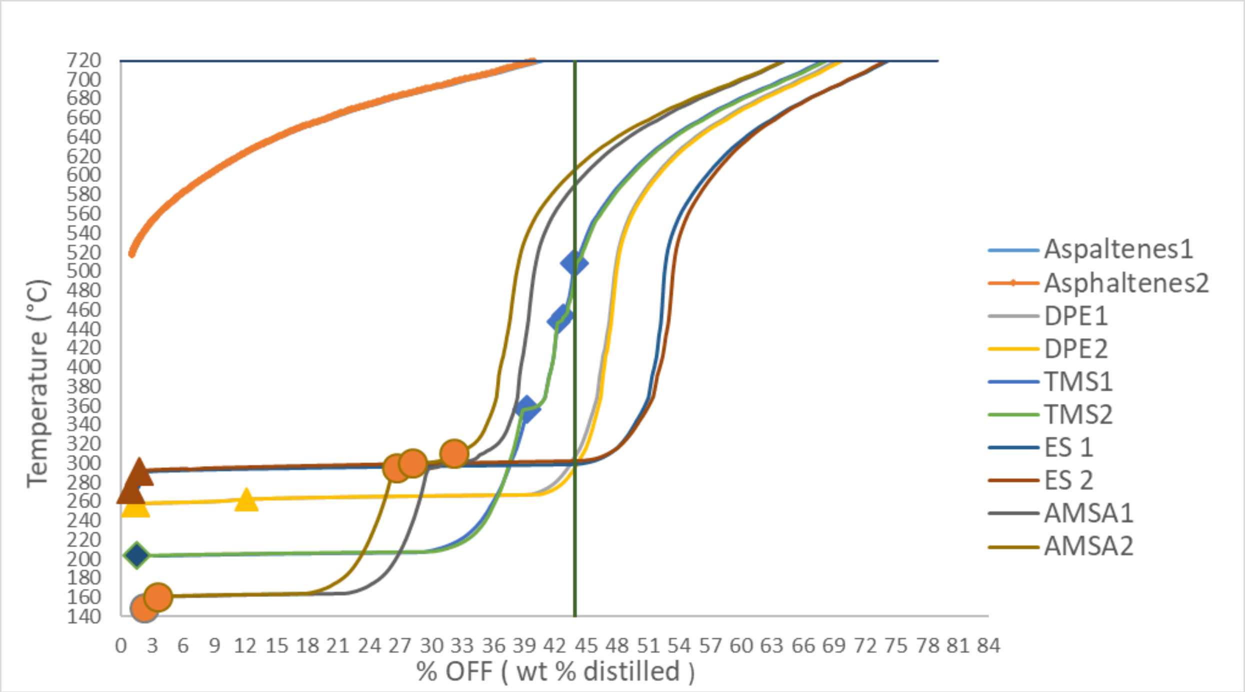

Figure 4. 10. Same simulated distillation results as shown in Figure 4.9, but with the normal boiling points of compounds identified in the products indicated.

Table 4. 18. Approximate boiling points of the product compounds obtained in the reaction of the probe molecule with asphaltenes from literature

Name of the compound	Normal boiling point (°C)
1,1-diphenylethylene	277[a]
1,1-diphenylethane	272.63[b]
E-stilbene	305-307[c]
Z-stilbene	307[d]
Bibenzyl	283[e]
2,4,6-trimethylstyrene	209[h]
1-isopropyl-2,4,6-trimethylbenzene	223[i]
α-Methylstyrene	161[j]
cumene	152.4[k]
2,3-Dimethylbutane-2,3-diyl)dibenzene	306[l]
2,4-diphenyl-4-methyl-pent-1-ene)	329[m]
hex-1-ene-2,5-diyldibenzene	346[n]

a,b- Serijan, K.T. and Wise, P.H., 1951. Dicyclic hydrocarbons. iii. diphenyl-and dicyclohexylalkanes through C15. *Journal of the American Chemical Society*, *73*(10), pp.4766-4769.

c- Laane, J., Haller, K., Sakurai, S., Morris, K., Autrey, D., Arp, Z., Chiang, W.Y. and Combs, A., 2003. Raman spectroscopy of vapors at elevated temperatures. *Journal of molecular structure*, *650*(1-3), pp.57-68; Bramwell, P.L., Gao, J., de Waal, B., de Jong, K.P., Gebbink, R.J.K. and de Jongh, P.E., 2016. A transition-metal-free hydrogenation catalyst: Pore-confined sodium alanate for the hydrogenation of alkynes and alkenes. *Journal of catalysis*, *344*, pp.129-135.

d- González, M., Toropov, A., Duchowicz, P. and Castro, E., 2004. QSPR calculation of normal boiling points of organic molecules based on the use of correlation weighting of atomic orbitals with extended connectivity of zero-and first-order graphs of atomic orbitals. *Molecules*, *9*(12), pp.1019-1033.

e- Kendler, S., Lambertus, G.R., Dunietz, B.D., Coy, S.L., Nazarov, E.G., Miller, R.A. and Sacks, R.D., 2007. Fragmentation pathways and mechanisms of aromatic compounds in atmospheric pressure studied by GC–DMS and DMS–MS. *International Journal of Mass Spectrometry*, *263*(2-3), pp.137-147.

i,l,m,n,- Scifinder.cas.org. (2019). *Experimental properties*. (online) Available at: https://scifinder.cas.org/scifinder/view/scifinder/scifinderExplore.jsf (Accessed 7 Aug. 2019).

h- Buck, F.R., Coles, K.F., Kennedy, G.T. and Morton, F., 1949. 502. Some nuclear-methylated styrenes and related compounds. Part I. *Journal of the Chemical Society (Resumed)*, pp.2377-2383.

j- Corbett, G.E. and Williams, G.H., 1966. Reactions of alkyl radicals. Part II. Reactions of alkylbenzenes with methyl radicals. Photolytic formation and reactions of ethyl and n-butyl radicals. *Journal of the Chemical Society B: Physical Organic*, pp.877-880.

k- Forziati, A.F. and Rossini, F.D., 1949. Physical properties of sixty API-NBS hydrocarbons. *J. Res. Natl. Bur. Stand*, *43*, pp.473-476.

As seen from Figures 4.9 and 4.10 showing the simulated distillation results, products of asphaltenes conversion at 250 °C, 4 MPa N_2 pressure are eluting at temperatures above 500 °C. Two peaks were observed as the products of ES: asphaltenes and DPE: asphaltenes reactions. In case of AMS: asphaltenes. five peaks were observed, which corresponds to the boiling points of AMS, cumene and addition products A-1, A-2, A-3. As seen from the boiling curves of the asphaltene: TMS reaction mixture heavy compounds formation is observed, which were not detectable using GC-MS, due to high-boiling point of the heavy compounds.

4.4 Discussion

4.4.1. Extraction of probe molecules

One of the challenging aspects of the work, is the extraction of the lighter reaction products from the mixtures after reaction to evaluate conversion. Although care was taken to determine the extraction efficiency (Figure 4.2), some variation was found in the results.

Since sampling takes place after the mixing stops and the settling starts, the taken samples may not exactly represent the mixture environment because settling of the molecules highly depend on the density of the molecules and the later the sampling occurs the lighter compounds are retrieved. Nevertheless, since the same exact procedure was followed for all the measurements, the obtained results were comparable.

In addition, another reason for the discrepancy of the results could be that the asphaltenes are insoluble in methanol, they are likely to trap probe molecules within the bulk and cause a reduced extraction. Under the same operating conditions, the solubility depends on the polarity index and saturation point, which depends on the chemical nature of the substances involved. Molecular size (contact between solute and solvent) affects the solubility of the substance. Moreover, as observed in the Figure 4.2, TPE extraction efficiency is lower compared to other compounds. Which could be due to its complex geometry (discussed in the Section 4.4.3) and solid nature.

Moreover, the accuracy level of the pipette was ±0.4 µl, which could lead to the deviations in the calculations.

4.4.2. Hydrogenation of DPE, TMS

High yield was achieved in the hydrogenation of DPE and TMS, at the value of 98%±1. The corresponding amount of ISTD was added to each mixture and was quantified by correlation of the area corresponding to the mass. These molecules experienced little steric resistance to the hydrogenation, although the hydrogenation experiments were not designed specifically to evaluate this aspect.

4.4.3 Reaction of probe molecules with asphaltenes and DHA compound

Thermodynamic data for hydrogen transfer reactions at 300 °C of some of the compounds studied was found in the work of Rüchardt et al. (1997) and is shown in Table 4.19. In addition to the thermodynamic data, some rate constants for the rate of hydrogen transfer compared to α-methylstyrene are shown. In these reported reactions, 9,10-dihydroanthracene (DHA) was the hydrogen donor.

Table 4. 19. Reaction parameters for the hydrogen acceptor compounds and DHA reactions at 300 °C, provided by Rüchardt et al. (1997)

Hydrogen acceptor	Name	$\Delta G^{\ddagger}$ $(kcal.mole^{-1})$	$\Delta H^{\ddagger}$ $(kcal.mole^{-1})$	$\frac{k}{k_{ams}}$
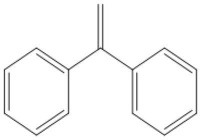	1,1-diphenylethylene	43.1±0.2	32.3±0.2	2.7
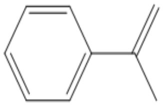	α-Methylstyrene	44.1±1.2	31.8±1.2	1
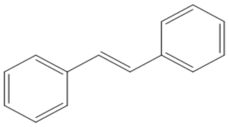	E-stilbene	47.6±0.1	37.6±0.1	0.045
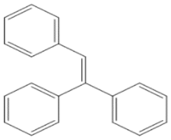	Triphenylethylene	47.7±0.6	35.9±0.6	0.051

For the current study, pseudo-first order reactions assumption was considered. According to Bernasconi (1986), for a reaction to be considered the pseudo-first order reaction the ratio of the reactants can be as little as 10:1, depending on the reaction. As molecular weight of asphaltenes is very high, its concentration in the solution is significantly lower than the concentration of the other compounds involved in the reaction, thus, pseudo-first order reactions assumption is reasonable.

If the assumption is made that all the parameters remain the same throughout the reactions, then from Table 4.19, it is evident that the rate of reaction for triphenylethylene is greater than the rate of reaction for E-stilbene. Therefore, the formation of the product (1,1,2-triphenylethane) in Experiment 7 should be greater than the formation of the product (bibenzyl) in Experiment 4. However, as seen from Tables 4.10 and 4.11, during Experiment 4 bibenzyl was formed in

0.084±0.001 mg/ml extent, but no product formation was observed during Experiment 7 which could be due to the steric requirements of asphaltenes, as TPE has more complex geometry than ES, as will be discussed later in Section 4.4.3.
No reactions were observed for 1,1,2,2-Tetraphenylethylene: asphaltenes mixtures, as seen in Table 4.17. Generally, activation energy increases as the steric requirements of the substituent of molecule increases, and the rate decrease at the same conditions (Brown, 1956). Thus, it could be interpreted in the following way: if the concentration of the saturated product decreases with the increase in asphaltenes concentration, it is attributed to the complex nature of the structure and high steric hindrance in the asphaltene molecules.

It was shown by Mathai (1960) that steric requirements of the TPE plays an important role in bromination. According to Mathai (1960), due to the lower stabilization energy of TPE compared to ES, TPE is more likely to react with the same common reactant at the given conditions at a higher rate. Moreover, E-stilbene have the tendency of isomerization at high temperatures which was observed in the current study. The difference between E-stilbene and Z-stilbene is about 3 kcal.mole^{-1} (Suzuki,2012). It was found by Mathai (1960) that TPE is more reactive than ES. However, steric hindrance of TPE can impose some limitations because of the size and structure of the reactant compound. Such that the effect of steric hindrance by TPE and tetraphenylethylene resulting in a lower rate of catalytic activity compared to ES at the same conditions was mentioned by Zhang et al., 2014.

As seen from the Tables 4.10; 4.15, the hydrogen transfer occurred during E-stilbene reaction with asphaltenes (Experiment 4), TMS:asphaltenes reactions (Experiment 13), but did not occur between (or peaks were too small to be identified) ES:DHA or TMS:DHA (Experiments 6 and Experiment 15, accordingly). Which can mean that there are compounds with donor properties in asphaltene that have bond dissociation energy (BDE) of less than that of DHA (76.3 -79.9 kcal mol^{-1}) (Luo, 2007; Klein et al., 2016).

As seen from the results in Tables 4.13 and 4.16, the number of addition products increases with the decrease in the asphaltene content. In Table 4.13 it could be seen that even if the selectivity of cumene in Experiment 11 is greater than in Experiment 10, due to addition of DHA, however, it is also worth noting that in Experiment 12 the selectivity for cumene is less than in Experiment 11. That effect was observed by Naghizada (2017) and was ascribed to the steric factors in asphaltenes. It could be ascribed to the complex nature of asphaltenes and presence of steric hindrance in asphaltene molecules. As seen from the Figure 4.7, heavy compound A-5 is formed, as suggested by GC-MS, which could be the addition product of DHA and cumene radical, which was not observed during Experiment 11 or 12.

Asphaltenes might not be capable of accommodation such a complex compound as A-5, which consists of 3 fused rings and 1 ring as substituent. However, as was observed in chapter 3, during DHN: asphaltenes reaction dimer of 1,2,3,4-tetrahydronaphthalene was observed. It could be that asphaltenes are capable of accommodation of dimers consisting of 2 fused rings on each end, but not the compound as complex as A-5, which has 3 joint rings in a row.

As seen in the Figure 4.8 during reaction of TMS:DHA (Experiment 15) no hydrogen transfer occurred, however TMS polymerized and the heavy product was eluted at retention time of 46 minutes. However, during TMS conversion at 250 °C, 4MPa N_2 pressure, 1HP products were formed, no visible peak was formed at 46 minutes, which could be due to decrease in steric constraints of TMS with addition DHA compound.

According to Suzuki (2012), in triphenylethylene at least two of the aromatic rings are pointed out of the ethylenic bond plane. 1,1-diphenylethylene two aromatic rings are pointed out of the ethylenic bond plane. As in the case of E-stilbene the structure is considered to be planar or almost polar. The structure of DPE molecule is favorable for the hydrogen abstraction due to its geometry. As seen in Table 4.9 due to its nature and structure DPE appears to be an effective hydrogen acceptor without the formation of addition products at high temperatures. As shown in the Table 4.11 asphaltenes might contain compounds with smaller BDE than DHA and it is possible for TPE molecules to access them as mass transport limitations decrease with addition of solvent (DHA) which can be considered to play the role of the inert solvent in the given case.

The increase in the bibenzyl amount with addition of DHA in Table 4.10 could be due to the decrease of mass transport limitation and better accesability of asphaltenes molecules by E-stilbene with addition of DHA.

It was proved to be difficult to comment on the conversion of the products due to unrecovered products formation.

As seen from Figures 4.9 and 4.10, it is possible to observe the trend of formation of addition products in the reactions using the SimDis technique, based on the boiling point information of compounds. SimDis can give more information about heavy compounds than GC-MS as the latter technique is unable to detect the heavy compounds containing carbon number above C-16.

Recovery was above 97% for all the reactions, due to the depressurizing some of the compounds were spilled out of the vial which were not considered during the quantification of reaction products. The quantification was proven to be difficult, as in the case of addition products the peaks response factor in GC-MS and GC-FID were different. Also, the amount of the unrecovered products was difficult to evaluate.

4.5 Conclusion

- Extraction efficiency for all the compounds increased with the addition of the donor compound during control experiments which could be due to possible trapping by asphaltenes molecules
- DPE was found to be an effective hydrogen acceptor without formation of heavier compounds at the reaction conditions.
- In case of TMS and AMS reactions with asphaltenes and DHA, more heavy compounds' formation was observed with addition of DHA which was ascribed to steric requirements of asphaltenes
- In case of TPE reaction with asphaltenes and TPE reaction with DHA, no quantifiable amount of 1,1,2-triphenylethane was formed, however, in case of reaction TPE: DHA: asphaltenes (Experiment 8), the mass concentration of 1,1,2-triphenylethane increased to 0.03±0.01 mg/ml which was ascribed to asphaltene complex structure and steric hindrance
- No peak or unquantifiable amount of bibenzyl was detected at the reaction of ES: DHA (Experiment 6), however of E-stilbene: DHA: asphaltene (Experiment 5) the concentration of bibenzyl in the mixture increased compared to the reaction E-stilbene: asphaltenes (Experiment 4)
- It was possible to confirm heavy compounds evaluation using the SIMDIS technique
- Steric requirements should be accounted during reaction of asphaltenes with probe molecules

4.6 References

Akchurin, T.I., Baibulatova, N.Z., Grabovskii, S.A., Talipova, P.P., Galkin, E.G. and Dokichev, V.A., 2016. Alkene hydrogenation over palladium supported on a carbon–silica material. *Kinetics and Catalysis*, *57*(5), pp.586-591.

Amini, M. and Etemadi, H., 2013. D-Glucosamine as an efficient and green additive for palladium-catalyzed Heck reaction. *Chemical Papers*, *67*(7), pp.759-763.

Bernasconi, C.F. ed., 1986. *Investigation of rates and mechanisms of reactions, general considerations and reactions at conventional rates* (Vol. 6). Wiley-Interscience.

Brown, H.C., 1956. Chemical effects of steric strains. *Journal of the Chemical Society (Resumed)*, pp.1248-1268.

Brown, W.G., Mighton, C.J. and Senkus, M., 1938. The Raman spectra of some hydrocarbons containing tertiary C—D linkages. *The Journal of Organic Chemistry*, *3*(1), pp.62-75.

D7169-11, A. (2019). ASTM D7169 - 11 Standard Test Method for Boiling Point Distribution of Samples with Residues Such as Crude Oils and Atmospheric and Vacuum Residues by High Temperature Gas Chromatography. (online) Astm.org. Available at: https://www.astm.org/DATABASE.CART/HISTORICAL/D7169-11.htm (Accessed 8 Sep. 2019).

Jin, Y.J., Choi, Y.G., Park, H. and Kwak, G., 2018. Near-room-temperature phase-change fluorescent molecular rotor and its hybrids. *Journal of Molecular Liquids*, *265*, pp.260-268.

Klein, J.E., Dereli, B., Que, L. and Cramer, C.J., 2016. Why metal–oxos react with dihydroanthracene and cyclohexadiene at comparable rates, despite having different C–H bond strengths. A computational study. *Chemical Communications*, *52*(69), pp.10509-10512.

Kooyman, E.C., 1955. The reactivity of alpha-methylenic groups towards free radicals: V. Azo-compounds and ketazines. *Recueil des Travaux Chimiques des Pays-Bas*, *74*(1), pp.117-126.

Kuimov, V.A., Gusarova, N.K., Malysheva, S.F. and Trofimov, B.A., 2018. Transition metal-free regioselective access to 9, 10-dihydroanthracenes via the reaction of anthracenes with elemental phosphorus in the KOH/DMSO system. *Tetrahedron letters*, *59*(52), pp.4533-4536.

Lin, Y.H., Williams, I.D. and Li, P., 1997. Selective oxidation of styrenes under oxygen catalyzed by cobalt chloride. *Applied Catalysis A: General*, *150*(2), pp.221-229.

Luo, Y.R., 2007. *Comprehensive handbook of chemical bond energies*. CRC press.

Mathai, I.M., 1960, October. The influence of substituents on the additive reactivity of ethylene derivatives. In *Proceedings of the Indian Academy of Sciences-Section A* (Vol. 52, No. 4, pp. 182-188). Springer India.

Mathieson, A.R., 1960. Polymerisation Ceiling Temperatures Of Some Substituted Styrenes. *JOURNAL OF THE CHEMICAL SOCIETY*, (JUN), pp.2778-2779.

McCormick, H.W., 1957. Ceiling temperature of α-methylstyrene. *Journal of Polymer Science*, *25*(111), pp.488-490.

Naghizada, N., 2017. Uncatalyzed hydrogen transfer during 100-250° C conversion of asphaltenes. M.Sc. Thesis, University of Alberta: Edmonton, Alberta, Canada.

Naghizada, N., Prado, G.H. and de Klerk, A., 2017. Uncatalyzed hydrogen transfer during 100–250 C conversion of asphaltenes. *Energy & fuels*, *31*(7), pp.6800-6811.

Nakamula, I., Yamanoi, Y., Yonezawa, T., Imaoka, T., Yamamoto, K. and Nishihara, H., 2008. Nanocage catalysts—rhodium nanoclusters encapsulated with dendrimers as accessible and stable catalysts for olefin and nitroarene hydrogenations. *Chemical Communications*, (44), pp.5716-5718.

Payan, F. and de Klerk, A., 2018. Hydrogen Transfer in Asphaltenes and Bitumen at 250° C. *Energy & fuels*, *32*(9), pp.9340-9348.

Pelletier, G., Lie, S., Mousseau, J.J. and Charette, A.B., 2012. One-pot synthesis of 1-iodoalkynes and trisubstituted alkenes from benzylic and allylic bromides. *Organic letters*, *14*(21), pp.5464-5467.

Peña-López, M., Sarandeses, L.A. and Perez Sestelo, J., 2013. Organogold (I) Phosphanes in Palladium-Catalyzed Cross-Coupling Reactions in Aqueous Media. *European Journal of Organic Chemistry*, *2013*(13), pp.2545-2554.

Ru, C.H., Guo, S.H., Pan, G.F., Zhu, X.Q., Gao, Y.R. and Wang, Y.Q., 2018. Synthesis of Hydrazines via Radical Generation and Addition of Azocarboxylic tert-Butyl Esters. *Organic letters*, *20*(7), pp.1910-1913.

Rüchardt, C., Gerst, M. and Ebenhoch, J., 1997. Uncatalyzed Transfer Hydrogenation and Transfer Hydrogenolysis: Two Novel Types of Hydrogen-Transfer Reactions. *Angewandte Chemie International Edition in English*, *36*(13-14), pp.1406-1430.

Sánchez-Lemus, M.C., Schoeggl, F., Taylor, S.D., Mahnel, T., Vrbka, P., Růžička, K., Fulem, M. and Yarranton, H.W., 2016. Vapor pressure and thermal properties of heavy oil distillation cuts. *Fuel*, *181*, pp.503-521.

Smith, A.J., Young, A., Rohrbach, S., O'Connor, E.F., Allison, M., Wang, H.S., Poole, D.L., Tuttle, T. and Murphy, J.A., 2017. Electron-Transfer and Hydride-Transfer Pathways in the Stoltz–Grubbs Reducing System (KOtBu/Et3SiH). *Angewandte Chemie*, *129*(44), pp.13935-13939.

Suzuki, H., 2012. *Electronic absorption spectra and geometry of organic molecules: An application of molecular orbital theory*. Elsevier.

Wu, S.W., Liu, J.L. and Liu, F., 2015. Metal-Free Microwave-Assisted Decarboxylative Elimination for the Synthesis of Olefins. *Organic letters*, *18*(1), pp.1-3.

Wyman, D.P. and Altares Jr, T., 1964. Difunctional anionic polymerization initiators from the reaction of butyllithium with trans-stilbene. *Die Makromolekulare Chemie: Macromolecular Chemistry and Physics*, *72*(1), pp.68-75.

Yaws, C.L., Narasimhan, P. and Gabbula, C., 2009. *Yaws' Handbook of Antoine Coefficients for Vapor Pressure (2nd Electronic Edition)*. New York: Knovel.

Zhang, W., Lu, G., Cui, C., Liu, Y., Li, S., Yan, W., Xing, C., Chi, Y.R., Yang, Y. and Huo, F., 2014. A family of metal-organic frameworks exhibiting size-selective catalysis with encapsulated noble-metal nanoparticles. *Advanced Materials*, *26*(24), pp.4056-4060.

Chapter 5 – Synthesis of hex-1-en-2-ylbenzene

5.1 Introduction

In the study of Palmer et al. (1942), it was mentioned that the alpha-substituted styrene is not polymerizable when subjected to elevated temperatures. Seymour (1948) in his study showed that under the polymerizing conditions vinylbenzene is polymerizable. Additionally, other nuclearly substituted aromatic compounds with a vinyl radical attached to the aromatic ring demonstrate similar properties when exposed to the same conditions. However, due to the thermal instability of the copolymers at elevated temperatures, the alpha substituted aromatic compounds with a vinyl radical do not polymerize under the polymerizing conditions.

In order to further investigate the steric requirements of the asphaltene fraction, it was decided to synthesize the compound that would be similar in structure to the α-methylstyrene, by synthesizing α-substituted olefinic alkylbenzene.

The synthesis of α-substituted alkylbenzene is possible via different pathways. However, due to the limited time, and in order to avoid the formation of byproducts with close boiling points, it was decided to synthesize the compound directly using ketone. It was of further interest to synthesize the compounds that would not copolymerize at higher temperatures so as to avoid the difficulties associated with the recovery of the reaction products.

For this purpose, Wittig and Haag (1955) and Tebbe olefination (Tebbe et al., 1978) reactions were considered. According to the study performed by Pine et al. (1991), Tebbe methylenation proved to have the higher yield, thus the synthesis was carried out using the Tebbe reagent, µ-Chloro-µ-methylenebis (cyclopentadienyl)titaniumdimethylaluminum. The reaction is shown in Figure 5.1.

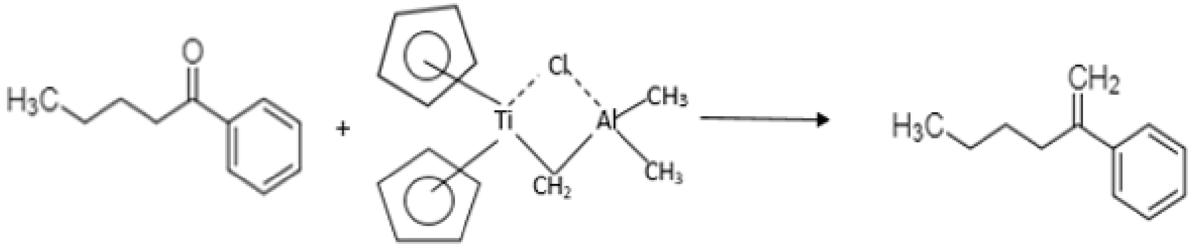

Figure 5. 1. Basic representation of the reaction. Tebbe methylenation of 1-phenylpentan-1-one to synthesize hex-1-en-2-ylbenzene.

The reaction pathway can be explained as follows with reference to Figure 5.2. Methylene titanocene (2) is obtained through the dissociation of Tebbe ragent (1) which happens when a Lewis base, such as THF, is added. Subsequently, methylene titanocene (2) produces oxometallacyclobutane (3) as a result of [2+2] cycloaddition reaction with carbonyl compounds. In the next step, Cp2Ti=O2 (Cp = cyclopentadienyl) is formed as a result of further [2+2] retro-cycloaddition of the oxometallacyclobutane (3). The major reason for the reaction to progress is the generation of the bond between titanium and oxygen (Cannizzo et al., 1985; Parashar, 2008; Grubbs et al., 2003; Li, 2014).

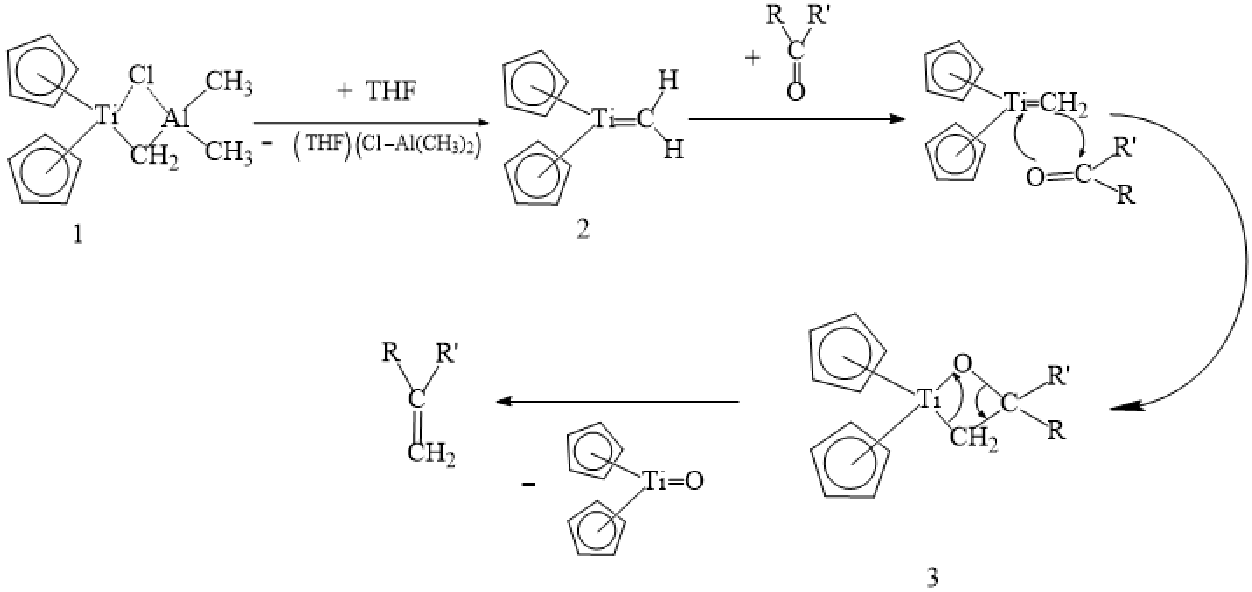

Figure 5. 2. Mechanism of Tebbe methylenation reaction (Li, 2014; Grubbs et al., 2003)

According to the literature it was possible to get the high yield of desired compound directly from ketone without intermediate stages (Pine et al., 1991). Moreover, one of its advantages is that the olefination occurs even at lower temperatures.

Most of the reactions with high yield were conducted at < 0°C temperatures (Yadav et al., 2013; Navickas et al., 2011; Thonhofer et al., 2016; Godage et al. 2003), and only some were conducted at higher temperatures (Gil et al., 2016; Abe et al., 2015; Jeong et al., 2006). Tetrahydrofuran (THF) was preferred over the other solvents, such as toluene, due to its low boiling point, therefore low temperature reactions were selected, as Tebbe reagent is soluble in THF at low temperatures (Straus et al., 2001).

However, due to the absence of stirring in the laboratory chillers the reaction was conducted at 0°C on the stirring plate, to ensure the adequate mixing of reactants. Synthesis was performed by the modified method reported in literature (Kobayashi et al., 2017; Otani et al., 2015; Fuwa et al., 2015; Pine et al., 1991; Raghavendra et al., 2017; Snyder and Brill, 2011).

5.2 Experimental work

5.2.1 Materials

The materials that were employed during the synthesis procedure are listed in Table 5.1.

Table 5. 1. Materials employed in this study

Chemical compound name	Formula	Purity %[a]	CASRN[b]	Supplier
1-Phenylheptan-1-one	$C_{13}H_{17}O$	98+	1671-75-6	Acros Organics
1-phenylpentan-1-one	$C_{11}H_{14}O$	99	1009-14-9	Alfa Aesar
Tetrahydrofuran (HPLC grade)	C_4H_8O	99.9	109-99-9	Fischer Chemical
Diethyl Ether	$(C_2H_5)_2O$	99	60-29-7	Acros Organics
Tebbe Reagent	$C_{13}H_{18}AlClTi$	0.5 M [c]	67719-69-1	Alfa Aesar
Sodium hydroxide	NaOH	1N	1310-73-2	Fischer Chemical
Sodium Chloride	NaCl	99.5	7647-14-5	Sigma-Aldrich
Sodium Sulfate	Na_2SO_4	99+	7757-82-6	Sigma-Aldrich

[a] - This is the purity of the material guaranteed by the supplier; material was not further purified.
[b]- CASRN = Chemical Abstracts Services Registry Number
[c]- 0.5 M in toluene.

5.2.2 Equipment and Procedure

The steps in the reaction are graphically presented in Figure 5.3 for easier reference. The detailed procedure is as follows:

511 mg of 1-Phenylpentan-1-one (3.15 mmol) and 2.29 ml of THF were added to the tared empty 100 ml round bottom flask. The mixture of ketone and THF was cooled together in FP50-HL Refrigerated/Heating Circulator purchased from Julabo, to -1 °C for 30 minutes. Subsequently,

7.44 ml (3.72 mmol, 6.896 g) of Tebbe reagent was added. The mixture was stirred for an hour at 0 °C (using ice from the freezer mixed with water for homogeneous temperature distribution) at 550 rpm. The temperature was measured with a temperature sensor.

A Mettler Toledo-XP1203S precision balance was used for the weighing of compounds. The maximum capacity of the scale is 1210 g, and the readability is 0.001g.

After reaction the mixture was diluted at room temperature with 14.3 ml diethyl ether and quenched with 0.6 ml (1M) sodium hydroxide that was added dropwise while stirring the mixture. The resultant mixture was filtered using ethyl acetate/hexane (1/50) solution to remove the solid materials.

As having inorganic compounds for the further analysis using GC-MS was undesirable, it was decided to wash the filtrate with brine (NaCl solution) and dry over Na_2SO_4 to remove the remaining water. The mixture was filtered using MF-Millipore Hydrophilic Filter papers with 0.22 µm pore size.

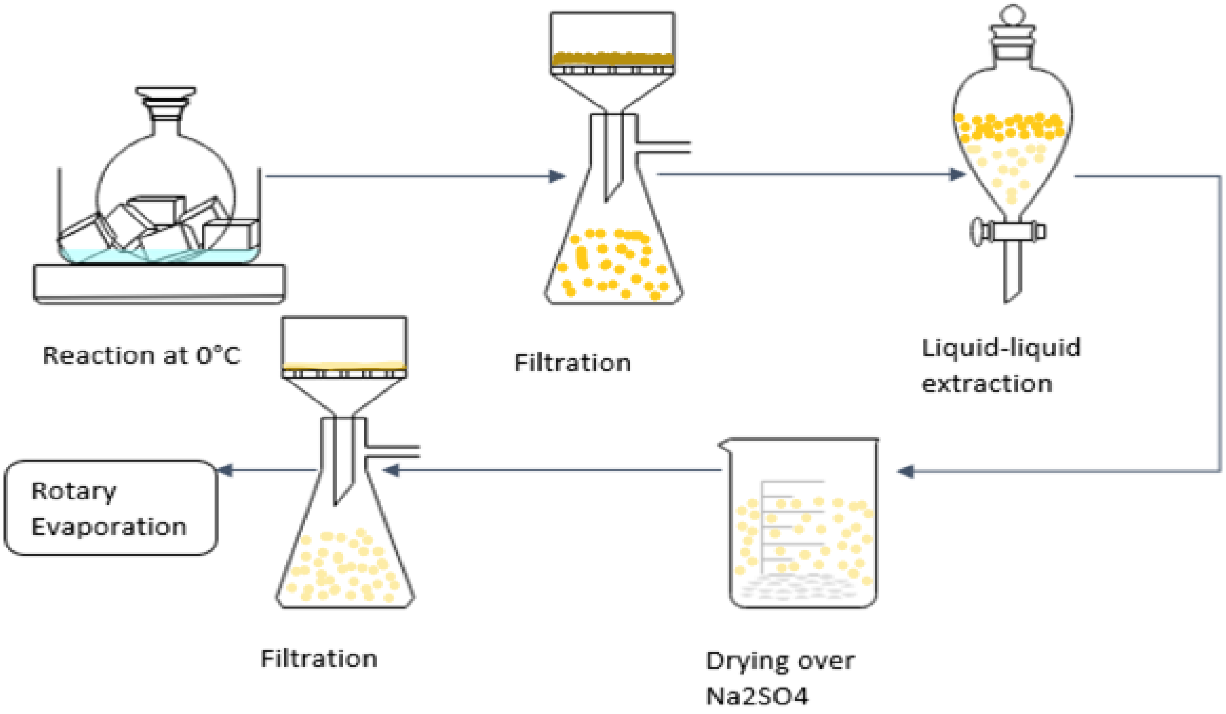

Figure 5. 3. Reaction setup for methylenation of 1-phenylpentan-1-one using Tebbe reagent to get the hex-1-en-2-ylbenzene

The solution was concentrated using Heidolph Hei-Vap rotary evaporator at 130 mbar at room temperature, slowly reducing the pressure and increasing the vacuum to 100 mbar absolute so as to avoid rapid excessive evaporation of the compounds. The small-scale reaction was performed twice to prove the reliability of the results.

Additional information, including some photos of the setup and intermediate products can be found in Appendix C.

5.2.3 Analyses

Gas chromatography-mass spectrometry (GC-MS) was employed to identify the products. The method and equipment used is as described in Chapter 4.

Quantification of the products was performed using gas chromatography with flame ionization detector (GC-FID). The equipment and method used is described in Chapter 3.

Toluene was used as an internal standard (ISTD) for the quantification of the 1-phenylpentan-1-one, in the absence of the hex-1-en-2-ylbenzene. Ideally the ISTD should be similar in properties to the compound being analyzed. It should be inert and is not supposed to react with any component of the reaction mixture.

The ISTD was dissolved in methanol. Three levels were considered with concentration of hex-1-en-2-ylbenzene as following: 1.937 mg/ml; 4.101 mg/ml; 6.277 mg/ml. And the concentration of the internal standard was kept the same at 2 mg/ml. All solutions for calibrations were run for three times to ensure the average value with the least standard deviation. Peaks of the product and 1-phenylpentan-1-one were integrated and quantified manually in the later stage for quantification by comparison of the weight/area ratio data, due to the traces of toluene in the mixture.

A regression coefficient $R^2=0.998$ was obtained for the calibration curve. The calibration data is shown in Appendix C.

Solutions were weighted using analytical balance ME 204 purchased from Mettler Toledo, with the maximum capacity of 220 g, and the readability of 0.1 mg. All the compounds were added using a syringe to 50 ml volumetric flask and Internal Standard of 100 mg was added to each mixture.

All the vials containing the calibrations solutions were stirred for half an hour at 250 rpm to have better extraction of the compounds.

5.3 Results

5.3.1 Identification of the reaction products

Reaction products were identified by GC-MS analysis. The detector was turned on after 5 min to avoid detector saturation while the solvent eluted.

Two main peaks appeared in the chromatogram and have high intensity (Figure 5.4). The reaction product, hex-1-en-2-ylbenzene, eluted with the retention time of 17 min and it was identified by its mass spectrum (Figure 5.5). The other major peak was unconverted reagent, 1-phenylpentan-1-one, eluted with the retention time of 20 min.

The small peaks were ascribed to the minor impurities and side-product present in the mixture and were not further analyzed.

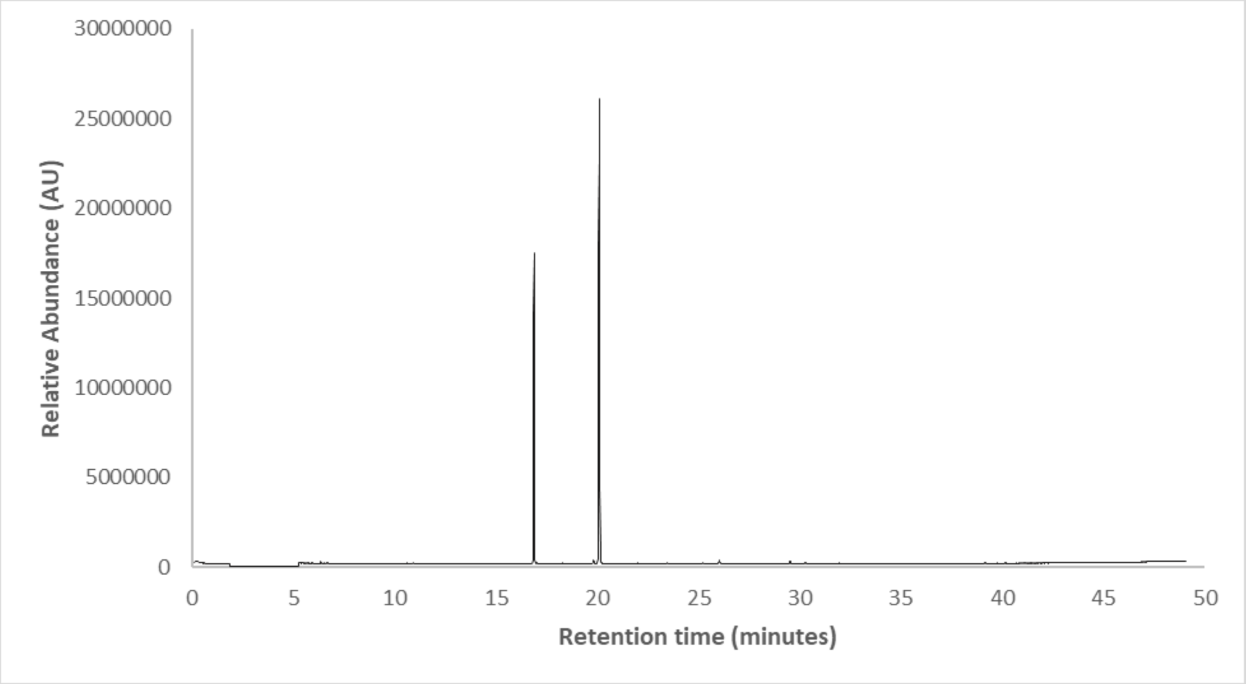

Figure 5. 4. Chromatogram of the products obtained from the Tebbe methylenation reaction of the 1-phenylpentan-1-one: Hex-1-en-2-ylbenzene (17 min) and 1-phenylpentan-1-one (20 min)

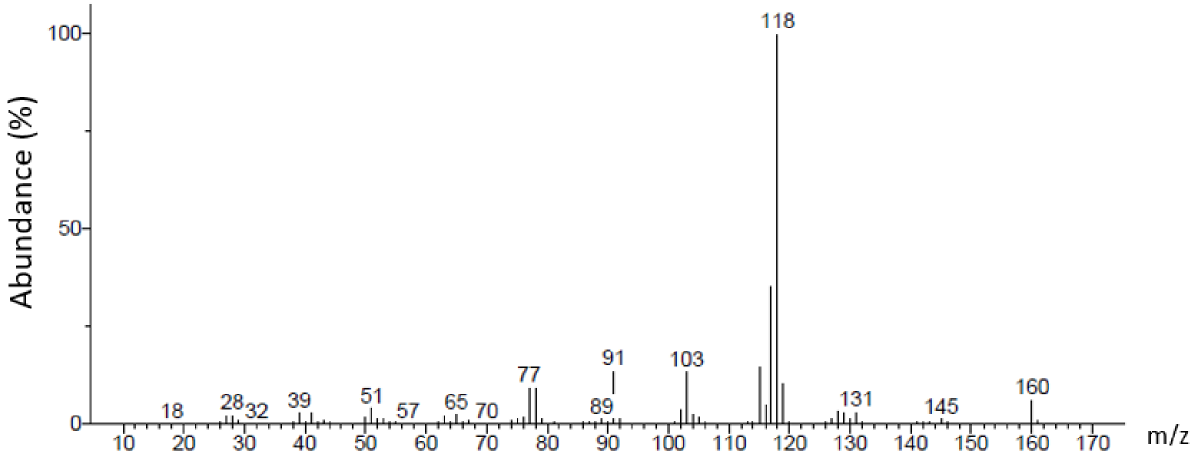

Figure 5. 5. Mass ionization spectrum for hex-1-en-2-ylbenzene obtained via GC-MS

The mass ionization spectrum results (Figure 5.5) correspond to the literature (Fiandanese et al., 1987; Cahiez et al. 2008). MS [70 eV, EI]: m/z (%): 160 (5.8 %) [M^+]; 131 (3 %); 118 (100 %); 103 (26 %); 91 (26%); 77 (73 %); 65 (1.4%); 51 (3%).

As seen from the mass ionization spectrum the molecular ion [M^+] at m/z =160 corresponds to the molecular weight of hex-1-en-2-ylbenzene.

5.4 Discussion

It was possible to get the desired compound hex-1-en-2-ylbenzene, however the yield appeared to be low at 60±3%. Some of the material was lost during the filtration steps and some of the compounds could not be removed from the Na_2SO_4 used for drying.

As mentioned in the work of Wernerova et al., (2010), the losses during the filtration, extraction, and evaporation as well as the losses during water removal stage with brine solution were unavoidable. Losses also occurred because of the glassware, which was not designed for small-scale reactions.

Due to the low yield, it was decided to abandon further efforts at scaling up the reaction and purifying the compound for the intended purpose. Interest in the behavior of hex-1-en-2-ylbenzene for the type of conversion reported in Chapter 4 remains, but it is left to future researchers to continue this work.

5.5 Conclusion

- It was possible to synthesizehex-1-en-2-ylbenzene directly from 1-phenylpentan-1-one by Tebbe methylenation.
- For this synthesis to be scaled up the yield needs to be improved and a separation strategy must be developed to purify the product.

5.6 References

Abe, H., Horii, Y., Hagiwara, M., Kobayashi, T. and Ito, H., 2015. Stereoselective synthesis of a highly oxygenated decahydrocyclopenta [g] chromene derivative: the common tricyclic framework of leucosceptrine and leucosesterterpenone. Chemical Communications, 51(28), pp.6108-6110.

Cahiez, G., Gager, O. and Habiak, V., 2008. Iron-catalyzed alkenylation of Grignard reagents by enol phosphates. *Synthesis*, *2008*(16), pp.2636-2644.

Cannizzo, L.F. and Grubbs, R.H., 1985. In situ preparation of (. mu.-chloro)(. mu.-methylene) bis (cyclopentadienyl)(dimethylaluminum) titanium (Tebbe's reagent). *The Journal of Organic Chemistry*, *50*(13), pp.2386-2387.

Fiandanese, V., Marchese, G., Naso, F. and Ronzini, L., 1987. Synthesis of 1, 1-disubstituted ethenes by means of sequential cross-coupling reactions. *Synthesis*, *1987*(11), pp.1034-1036.

Fuwa, H., Sakamoto, K., Muto, T. and Sasaki, M., 2015. Concise synthesis of the C15–C38 fragment of okadaic acid, a specific inhibitor of protein phosphatases 1 and 2A. *Tetrahedron*, *71*(37), pp.6369-6383.

Gil, A., Lamariano-Merketegi, J., Lorente, A., Albericio, F. and Álvarez, M., 2016. Enantioselective Synthesis of the Polyhydroxylated Chain of Oscillariolide and Phormidolides A–C. *Organic letters*, *18*(18), pp.4485-4487.

Godage, H.Y., Chambers, D.J., Evans, G.R. and Fairbanks, A.J., 2003. Stereoselective synthesis of C-glycosides from carboxylic acids: the tandem Tebbe–Claisen approach. *Organic & biomolecular chemistry*, *1*(21), pp.3772-3786.

Grubbs, R.H., Trnka, T.M. and Sanford, M.S., 2003. Transition metal–carbene complexes in olefin metathesis and related reactions. *Curr. Methods Inorg. Chem*, *3*, pp.187-231.

Jeong, J.H. and Weinreb, S.M., 2006. Formal total synthesis of the cytotoxic marine ascidian alkaloid haouamine A. *Organic letters*, *8*(11), pp.2309-2312.

Kobayashi, T., Yamanoue, K., Abe, H. and Ito, H., 2017. Diastereoselective Total Synthesis of (±)-Toxicodenane A. *European Journal of Organic Chemistry*, *2017*(45), pp.6693-6699.

Li, J.J., 2014. *Name Reactions: A Collection of Detailed Mechanisms and Synthetic Applications Fifth Edition*. Springer Science & Business Media.

Navickas, V., Rink, C. and Maier, M.E., 2011. Synthetic Studies towards Leiodermatolide: Rapid Stereoselective Syntheses of Key Fragments. *Synlett*, *2011*(02), pp.191-194.

Otani, T., Tamai, Y., Seki, K., Kikuchi, T., Miyazawa, T. and Saito, T., 2015. Stereo-controlled synthesis of polyheterocycles via the diene-transmissive hetero-Diels–Alder reaction of β, γ-unsaturated α-keto esters. *Organic & biomolecular chemistry*, *13*(21), pp.5875-5879.

Palmer, R.C., 1942. Developments in terpene chemicals. *Industrial & Engineering Chemistry*, *34*(9), pp.1028-1034.

Parashar, R.K., 2008. Carbon–Carbon Double Bond Forming Reactions. *Reaction Mechanisms in Organic Synthesis*, pp.148-190.

Pine, S.H., Shen, G.S. and Hoang, H., 1991. Ketone methylenation using the Tebbe and Wittig reagents-a comparison. *Synthesis*, *1991*(02), pp.165-167.

Poole, C.F. and Poole, S.K., 2012. *Chromatography today*. Elsevier.

Raghavendra, S., Tadiparthi, K. and Yadav, J.S., 2017. Total syntheses of Prelactone V and Prelactone B. *Carbohydrate research*, *442*, pp.17-19.

Seymour, R.B., Monsanto Chemicals Ltd, 1948. *Copolymers of fumarodinitrile and alpha-substituted styrenes*. U.S. Patent 2,439,226.

Snyder, S.A. and Brill, Z.G., 2011. Structural Revision and Total Synthesis of Caraphenol B and C. *Organic letters*, *13*(20), pp.5524-5527.

Straus, D.A., Morshed, M.M., Dudley, M.E. and Hossain, M.M., 2001. μ-Chlorobis (cyclopentadienyl)(dimethylaluminum)-μ-methylenetitanium. *Encyclopedia of Reagents for Organic Synthesis*.

Tebbe, F.N., Parshall, G.W. and Reddy, G.D., 1978. Olefin homologation with titanium methylene compounds. *Journal of the American chemical society*, *100*(11), pp.3611-3613.

Thonhofer, M., Weber, P., Santana, A.G., Tysoe, C., Fischer, R., Pabst, B.M., Paschke, E., Schalli, M., Stütz, A.E., Tschernutter, M. and Windischhofer, W., 2016. Synthesis of C-5a-substituted derivatives of 4-epi-isofagomine: notable β-galactosidase inhibitors and activity promotors of GM1-gangliosidosis related human lysosomal β-galactosidase mutant R201C. *Carbohydrate research*, *429*, pp.71-80.

Wernerova, M. and Hudlicky, T., 2010. On the practical limits of determining isolated product yields and ratios of stereoisomers: reflections, analysis, and redemption. *Synlett*, *2010*(18), pp.2701-2707.

Wittig, G. and Haag, W., 1955. Über Triphenyl-phosphinmethylene als olefinbildende Reagenzien (II. Mitteil. 1). *Chemische Berichte*, *88*(11), pp.1654-1666.

Yadav, J.S., Goreti, R., Pabbaraja, S. and Sridhar, B., 2013. Short route to platencin. *Organic letters*, *15*(14), pp.3782-3785.

Chapter 6 – Major conclusions and Future work

6.1 Conclusions

The objective of this study was determination of the nature of radicals present in asphaltenes and investigation of asphaltenes steric requirements. Understanding of asphaltene requirements was considered to be beneficial for further development of asphaltenes processing, such as accounting for steric requirements of donor/acceptor compounds.

- With air and N_2 purges, the free radical concentration of the asphaltenes decreases over time however this decrease is not consistent such that compared to air when the asphaltenes are purged with N_2 radicals concentration drops more noticeable.
- It was deducted that the higher free radicals concentration of samples purged with air is not due to oxidation-aging but due to the paramagnetic nature of the oxygen molecules.
- The reason for radical persistence in asphaltenes may not be necessarily attributed to caging, as with addition of 1,2-dihydronaphthalene the free radical concentration of the mixture was higher than the free radical concentration of asphaltenes conversion products.
- During reaction of 1,2-dihydronaphthalene with asphaltenes it was observed that the hydrogen transfer was about 100 time larger than the amount of free radicals.
- Adding hydrogen donor does not always ensure decrease in free radicals concentration depending on the nature of donor compound.
- Although DHN undergoes self-initiation and conversion at reaction conditions, no radical content was detected using ESR technique.
- The increase in the extraction of probe molecules with the increase of the donor (DHA) compound's concentration was observed, which was attributed to the possible trapping by asphaltene molecules.
- DPE is a good hydrogen acceptor that doesn't lead to formation of undesired heavy compounds and gives rise to a high product yield.
- More heavy compounds were formed with addition of DHA molecule to the asphaltene mixture with TMS and AMS that is assumed to happen steric requirements.

- No 1,1,2-triphenylethane was observed after the reaction of TPE with asphaltenes and DHA. However, its mass concentration was found to be 0.03±0.01 mg/ml after the TPE: DHA: asphaltenes reaction.
- The bibenzyl concentration was higher in E-stilbene: DHA: asphaltene (Experiment 5) than E-stilbene: asphaltenes (Experiment 4) and ES: DHA (Experiment 6) which is considered to be a result of complex asphaltenes structure.
- Although the obtained yield was lower than the predicted, about 60% hex-1-en-2-yl benzene yield was attained from the reaction of 1-phenylpentan-1-one with Tebbe reagent.

6.2 Future work

During asphaltenes reaction with probe molecules the mass of unrecovered products is impossible to predict. Moreover, quantification of addition products formed after the reaction was proved to be difficult, as Response Factors in GC-MS and GC-FID were different. For further investigation of the topic inert solvent can be employed.

BIBLIOGRAPHY

Abe, H., Horii, Y., Hagiwara, M., Kobayashi, T. and Ito, H., 2015. Stereoselective synthesis of a highly oxygenated decahydrocyclopenta [g] chromene derivative: the common tricyclic framework of leucosceptrine and leucosesterterpenone. Chemical Communications, 51(28), pp.6108-6110.

Acevedo, S., Castro, A., Negrin, J.G., Fernández, A., Escobar, G., Piscitelli, V., Delolme, F. and Dessalces, G., 2007. Relations between asphaltene structures and their physical and chemical properties: The rosary-type structure. *Energy & fuels*, *21*(4), pp.2165-2175.

Acevedo, S., Escobar, G., Ranaudo, M.A., Pinate, J., Amorín, A., Díaz, M. and Silva, P., 1997. Observations about the structure and dispersion of petroleum asphaltenes aggregates obtained from dialysis fractionation and characterization. *Energy & Fuels*, *11*(4), pp.774-778.

Akchurin, T.I., Baibulatova, N.Z., Grabovskii, S.A., Talipova, P.P., Galkin, E.G. and Dokichev, V.A., 2016. Alkene hydrogenation over palladium supported on a carbon–silica material. *Kinetics and Catalysis*, *57*(5), pp.586-591.

Ali, H. (2016). *Reaction Mechanism in Organic Chemistry*. 1st ed. S. Chand, p.111.

Alimohammadi, S., Zendehboudi, S. and James, L., 2019. A comprehensive review of asphaltene deposition in petroleum reservoirs: Theory, challenges, and tips. *Fuel*, *252*, pp.753-791.

Amini, M. and Etemadi, H., 2013. D-Glucosamine as an efficient and green additive for palladium-catalyzed Heck reaction. *Chemical Papers*, *67*(7), pp.759-763.

Ancheyta, J. and Speight, J.G., 2007. *Hydroprocessing of heavy oils and residua*. CRC Press.

Ancheyta, J., 2016. *Deactivation of heavy oil hydroprocessing catalysts: fundamentals and modeling*. John Wiley & Sons.

Babu, D.R. and Cormack, D.E., 1983. Low temperature oxidation of Athabasca bitumen. *The Canadian Journal of Chemical Engineering*, *61*(4), pp.575-580.

Bachmann, W.E. and Wiselogle, F.Y., 1936. The relative stability of pentaarylethanes. iii. 1 the reversible dissociation of pentaarylethanes. *The Journal of Organic Chemistry*, *1*(4), pp.354-382.

Badre, S., Goncalves, C.C., Norinaga, K., Gustavson, G. and Mullins, O.C., 2006. Molecular size and weight of asphaltene and asphaltene solubility fractions from coals, crude oils and bitumen. *Fuel*, *85*(1), pp.1-11.

Banerjee, D.K., 2012. *Oil sands, heavy oil & bitumen: from recovery to refinery*. PennWell Books.

Benson, S.W., 1985. Disproportionation of free radicals. *The Journal of Physical Chemistry*, *89*(20), pp.4366-4369.

Bernasconi, C.F. ed., 1986. *Investigation of rates and mechanisms of reactions, general considerations and reactions at conventional rates* (Vol. 6). Wiley-Interscience.

Bersohn, M. and Baird, J.C., 1966. Introduction to electron paramagnetic resonance.

Bramwell, P.L., Gao, J., de Waal, B., de Jong, K.P., Gebbink, R.J.K. and de Jongh, P.E., 2016. A transition-metal-free hydrogenation catalyst: Pore-confined sodium alanate for the hydrogenation of alkynes and alkenes. *Journal of catalysis*, *344*, pp.129-135.

Brown, H.C., 1956. Chemical effects of steric strains. *Journal of the Chemical Society (Resumed)*, pp.1248-1268.

Brown, R.C. and Wang, K., 2017. *Fast Pyrolysis of Biomass: Advances in Science and Technology* (Vol. 50). Royal Society of Chemistry.

Brown, W.G., Mighton, C.J. and Senkus, M., 1938. THE RAMAN SPECTRA OF SOME HYDROCARBONS CONTAINING TERTIARY C—D LINKAGES. *The Journal of Organic Chemistry*, *3*(1), pp.62-75.

Buch, L., Groenzin, H., Buenrostro-Gonzalez, E., Andersen, S.I., Lira-Galeana, C. and Mullins, O.C., 2003. Molecular size of asphaltene fractions obtained from residuum hydrotreatment☆. *Fuel*, *82*(9), pp.1075-1084.

Buck, F.R., Coles, K.F., Kennedy, G.T. and Morton, F., 1949. 502. Some nuclear-methylated styrenes and related compounds. Part I. *Journal of the Chemical Society (Resumed)*, pp.2377-2383.

Burtis, C.A. and Bruns, D.E., 2014. *Tietz fundamentals of clinical chemistry and molecular diagnostics-e-book*. Elsevier Health Sciences.

Cahiez, G., Gager, O. and Habiak, V., 2008. Iron-catalyzed alkenylation of Grignard reagents by enol phosphates. *Synthesis*, *2008*(16), pp.2636-2644.

Caldin, E.F. and Gold, V., 2013. *Proton-transfer reactions*. Springer.

Campbell, C.J. and Laherrère, J.H., 1998. The end of cheap oil. *Scientific American*, *278*(3), pp.78-83.

Canadian Association of Petroleum Producers (2019). *Canada's Energy Resources*. (online) Canadian Association of Petroleum Producers. Available at: https://www.capp.ca/canadian-oil-and-natural-gas/canadas-petroleum-resources (Accessed 26 Aug. 2019).

Cannizzo, L.F. and Grubbs, R.H., 1985. In situ preparation of (. mu.-chloro)(. mu.-methylene) bis (cyclopentadienyl)(dimethylaluminum) titanium (Tebbe's reagent). *The Journal of Organic Chemistry*, *50*(13), pp.2386-2387.

Carbognani, L. and Rogel, E., 2002. Solvent swelling of petroleum asphaltenes. *Energy & fuels*, *16*(6), pp.1348-1358.

Chang, H.L., Wong, G.K., Lin, J.R. and Yen, T.F., 2000. Electron spin resonance study of bituminous substances and asphaltenes. In *Developments in petroleum science* (Vol. 40, pp. 229-280). Elsevier.

Corbett, G.E. and Williams, G.H., 1966. Reactions of alkyl radicals. Part II. Reactions of alkylbenzenes with methyl radicals. Photolytic formation and reactions of ethyl and n-butyl radicals. *Journal of the Chemical Society B: Physical Organic*, pp.877-880.

Czarnecki, J., Masliyah, J., Xu, Z. and Dobras, M., 2013. Handbook on Theory and Practice of Bitumen Recovery from Athabasca Oil Sands. *Volume II Industrial Practice, Canada: Kingsley Knowledge Publishing*.

D7169-11, A. (2019). ASTM D7169 - 11 Standard Test Method for Boiling Point Distribution of Samples with Residues Such as Crude Oils and Atmospheric and Vacuum Residues by High Temperature Gas Chromatography. (online) Astm.org. Available at: https://www.astm.org/DATABASE.CART/HISTORICAL/D7169-11.htm (Accessed 8 Sep. 2019).

Dellinger, B., Lomnicki, S., Khachatryan, L., Maskos, Z., Hall, R.W., Adounkpe, J., McFerrin, C. and Truong, H., 2007. Formation and stabilization of persistent free radicals. *Proceedings of the Combustion Institute*, *31*(1), pp.521-528.

Denisov, E.T., Denisova, T.G. and Pokidova, T.S., 2005. *Handbook of free radical initiators*. John Wiley & Sons.

Desgranges, C. and Delhommelle, J., 2017. Coarse-Grained Model and Boiling Point Prediction for Asphaltene Model Compounds via HMC-WL Simulations. *Energy & Fuels*, *31*(10), pp.10699-10705.

DeTar, D.F., 1967. Theoretical study of the elementary steps involved in the reaction of benzoyl peroxide with benzene. *Journal of the American Chemical Society*, *89*(16), pp.4058-4068.

Dietz, W.A., 1967. Response factors for gas chromatographic analyses. *Journal of Chromatographic Science*, *5*(2), pp.68-71.

Durand, B. ed., 1980. Kerogen: Insoluble organic matter from sedimentary rocks. Editions technip.

Eaton, G. R., Eaton, S. S., Barr, D. P., & Weber, R. T. (2010). *Quantitative Epr*. Springer Science & Business Media.

Eberhardt, M.K., 2000. *Reactive oxygen metabolites: chemistry and medical consequences*. CRC press.

Fiandanese, V., Marchese, G., Naso, F. and Ronzini, L., 1987. Synthesis of 1, 1-disubstituted ethenes by means of sequential cross-coupling reactions. *Synthesis*, *1987*(11), pp.1034-1036.

Fischer, H., 1986. Unusual selectivities of radical reactions by internal suppression of fast modes. *Journal of the American Chemical Society*, *108*(14), pp.3925-3927.

Fischer, H., 2001. The persistent radical effect: a principle for selective radical reactions and living radical polymerizations. *Chemical reviews*, *101*(12), pp.3581-3610.

Flagan, R. C., & Seinfeld, J. H. (2012). *Fundamentals of air pollution engineering*. Courier Corporation.

Forrester, A.R., Hay, J.M. and Thomson, R.H., 1968. Organic chemistry of stable free radicals.

Forziati, A.F. and Rossini, F.D., 1949. Physical properties of sixty API-NBS hydrocarbons. *J. Res. Natl. Bur. Stand*, *43*, pp.473-476.

Fossey, J., Lefort, D. and Sorba, J. (1995). *Free radicals in organic chemistry*. Chichester: John Wiley & Sons.

Fox, M. and Whitesell, J. (2004). *Organic chemistry*. Sudbury, Mass.: Jones and Bartlett Publishers

Fuwa, H., Sakamoto, K., Muto, T. and Sasaki, M., 2015. Concise synthesis of the C15–C38 fragment of okadaic acid, a specific inhibitor of protein phosphatases 1 and 2A. *Tetrahedron*, *71*(37), pp.6369-6383.

Gafurov, M., Mamin, G., Gracheva, I., Murzakhanov, F., Ganeeva, Y., Yusupova, T. and Orlinskii, S., 2019. High-Field (3.4 T) ENDOR Investigation of Asphaltenes in Native Oil and Vanadyl Complexes by Asphaltene Adsorption on Alumina Surface. *Geofluids*, *2019*.

Ganshirt, H., 1955. Quantitative Evaluation of Thin-Layer Chromatography. *Thin-Layer Chromatography, A Laboratory Handbook*, pp.133-155.

Gil, A., Lamariano-Merketegi, J., Lorente, A., Albericio, F. and Álvarez, M., 2016. Enantioselective Synthesis of the Polyhydroxylated Chain of Oscillariolide and Phormidolides A–C. *Organic letters*, *18*(18), pp.4485-4487.

Godage, H.Y., Chambers, D.J., Evans, G.R. and Fairbanks, A.J., 2003. Stereoselective synthesis of C-glycosides from carboxylic acids: the tandem Tebbe–Claisen approach. *Organic & biomolecular chemistry*, *1*(21), pp.3772-3786.

González, M., Toropov, A., Duchowicz, P. and Castro, E., 2004. QSPR calculation of normal boiling points of organic molecules based on the use of correlation weighting of atomic orbitals with extended connectivity of zero-and first-order graphs of atomic orbitals. *Molecules*, *9*(12), pp.1019-1033.

Gray, M.R., 2015. *Upgrading oilsands bitumen and heavy oil*. University of Alberta.

Gray, M.R., Assenheimer, G., Boddez, L. and McCaffrey, W.C., 2004. Melting and fluid behavior of asphaltene films at 200− 500 C. *Energy & fuels*, *18*(5), pp.1419-1423.

Greenfield, M.L., 2011. Molecular modelling and simulation of asphaltenes and bituminous materials. *International Journal of Pavement Engineering*, *12*(4), pp.325-341.

Griller, D. and Ingold, K.U., 1976. Persistent carbon-centered radicals. *Accounts of Chemical Research*, *9*(1), pp.13-19.

Groenzin, H. and Mullins, O.C., 1999. Asphaltene molecular size and structure. *The Journal of Physical Chemistry A*, *103*(50), pp.11237-11245.

Grubbs, R.H., Trnka, T.M. and Sanford, M.S., 2003. Transition metal–carbene complexes in olefin metathesis and related reactions. *Curr. Methods Inorg. Chem*, *3*, pp.187-231.

Gruenwedel, D.W. and Whitaker, J.R. eds., 1986. *Food Analysis: Principles and Techniques (In 4 Volumes)*. CRC Press.

Guedes, C.L.B., Di Mauro, E., Antunes, V. and Mangrich, A.S., 2003. Photochemical weathering study of Brazilian petroleum by EPR spectroscopy. *Marine Chemistry*, *84*(1-2), pp.105-112.

Hademenos, G.J., 1999. *Schaum's Outline of Organic Chemistry*. McGraw Hill Professional.

Hart, A., 2014. A review of technologies for transporting heavy crude oil and bitumen via pipelines. *Journal of Petroleum Exploration and Production Technology*, *4*(3), pp.327-336.

Hicks, R. ed., 2011. *Stable radicals: fundamentals and applied aspects of odd-electron compounds*. John Wiley & Sons.

Hicks, R.G., 2007. What's new in stable radical chemistry? *Organic & biomolecular chemistry*, *5*(9), pp.1321-1338.

Hortal, A.R., Martínez-Haya, B., Lobato, M.D., Pedrosa, J.M. and Lago, S., 2006. On the determination of molecular weight distributions of asphaltenes and their aggregates in laser desorption ionization experiments. *Journal of mass spectrometry*, *41*(7), pp.960-968.

Isaacs, E., 2005. Canadian Oil Sands: development and future outlook. *Alberta Energy Research Institute, Calgary*.

Janzen, E.G., 1969. Substituent effects on electron spin resonance spectra and stability of free radicals. *Accounts of Chemical Research*, *2*(9), pp.279-288.

Jeong, J.H. and Weinreb, S.M., 2006. Formal total synthesis of the cytotoxic marine ascidian alkaloid haouamine A. *Organic letters*, *8*(11), pp.2309-2312.

Jia, N., Moore, R.G., Mehta, S.A., Van Fraassen, K., Ursenbach, M. and Zalewski, E., 2004, January. Compositional changes for Athabasca bitumen in the presence of oxygen under low temperature conditions. In *Canadian International Petroleum Conference*. Petroleum Society of Canada.

Jin, Y.J., Choi, Y.G., Park, H. and Kwak, G., 2018. Near-room-temperature phase-change fluorescent molecular rotor and its hybrids. *Journal of Molecular Liquids*, *265*, pp.260-268.

Katritzky, A.R., Ignatchenko, E.S., Barcock, R.A., Lobanov, V.S. and Karelson, M., 1994. Prediction of gas chromatographic retention times and response factors using a general qualitative structure-property relationships treatment. *Analytical Chemistry*, *66*(11), pp.1799-1807.

Kelley, R.D. and Klein, R., 1974. Cross disproportionation of alkyl radicals. *The Journal of Physical Chemistry*, *78*(16), pp.1586-1595.

Kendler, S., Lambertus, G.R., Dunietz, B.D., Coy, S.L., Nazarov, E.G., Miller, R.A. and Sacks, R.D., 2007. Fragmentation pathways and mechanisms of aromatic compounds in atmospheric pressure studied by GC–DMS and DMS–MS. *International Journal of Mass Spectrometry*, *263*(2-3), pp.137-147.

Khulbe, K.C., Mann, R.S., Lamarche, G. and Lamarche, A.M., 1992. Electron spin resonance study of the thermal decomposition of solvent extracted Athabasca tar sand bitumen. *Fuel processing technology*, *31*(2), pp.91-103.

Klein, J.E., Dereli, B., Que, L. and Cramer, C.J., 2016. Why metal–oxos react with dihydroanthracene and cyclohexadiene at comparable rates, despite having different C–H bond strengths. A computational study. *Chemical Communications*, *52*(69), pp.10509-10512.

Kobayashi, T., Yamanoue, K., Abe, H. and Ito, H., 2017. Diastereoselective Total Synthesis of (±)-Toxicodenane A. *European Journal of Organic Chemistry*, *2017*(45), pp.6693-6699.

Komsta, L., Waksmundzka-Hajnos, M. and Sherma, J. eds., 2013. *Thin layer chromatography in drug analysis*. CRC Press.

Kooyman, E.C., 1955. The reactivity of alpha-methylenic groups towards free radicals: V. Azo-compounds and ketazines. *Recueil des Travaux Chimiques des Pays-Bas*, *74*(1), pp.117-126.

Kopsch, H., 1994. On the thermal behavior of petroleum asphaltenes. *Thermochimica acta*, *235*(2), pp.271-275.

Kossiakoff, A. and Rice, F.O., 1943. Thermal decomposition of hydrocarbons, resonance stabilization and isomerization of free radicals1. *Journal of the American Chemical Society*, *65*(4), pp.590-595.

Kudynska, J. and Buckmaster, H.A., 1996. Low-temperature oxidation kinetics of high-volatile bituminous coal studied by dynamic in situ 9 GHz cwepr spectroscopy. *Fuel*, *75*(7), pp.872-878.

Kuimov, V.A., Gusarova, N.K., Malysheva, S.F. and Trofimov, B.A., 2018. Transition metal-free regioselective access to 9, 10-dihydroanthracenes via the reaction of anthracenes with elemental phosphorus in the KOH/DMSO system. *Tetrahedron letters*, *59*(52), pp.4533-4536.

Kuznicki, T., Masliyah, J.H. and Bhattacharjee, S., 2008. Molecular dynamics study of model molecules resembling asphaltene-like structures in aqueous organic solvent systems. *Energy & Fuels*, *22*(4), pp.2379-2389.

Laane, J., Haller, K., Sakurai, S., Morris, K., Autrey, D., Arp, Z., Chiang, W.Y. and Combs, A., 2003. Raman spectroscopy of vapors at elevated temperatures. *Journal of molecular structure*, *650*(1-3), pp.57-68

Lai, W., Li, C., Chen, H. and Shaik, S., 2012. Hydrogen-abstraction reactivity patterns from A to Y: the valence bond way. *Angewandte Chemie International Edition*, *51*(23), pp.5556-5578.

Lalevée, J. and Fouassier, J.P., 2012. Overview of radical initiation. *Encyclopedia of Radicals in Chemistry, Biology and Materials*.

Li, J.J., 2014. *Name Reactions: A Collection of Detailed Mechanisms and Synthetic Applications Fifth Edition*. Springer Science & Business Media.

Lin, Y.H., Williams, I.D. and Li, P., 1997. Selective oxidation of styrenes under oxygen catalyzed by cobalt chloride. *Applied Catalysis A: General*, *150*(2), pp.221-229.

Luo, Y. R. (2002). *Handbook of bond dissociation energies in organic compounds*. CRC press.

Luo, Y.R., 2007. *Comprehensive handbook of chemical bond energies*. CRC press.

Mahoney, L.R., Mendenhall, G.D. and Ingold, K.U., 1973. Calorimetric and equilibrium studies on some stable nitroxide and iminoxy radicals. Approximate oxygen-hydrogen bond dissociation energies in hydroxylamines and oximes. *Journal of the American Chemical Society*, *95*(26), pp.8610-8614.

Masliyah, J., Czarnecki, J. and Xu, Z., 2011. Handbook on theory and practice of bitumen recovery from Athabasca oil sands, volume 1: Theoretical basis. *Canada: Kingsley Knowledge Publishing*.

Mathai, I.M., 1960, October. The influence of substituents on the additive reactivity of ethylene derivatives. In *Proceedings of the Indian Academy of Sciences-Section A* (Vol. 52, No. 4, pp. 182-188). Springer India.

Mathieson, A.R., 1960. POLYMERISATION CEILING TEMPERATURES OF SOME SUBSTITUTED STYRENES. *JOURNAL OF THE CHEMICAL SOCIETY*, (JUN), pp.2778-2779.

Matyjaszewski, K. and Davis, T.P., 2003. *Handbook of radical polymerization*. John Wiley & Sons.

McCormick, H.W., 1957. Ceiling temperature of α-methylstyrene. *Journal of Polymer Science*, *25*(111), pp.488-490.

Melezhik, V., Prave, A.R., Hanski, E.J., Fallick, A.E., Lepland, A., Kump, L.R. and Strauss, H. eds., 2012. *Reading the Archive of Earth's Oxygenation: Volume 3: Global Events and the Fennoscandian Arctic Russia-Drilling Early Earth Project*. Springer Science & Business Media.

Merck, E., 1980. *Dyeing reagents for thin layer and paper chromatography*. E. Merck.

Mitchell, D.L. and Speight, J.G., 1973. The solubility of asphaltenes in hydrocarbon solvents. *Fuel*, *52*(2), pp.149-152.

Molton, P.M., Demmitt, T.F., Donovan, J.M. and Miller, R.K., 1978. Mechanism of conversion of cellulose wastes to liquid fuels in alkaline solution. In: D.L. Klass (Ed.), Energy from Biomass and Wastes III. Institute of Gas Technology, Chicago, IL, p. 293.

Montanari, L., Clericuzio, M., Del Piero, G., & Scotti, R. (1998). Asphaltene radicals and their interaction with molecular oxygen: An EPR probe of their molecular characteristics and tendency to aggregate. *Applied Magnetic Resonance*, *14*(1), 81-100.

Morimoto, M., Sugimoto, Y., Saotome, Y., Sato, S. and Takanohashi, T., 2010. Effect of supercritical water on upgrading reaction of oil sand bitumen. The Journal of Supercritical Fluids, 55(1), pp.223-231.

Moss, R.A., Platz, M. and Jones, M. eds., 2004. *Reactive intermediate chemistry* (p. 1084). Hoboken, NJ: Wiley-Interscience.

Mujica, V., Nieto, P., Puerta, L. and Acevedo, S., 2000. Caging of molecules by asphaltenes. A model for free radical preservation in crude oils. *Energy & fuels*, *14*(3), pp.632-639.

Mukherjee, S. and Boudouris, B.W., 2017. *Organic Radical Polymers: New Avenues in Organic Electronics*. New York: Springer.

Mullins, O.C., Sheu, E.Y., Hammami, A. and Marshall, A.G., 2007. *Asphaltenes, heavy oils, and petroleomics*. Springer Science & Business Media.

Naghizada, N., 2017. Uncatalyzed hydrogen transfer during 100-250 ° C conversion of asphaltenes. M.Sc. Thesis, University of Alberta: Edmonton, Alberta, Canada.

Naghizada, N., Prado, G.H. and de Klerk, A., 2017. Uncatalyzed hydrogen transfer during 100–250 °C conversion of asphaltenes. *Energy & Fuels*, *31*(7), pp.6800-6811.

Nakamula, I., Yamanoi, Y., Yonezawa, T., Imaoka, T., Yamamoto, K. and Nishihara, H., 2008. Nanocage catalysts—rhodium nanoclusters encapsulated with dendrimers as accessible and stable catalysts for olefin and nitroarene hydrogenations. *Chemical Communications*, (44), pp.5716-5718.

Navickas, V., Rink, C. and Maier, M.E., 2011. Synthetic Studies towards Leiodermatolide: Rapid Stereoselective Syntheses of Key Fragments. *Synlett*, *2011*(02), pp.191-194.

Niizuma, S., Steele, C.T., Gunning, H.E. and Strausz, O.P., 1977. Electron spin resonance study of free radicals in Athabasca asphaltene. *Fuel*, *56*(3), pp.249-256.

Nonhebel, D.C., Tedder, J.M. and Walton, J.C., 1979. *Radicals*. CUP Archive.

Oil Sands Magazine. (2019). *World | Oil Sands Magazine*. (online) Available at: https://www.oilsandsmagazine.com/energy-statistics/world#reserves (Accessed 1 Sep. 2019).

Oliviero Rossi, C., Caputo, P., Ashimova, S., Fabozzi, A., D'Errico, G. and Angelico, R., 2018. Effects of natural antioxidant agents on the bitumen aging process: An epr and rheological investigation. *Applied Sciences*, *8*(8), p.1405.

Otani, T., Tamai, Y., Seki, K., Kikuchi, T., Miyazawa, T. and Saito, T., 2015. Stereo-controlled synthesis of polyheterocycles via the diene-transmissive hetero-Diels–Alder reaction of β, γ-unsaturated α-keto esters. *Organic & biomolecular chemistry*, *13*(21), pp.5875-5879.

Ouellette, R.J. and Rawn, J.D., 2015. *Organic Chemistry Study Guide: Key Concepts, Problems, and Solutions*. Elsevier.

Owen, N.A., Inderwildi, O.R. and King, D.A., 2010. The status of conventional world oil reserves—Hype or cause for concern?. *Energy policy*, *38*(8), pp.4743-4749.

Palmer, R.C., 1942. Developments in terpene chemicals. *Industrial & Engineering Chemistry*, *34*(9), pp.1028-1034.

Parashar, R.K., 2008. Carbon–Carbon Double Bond Forming Reactions. *Reaction Mechanisms in Organic Synthesis*, pp.148-190.

Parsons, A.F., 2000. An introduction to free radical chemistry. Wiley-Blackwell.

Payan, F. and de Klerk, A., 2018. Hydrogen Transfer in Asphaltenes and Bitumen at 250° C. *Energy & fuels*, *32*(9), pp.9340-9348.

Pelletier, G., Lie, S., Mousseau, J.J. and Charette, A.B., 2012. One-pot synthesis of 1-iodoalkynes and trisubstituted alkenes from benzylic and allylic bromides. *Organic letters*, *14*(21), pp.5464-5467.

Peña-López, M., Sarandeses, L.A. and Perez Sestelo, J., 2013. Organogold (I) Phosphanes in Palladium-Catalyzed Cross-Coupling Reactions in Aqueous Media. *European Journal of Organic Chemistry*, *2013*(13), pp.2545-2554.

Perchyonok, V.T., 2011. Radical reactions in aqueous media. *Encyclopedia of Inorganic and Bioinorganic Chemistry*, pp.1-22.

Perkins, M.J., 1980. Spin trapping. In *Advances in physical organic chemistry* (Vol. 17, pp. 1-64). Academic Press.

Petrakis, L. and Grandy, D.W., 1978. Electron spin resonance spectrometric study of free radicals in coals. *Analytical Chemistry*, *50*(2), pp.303-308.

Pine, S.H., Shen, G.S. and Hoang, H., 1991. Ketone methylenation using the Tebbe and Wittig reagents-a comparison. *Synthesis*, *1991*(02), pp.165-167.

Pomerantz, A.E., Wu, Q., Mullins, O.C. and Zare, R.N., 2015. Laser-based mass spectrometric assessment of asphaltene molecular weight, molecular architecture, and nanoaggregate number. *Energy & Fuels*, *29*(5), pp.2833-2842.

Poole, C.F. and Poole, S.K., 2012. *Chromatography today*. Elsevier.

Poole, C.F., 2003. *The essence of chromatography*. Elsevier.

Poutsma, M.L., 2010. The radical stabilization energy of a substituted carbon-centered free radical depends on both the functionality of the substituent and the ordinality of the radical. *The Journal of organic chemistry*, *76*(1), pp.270-276.

Rabinowitch, E. and Wood, W.C., 1936. The collison mechanism and the primary photochemical process in solutions. *Transactions of the Faraday Society*, *32*, pp.1381-1387.

Raghavendra, S., Tadiparthi, K. and Yadav, J.S., 2017. Total syntheses of Prelactone V and Prelactone B. *Carbohydrate research*, *442*, pp.17-19.

Redelius, P., 2009. Asphaltenes in bitumen, what they are and what they are not. *Road Materials and Pavement Design*, *10*(sup1), pp.25-43.

Richard, S., 2014. A more sustainable way to win oil from oil sands. *Journal of Sustainable Energy Engineering*, *1*(4), pp.286-298.

Ru, C.H., Guo, S.H., Pan, G.F., Zhu, X.Q., Gao, Y.R. and Wang, Y.Q., 2018. Synthesis of Hydrazines via Radical Generation and Addition of Azocarboxylic tert-Butyl Esters. *Organic letters*, *20*(7), pp.1910-1913.

Rüchardt, C., Gerst, M. and Ebenhoch, J., 1997. Uncatalyzed Transfer Hydrogenation and Transfer Hydrogenolysis: Two Novel Types of Hydrogen-Transfer Reactions. *Angewandte Chemie International Edition in English*, *36*(13-14), pp.1406-1430.

Sánchez-Lemus, M.C., Schoeggl, F., Taylor, S.D., Mahnel, T., Vrbka, P., Růžička, K., Fulem, M. and Yarranton, H.W., 2016. Vapor pressure and thermal properties of heavy oil distillation cuts. *Fuel*, *181*, pp.503-521.

Schmidt, L. D. (1945). Changes in coal during storage. *Chemistry of coal utilization*, *18*, 627-676.

Schultz, K.F. and Selucky, M.L., 1981. Esr measurements on asphaltene and resin fractions from various separation methods. *Fuel*, *60*(10), pp.951-956.

Schulze, M., Scherer, A., Hampel, F., Stryker, J.M. and Tykwinski, R.R., 2016. Synthesis and Aggregation Behavior of Chiral Naphthoquinoline Petroporphyrin Asphaltene Model Compounds. *Chemistry–A European Journal*, *22*(10), pp.3378-3386.

Scifinder.cas.org. (2019). *Experimental properties*. (online) Available at: https://scifinder.cas.org/scifinder/view/scifinder/scifinderExplore.jsf (Accessed 7 Aug. 2019).

Scotti, R. and Montanari, L., 1998. Molecular structure and intermolecular interaction of asphaltenes by FT-IR, NMR, EPR. In *Structures and dynamics of asphaltenes* (pp. 79-113). Springer, Boston, MA.

Serijan, K.T. and Wise, P.H., 1951. Dicyclic hydrocarbons. iii. diphenyl-and dicyclohexylalkanes through C15. *Journal of the American Chemical Society*, *73*(10), pp.4766-4769.

Seymour, R.B., Monsanto Chemicals Ltd, 1948. *Copolymers of fumarodinitrile and alpha-substituted styrenes*. U.S. Patent 2,439,226.

Sheu, E.Y. and Mullins, O.C., 1995. *Fundamentals and applications*. New York: Plenum Press.

Shin, S., Lee, J.M., Hwang, J.W., Jung, H.W., Nho, N.S. and Lee, K.B., 2014. Physical and rheological properties of deasphalted oil produced from solvent deasphalting. *Chemical Engineering Journal*, *257*, pp.242-247.

Siddiquee, M. N., de Klerk, A., & Nazemifard, N. (2016). Application of microfluidics to control product selectivity during non-catalytic oxidation of naphthenic-aromatic hydrocarbons. *Reaction Chemistry & Engineering*, *1*(4), 418-435.

Siddiquee, M.N. and de Klerk, A., 2014. Hydrocarbon addition reactions during low-temperature autoxidation of oilsands bitumen. *Energy & Fuels*, *28*(11), pp.6848-6859.

Siddiqui, M.N. and Ali, M.F., 1999. Studies on the aging behavior of the Arabian asphalts. *Fuel*, *78*(9), pp.1005-1015.

Slangen, H.J.M., 1970. Determination of the spin concentration by electron spin resonance. *Journal of Physics E: Scientific Instruments*, *3*(10), p.775.

Smith, A.J., Young, A., Rohrbach, S., O'Connor, E.F., Allison, M., Wang, H.S., Poole, D.L., Tuttle, T. and Murphy, J.A., 2017. Electron-Transfer and Hydride-Transfer Pathways in the Stoltz–Grubbs Reducing System (KOtBu/Et3SiH). *Angewandte Chemie*, *129*(44), pp.13935-13939.

Snyder, L.R., Kirkland, J.J. and Dolan, J.W., 2010. Basic concepts and the control of separation. *Introduction to Modern Liquid Chromatography*, pp.19-86.

Snyder, S.A. and Brill, Z.G., 2011. Structural Revision and Total Synthesis of Caraphenol B and C. *Organic letters*, *13*(20), pp.5524-5527.

Speight, J.G., 2014. *The chemistry and technology of petroleum*. CRC Press.

Speight, J.G., 2019. Handbook of Petrochemical Processes. CRC Press.

Straus, D.A., Morshed, M.M., Dudley, M.E. and Hossain, M.M., 2001. μ-Chlorobis (cyclopentadienyl)(dimethylaluminum)-μ-methylenetitanium. *Encyclopedia of Reagents for Organic Synthesis*.

Strausz, O.P. and Lown, E.M., 2003. *The chemistry of Alberta oil sands, bitumens and heavy oils* (pp. 588-592). Calgary, Alberta, Canada: Alberta Energy Research Institute.

Strausz, O.P., Mojelsky, T.W. and Lown, E.M., 1992. The molecular structure of asphaltene: an unfolding story. *Fuel*, *71*(12), pp.1355-1363.

Suzuki, H., 2012. *Electronic absorption spectra and geometry of organic molecules: An application of molecular orbital theory*. Elsevier.

Tannous, J.H. and de Klerk, A., 2019. Quantification of the Free Radical Content of Oilsands Bitumen Fractions. *Energy & Fuels*.

Tebbe, F.N., Parshall, G.W. and Reddy, G.D., 1978. Olefin homologation with titanium methylene compounds. *Journal of the American chemical society*, *100*(11), pp.3611-3613.

Thonhofer, M., Weber, P., Santana, A.G., Tysoe, C., Fischer, R., Pabst, B.M., Paschke, E., Schalli, M., Stütz, A.E., Tschernutter, M. and Windischhofer, W., 2016. Synthesis of C-5a-substituted derivatives of 4-epi-isofagomine: notable β-galactosidase inhibitors and activity promotors of GM1-gangliosidosis related human lysosomal β-galactosidase mutant R201C. *Carbohydrate research*, *429*, pp.71-80.

Togo, H., 2004. *Advanced free radical reactions for organic synthesis*. Elsevier.

Trotman-Dickenson, A.F., 1965. The abstraction of hydrogen atoms by free radicals. *Advances in free radical chemistry*, *1*, pp.1-38.

Turuga, A.S.S., 2017. Effect of Solvent Deasphalting Process on the Properties of Deasphalted Oil and Asphaltenes from Bitumen. M.Sc. Thesis, University of Alberta: Edmonton, Alberta, Canada.

Van Boekel, M.A., 2008. *Kinetic modeling of reactions in foods*. CRC press.

Walter, R.I., 1966. Substituent effects on the properties of stable aromatic free radicals. The criterion for non-hammett behavior1. *Journal of the American Chemical Society*, *88*(9), pp.1923-1930.

Wang, H., Dlugogorski, B.Z. and Kennedy, E.M., 2003. Coal oxidation at low temperatures: oxygen consumption, oxidation products, reaction mechanism and kinetic modelling. *Progress in energy and combustion science*, *29*(6), pp.487-513.

Wang, P., Dong, Z.J., Tan, Y.Q. and Liu, Z.Y., 2015. Investigating the interactions of the saturate, aromatic, resin, and asphaltene four fractions in asphalt binders by molecular simulations. *Energy & Fuels*, *29*(1), pp.112-121.

Waples, D.W., 1981. Organic geochemistry for exploration geologists. Burgess Pub. Co..

Wernerova, M. and Hudlicky, T., 2010. On the practical limits of determining isolated product yields and ratios of stereoisomers: reflections, analysis, and redemption. *Synlett*, *2010*(18), pp.2701-2707.

Wittig, G. and Haag, W., 1955. Über Triphenyl-phosphinmethylene als olefinbildende Reagenzien (II. Mitteil. 1). *Chemische Berichte*, *88*(11), pp.1654-1666.

Wu, S.W., Liu, J.L. and Liu, F., 2015. Metal-Free Microwave-Assisted Decarboxylative Elimination for the Synthesis of Olefins. *Organic letters*, *18*(1), pp.1-3.

Wyman, D.P. and Altares Jr, T., 1964. Difunctional anionic polymerization initiators from the reaction of butyllithium with trans-stilbene. *Die Makromolekulare Chemie: Macromolecular Chemistry and Physics*, *72*(1), pp.68-75.

Yadav, J.S., Goreti, R., Pabbaraja, S. and Sridhar, B., 2013. Short route to platencin. *Organic letters*, *15*(14), pp.3782-3785.

Yaws, C.L., Narasimhan, P. and Gabbula, C., 2009. *Yaws' Handbook of Antoine Coefficients for Vapor Pressure (2nd Electronic Edition)*. New York: Knovel.

Yen, T.F., Erdman, J.G. and Saraceno, A.J., 1962. Investigation of the Nature of Free Radicals in Petroleum Asphaltenes and Related Substances by Electron Spin Resonance. *Analytical Chemistry*, *34*(6), pp.694-700.

Yordanov, N. D., & Christova, A. (1994). DPPH as a primary standard for quantitative EPR spectrometry. *Applied Magnetic Resonance*, *6*(1-2), 341-345.

Zachariah, A., Wang, L., Yang, S., Prasad, V. and de Klerk, A., 2013. Suppression of coke formation during bitumen pyrolysis. *Energy & Fuels*, *27*(6), pp.3061-3070.

Zard, S.Z., 2003. *Radical reactions in organic synthesis* (No. 7). Oxford University Press on Demand.

Zhang, N., Zhao, S., Sun, X., Xu, Z. and Xu, C., 2010. Storage stability of the visbreaking product from Venezuela heavy oil. *Energy & Fuels*, *24*(7), pp.3970-3976.

Zhang, Q., Sun, H.H. and Geng, J.G., 2011. Chemical Effects of Environmental Factors on Asphalt Aging. In *Advanced Materials Research* (Vol. 243, pp. 1067-1071). Trans Tech Publications.

Zhang, W., Lu, G., Cui, C., Liu, Y., Li, S., Yan, W., Xing, C., Chi, Y.R., Yang, Y. and Huo, F., 2014. A family of metal-organic frameworks exhibiting size-selective catalysis with encapsulated noble-metal nanoparticles. *Advanced Materials*, *26*(24), pp.4056-4060.

Zou, R. and Liu, L., 1994. Role of Asphaltenes in Petroleum Cracking and Refining. In *Developments in Petroleum Science* (Vol. 40, pp. 339-363). Elsevier.

Appendix A

Supplementary information of Chapter 3 –Behavior and amount of free radicals in asphaltenes

A.1. Calibration data and curves

Calibration was performed using GC-FID, using α-Methylnaphthalene as an internal standard (ISTD). The α-Methylnaphthalene was selected as an ISTD as it is extracted in methanol and does not react with the compounds. The data is represented in the following table.

Table A. 1. Data for calibration of DHN; THN; N compounds

	Levels			
	1	1	1	1
THN				
Concentration (mg/ml)	0.6	1.1	1.6	2.1
Amount THN/Amount ISTD	0.275	0.556	0.787	1.039
Area THN/Area ISTD	0.264	0.522	0.746	1.009
DHN				
Concentration (mg/ml)	1.1	1.6	2.2	2.6
Amount DHN/Amount ISTD	0.55	0.798	1.074	1.271
Area DHN/Area ISTD	0.508	0.737	0.986	1.175
N				
Concentration (mg/ml)	0.8	1.1	1.4	1.7
Amount N/Amount ISTD	0.41	0.570707	0.70297	0.837438
Area N/Area ISTD	0.401	0.534	0.678	0.815
ISTD				
Concentration (mg/ml)	2.0	2.0	2.0	2.0

For each level the probe molecules and ISTD at the corresponding concentrations were inserted into the 100ml volumetric flask, methanol was added up to 100 ml. The mixture was stirred for half an hour on the stirring plate using a magnetic stirrer. All mixtures were injected three times to get the average value for each point on the curve (level). All calibration showed regression line coefficients *R*2>0.99.

Reaction products were extracted using methanol, then ISTD was added at 2mg/ml to each sample to ensure the adequate response factor for each mixture. The mixture was filtered and inserted into the autosampler vials using the syringe for further quantification. Quantification was performed by ratio of integration of the peaks of each compound to the internal standard peak. The quantification was performed by GC-FID using the linear correlation equations given in the calibration figures.

Calibration curves for 1,2,3,4-tetrahydronaphthalene and naphthalene built based on the data given in Table A.1 are represented below in the Figures A.1 and A.2. Calibration curve for 1,2-dihydronaphthalene is shown in Section 3.2.3.3 of Chapter 3, Figure 3.4.

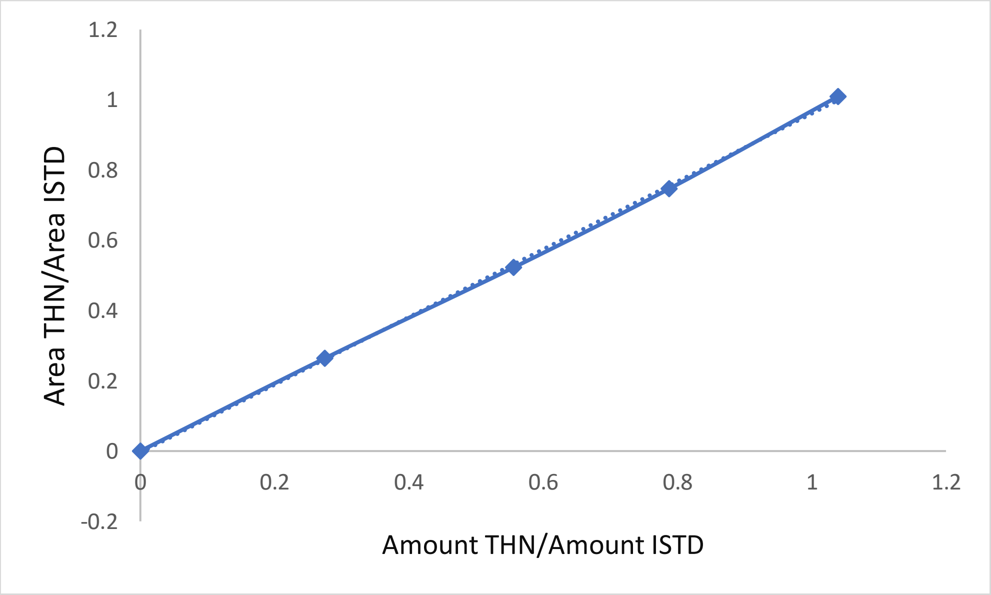

Figure A. 1. Calibration curve for 1,2,3,4-tetrahydronaphthalene obtained by GC-FID using α-Methylnaphthalene as an internal standard. Regression coefficient: R2=0.999; Linear equation: y=9.649E-1x-4.285E-3. Retention time of 1,2,3,4-tetrahydronaphthalene 14.607 minutes

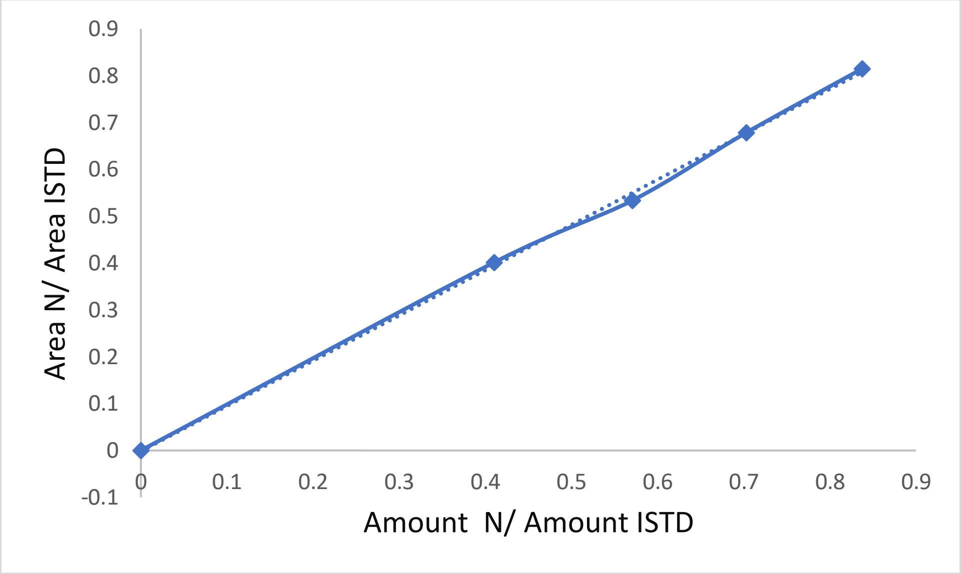

Figure A. 2. Calibration curve for naphthalene obtained by GC-FID using α-Methylnaphthalene as an internal standard. Regression coefficient: R2=0.999; Linear equation: y=9.662E-1x-1.612E-3. Retention time of naphthalene is 16.636 minutes.

A.2. Formulas employed in calculations

Calculations represented in Chapter 3 and Chapter 4 were derived from the following formulas:

Eq. A.1 demonstrates the equation used to calculate the H donated by asphaltenes.

$$\mathrm{H} = 2 \times (\mathrm{mT}) + 2 \times (\mathrm{mN}) - 2 \times \mathrm{m}(\mathrm{DH}-6, \mathrm{DH}-7) \qquad \text{Eq. A. 1}$$

Number of mmol by the reaction completion per mg of DHN was calculated using Eq. A.2.

$$\mathrm{n} = \frac{1}{\mathrm{MW(DHN)}} \times \frac{1}{\left((\mathrm{mD})+(\mathrm{mT})+(\mathrm{mN})+\mathrm{m}\ (\mathrm{unrecovered})+2*\mathrm{m}\ (\mathrm{dimers})\right)} \qquad \text{Eq. A.2}$$

Number of Hydrogen atoms transferred per 1 mg of asphaltenes was determined based on the following equation.

$$\mathrm{H\ transfer} = \mathrm{n} \times \mathrm{Na} \times \mathrm{H} \qquad \text{Eq. A.3}$$

The following abbreviation was used to simplify the equations.

m=mmol, mT=mmol of 1,2,3,4-tetrahydronaphthalene, mN=mmol of naphthalene, mD=mmol of 1,2-dihydronaphthalene, mDH-6=mmol of DH-6, mDH-7=mmol of DH-7, Na=Avogadro constant, $6.02*10^{23}$ mole^{-1}; C=conversion of probe molecule ; S=selectivity

Material balance based on the law of conservation of mass: [modified from Naghizada et al., 2017]

$$\mathrm{i} = \mathrm{mm} + \mathrm{mpr} + \mathrm{mb} + \mathrm{mu} \qquad \text{Eq. A.4}$$

$$\mathrm{mc} = \mathrm{i} - \mathrm{mm} \qquad \text{Eq. A.5}$$

$$\mathrm{mu} = \mathrm{mc} - \mathrm{mpr} - \mathrm{mb} \qquad \text{Eq. A.6}$$

Where i= intial mass of probe molecule, mm= mass of probe molecule measured after the reaction, mpr= mass of product measured after reaction, mb= mass of byproducts, mu= unrecovered mass, mc= mass consumed

$$\mathrm{C}(\%) = \frac{\mathrm{i}-\mathrm{mm}}{\mathrm{i}} * 100\% \qquad \text{Eq. A.7}$$

$$\mathrm{S(a)}(\%) = \frac{\text{mmol of product (a)}}{\text{consumed mmol of probe molecule}} * 100\% \qquad \text{Eq. A.8}$$

Where (a) can be either by-product or unrecovered product or main product.

A.3. GC-FID chromatograms of the reaction products in methanol extract

GC-FID chromatograms of the DHN: asphaltenes reaction products in methanol extract are represented in the Figures A.3-A.5.

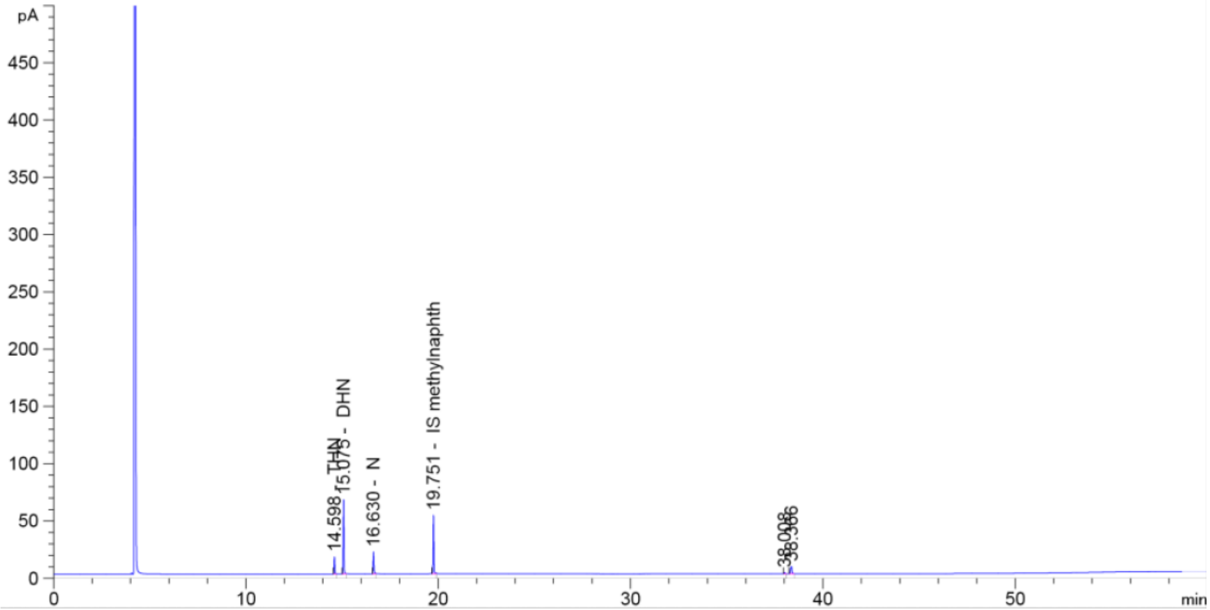

Figure A. 3. Chromatogram of DHN: asphaltenes reaction products (1:1 wt/wt ratio) in methanol extract obtained by GC-FID

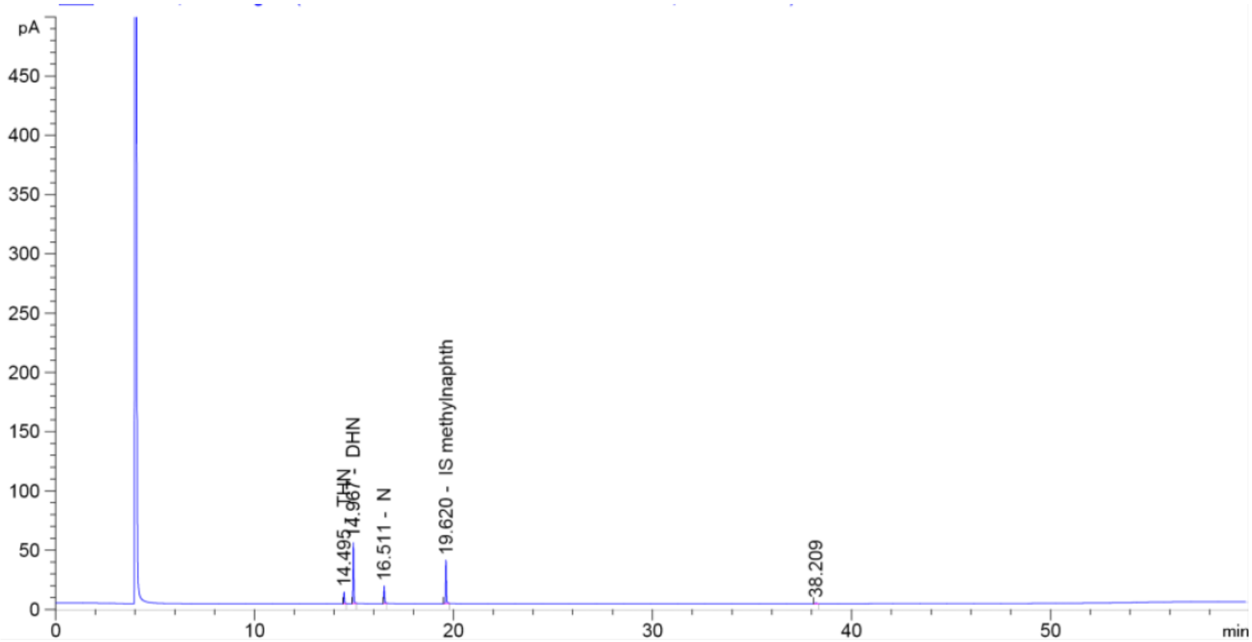

Figure A. 4. Chromatogram of DHN: asphaltenes reaction products (1.6:1 wt/wt ratio) in methanol extract obtained by GC-FID

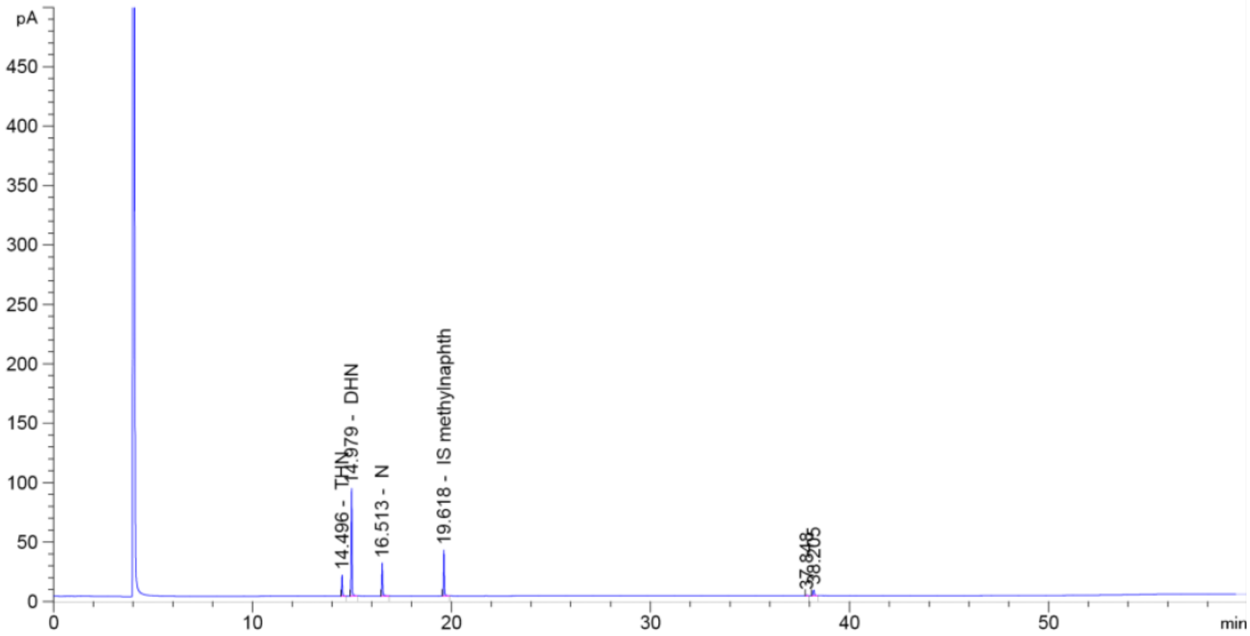

Figure A. 5. Chromatogram of DHN: asphaltenes reaction products (2.4:1 wt/wt ratio) in methanol extract obtained by GC-FID

Appendix B

Supplementary information of Chapter 4- Investigation of asphaltenes steric requirements.

B.1. Temperature profile

Temperature profile of the reactors was measured as a function of time using thermocouple. As seen from the Figure B.1 it took around 18 minutes for a reactor to reach the reaction temperature of $250\,°C$.

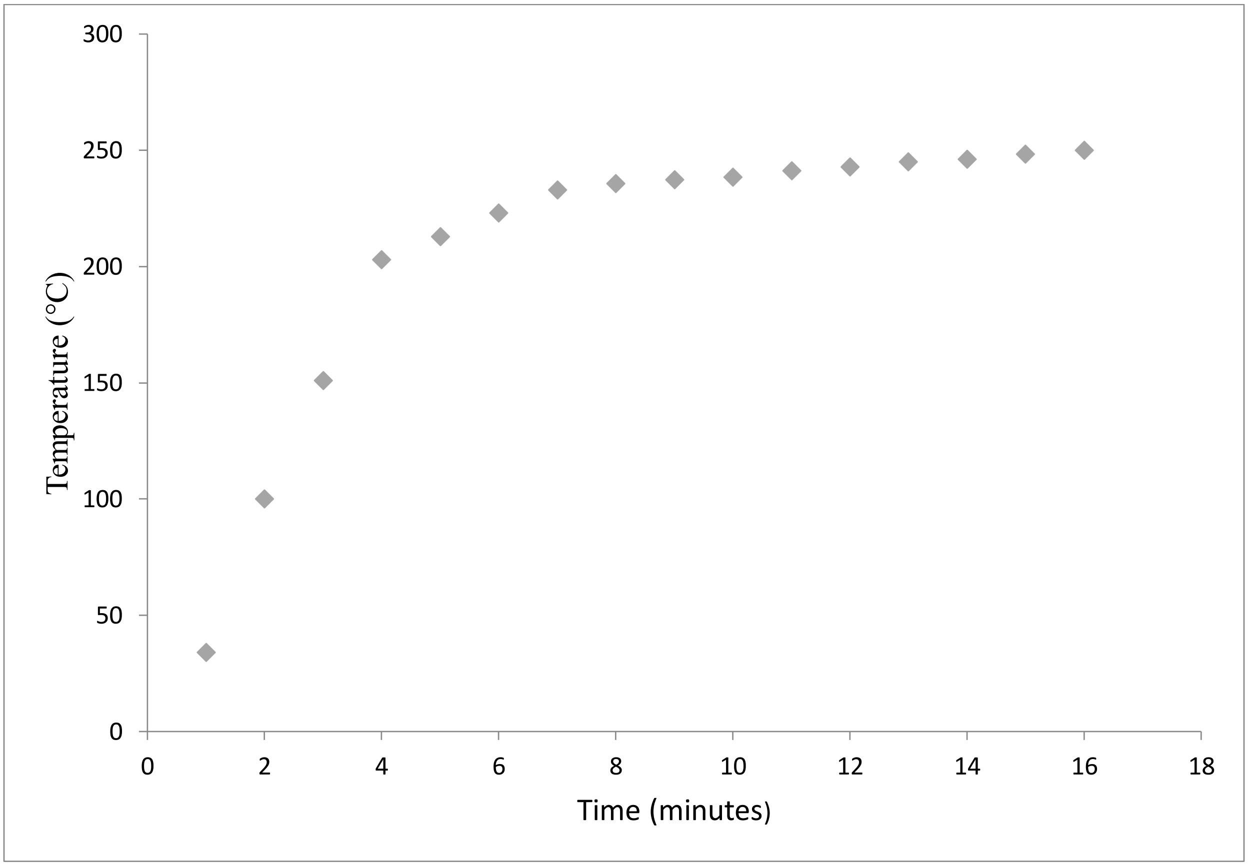

Figure B. 1. Temperature profile of the reactors vs time

B.2. Calibration curves

Calibration procedure performed is described in the chapter 4. The data can be found in Chapter 4, Section 4.3.1.1. The curves were plotted as a function of Area of probe molecule/Area of ISTD and Amount of probe molecule/ Amount of ISTD to obtain the linear equation and a regression factor, R^2.

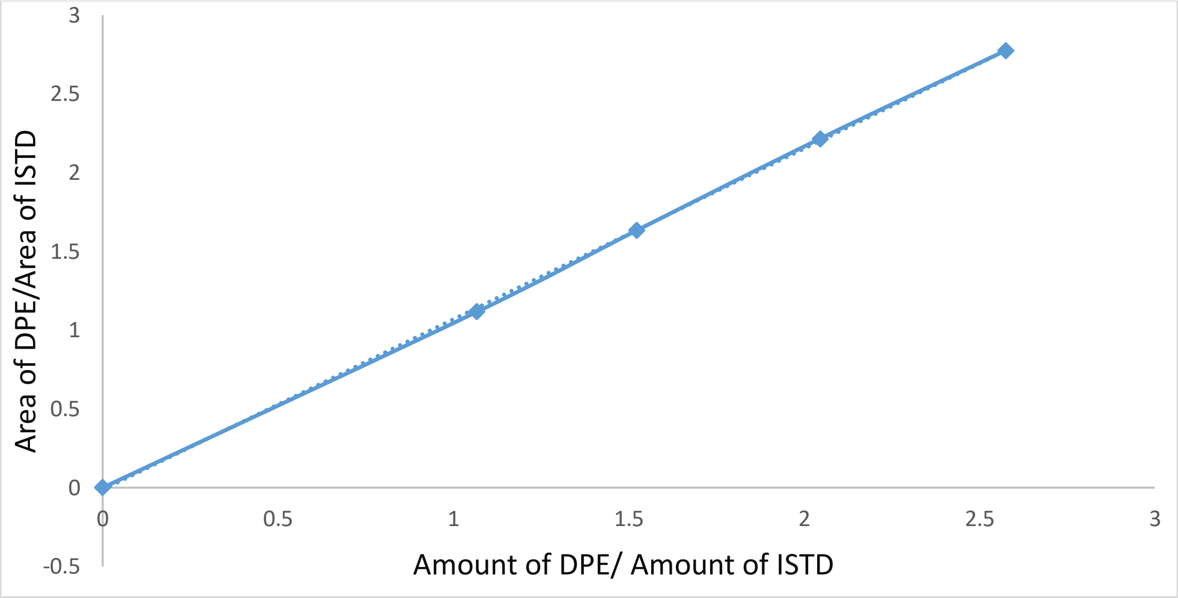

Figure B. 2. Calibration curve for 1,1-diphenylethylene. Quantification was performed using GC- FID, using α-Methylnaphthalene as an internal standard. Regression coefficient: R^2=0.999; Linear equation: y=1.082x-1.3057E-2. Retention time of 1,1-diphenylethylene: 22.874 minutes

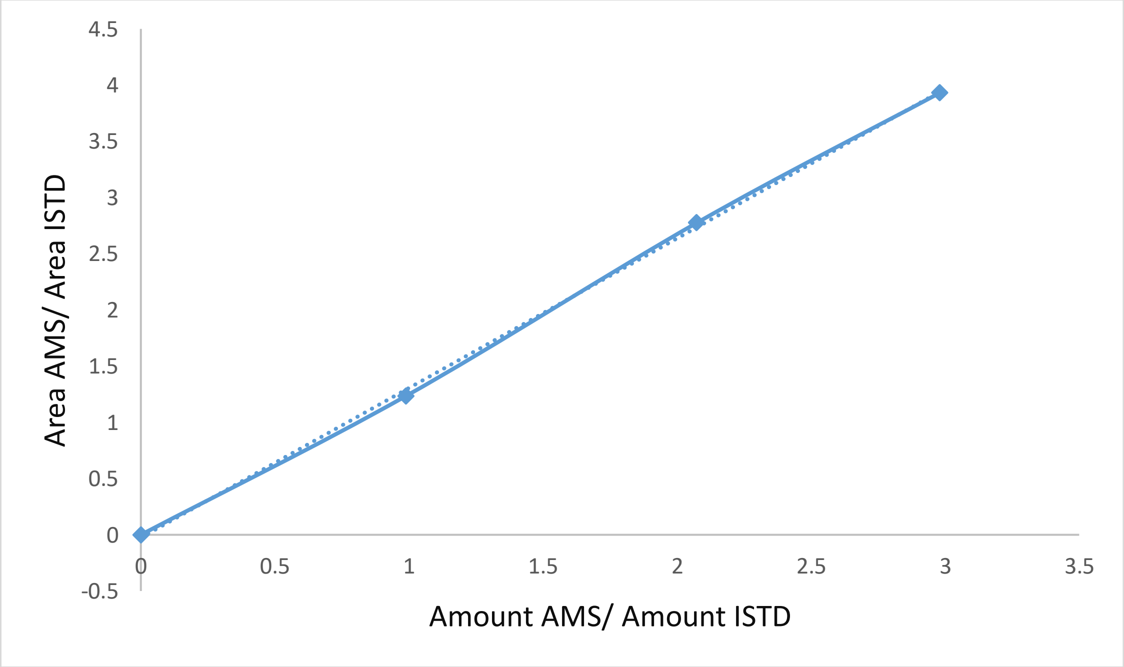

Figure B. 3. Calibration curve for α-Methylstyrene. Quantification was performed using GC-FID, using cyclohexane as an internal standard. Regression coefficient: R^2=0.999; Linear equation: y=1.33076x-2.512E-2. Retention time of α-Methylstyrene: 10.311 minutes

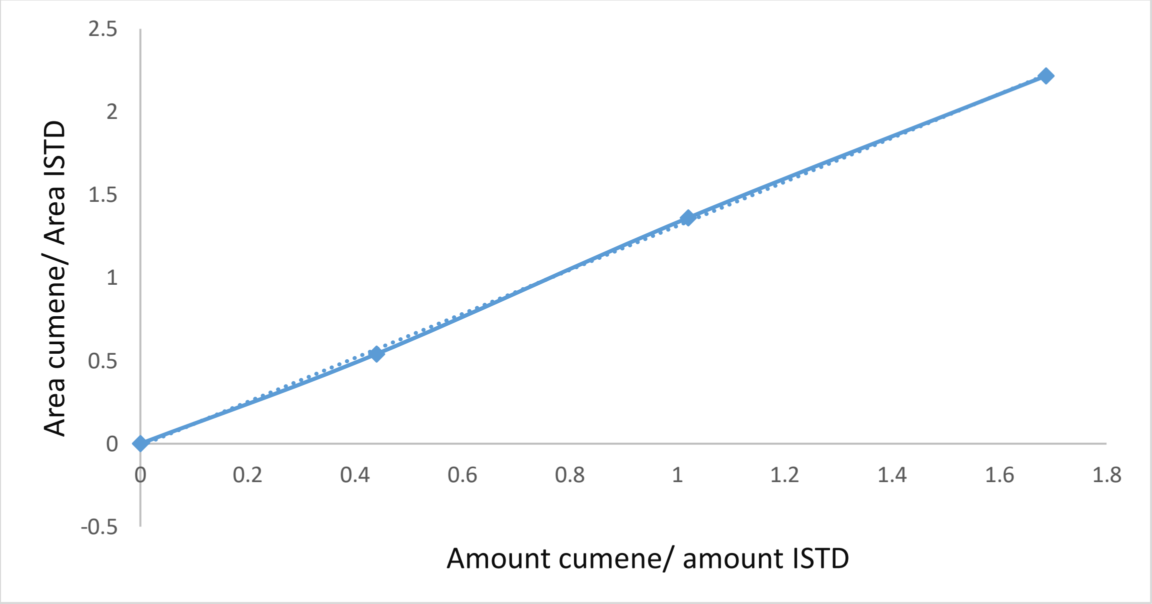

Figure B. 4. Calibration curve for cumene. Quantification was performed using GC- FID, using cyclohexane as an internal standard. Regression coefficient: R^2=0.999; Linear equation: y=1.325x-1.303E-2. Retention time of cumene: 8.686 minutes

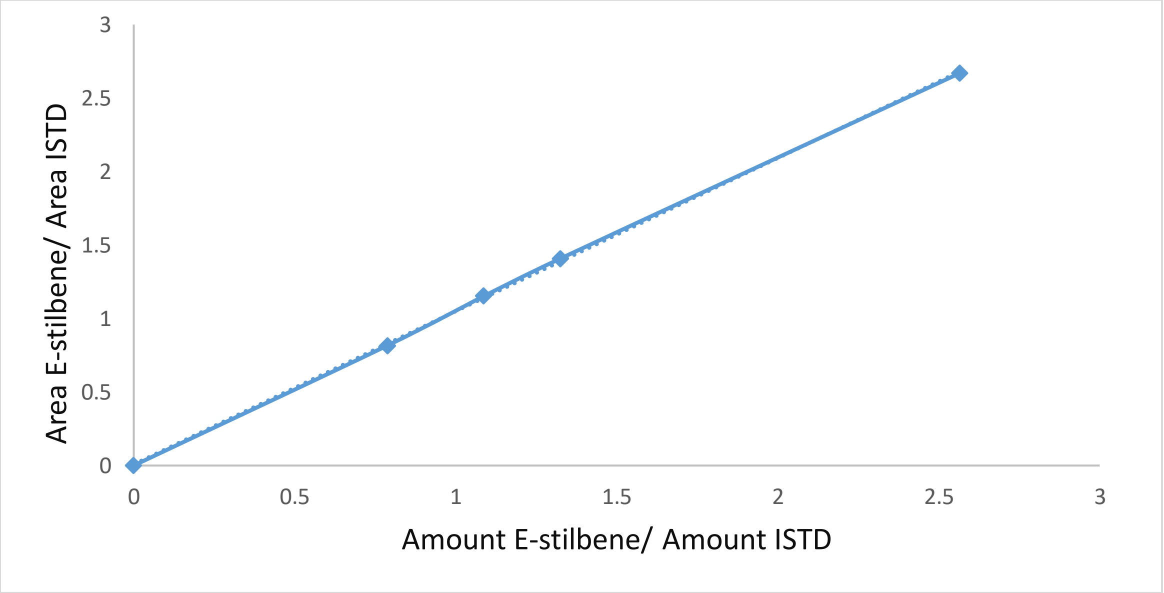

Figure B. 5. Calibration curve for E-stilbene. Quantification was performed using GC- FID, using α-Methylnaphthalene as an internal standard. Regression coefficient: R^2=0.999; Linear equation: y=1.042x-7.848E-3. Retention time of E-stilbene: 28.672 minutes

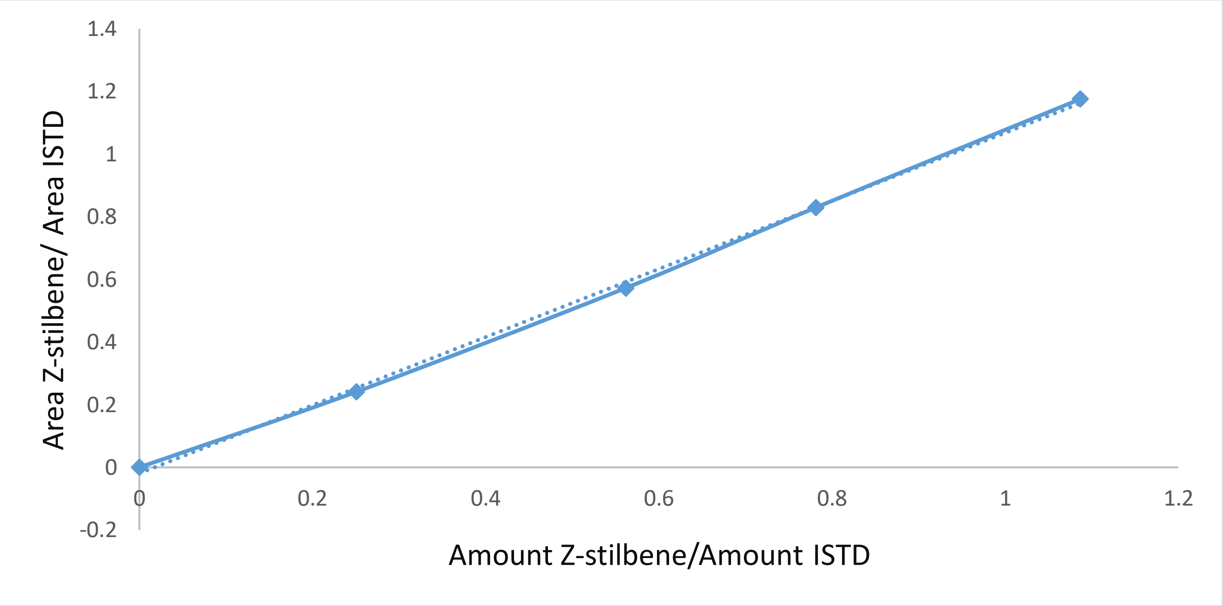

Figure B. 6. Calibration Curve for Z-stilbene. Quantification was performed using GC- FID, using α-Methylnaphthalene as an internal standard. Regression coefficient: R^2=0.999; Linear equation: y=1.087x-1.897E-2. Retention time of Z-stilbene: 22.920 minutes

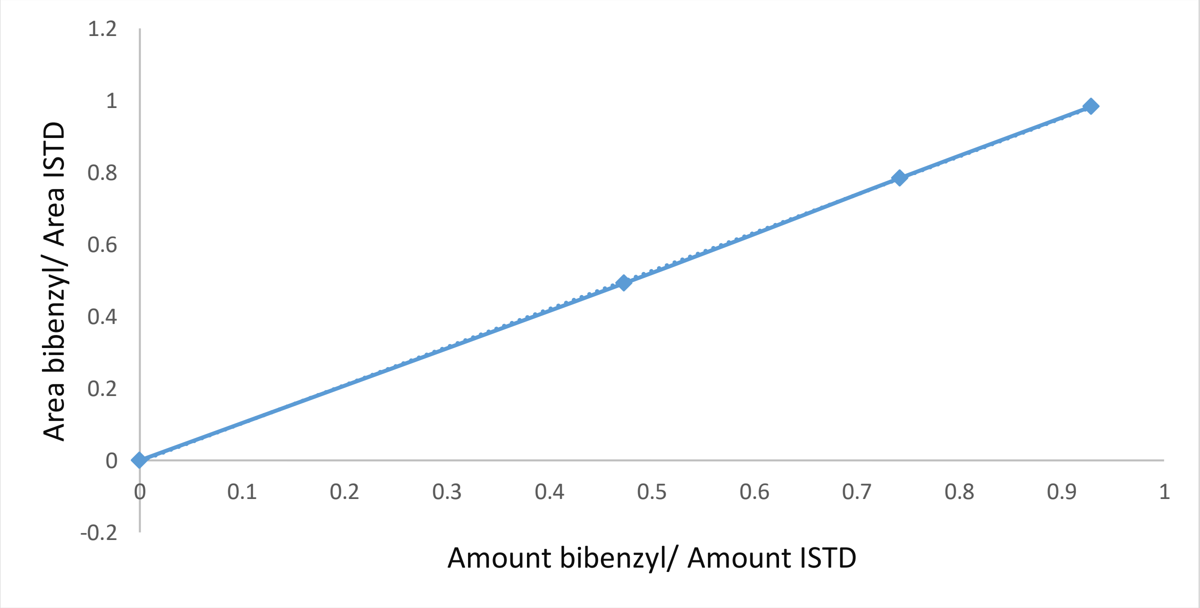

Figure B. 7. Calibration curve for Bibenzyl. Quantification was performed using GC- FID, using α-Methylnaphthalene as an internal standard. Regression coefficient: R^2=0.999; Linear equation: y=1.058x-2.648E-3. Retention time of bibenzyl: 23.455 minutes

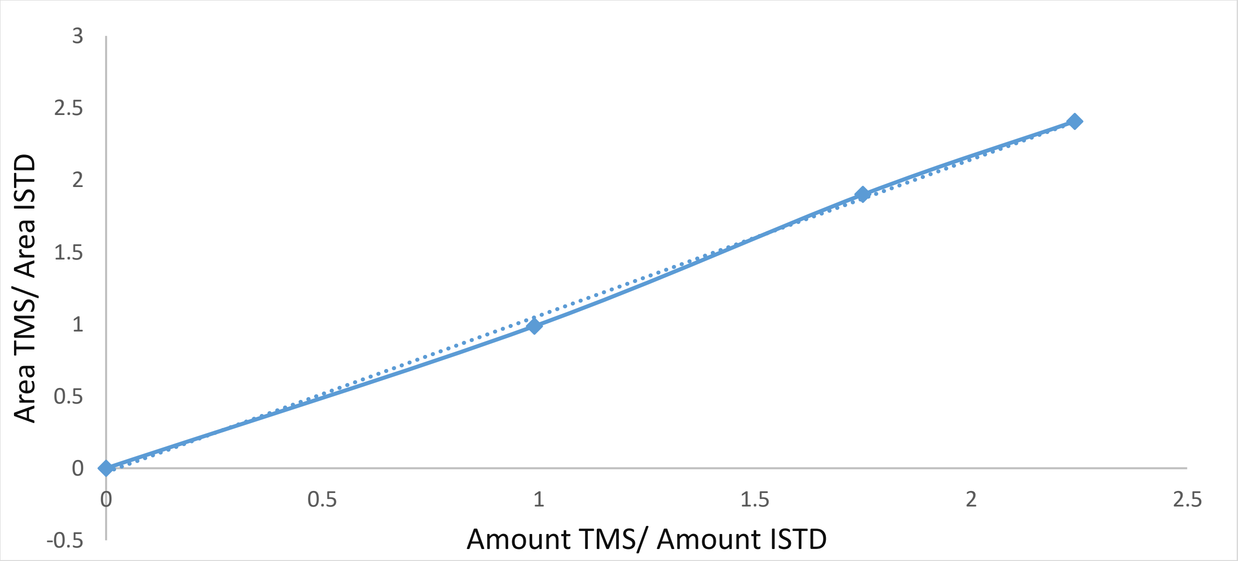

Figure B. 8. Calibration curve for 2,4,6-trimethylstyrene. Quantification was performed using GC- FID, using cyclohexane as an internal standard. Regression coefficient: $R^2=0.999$; Linear equation: $y=1.085x-2.785E-2$. Retention time of 2,4,6-trimethylstyrene: 14.407 minutes

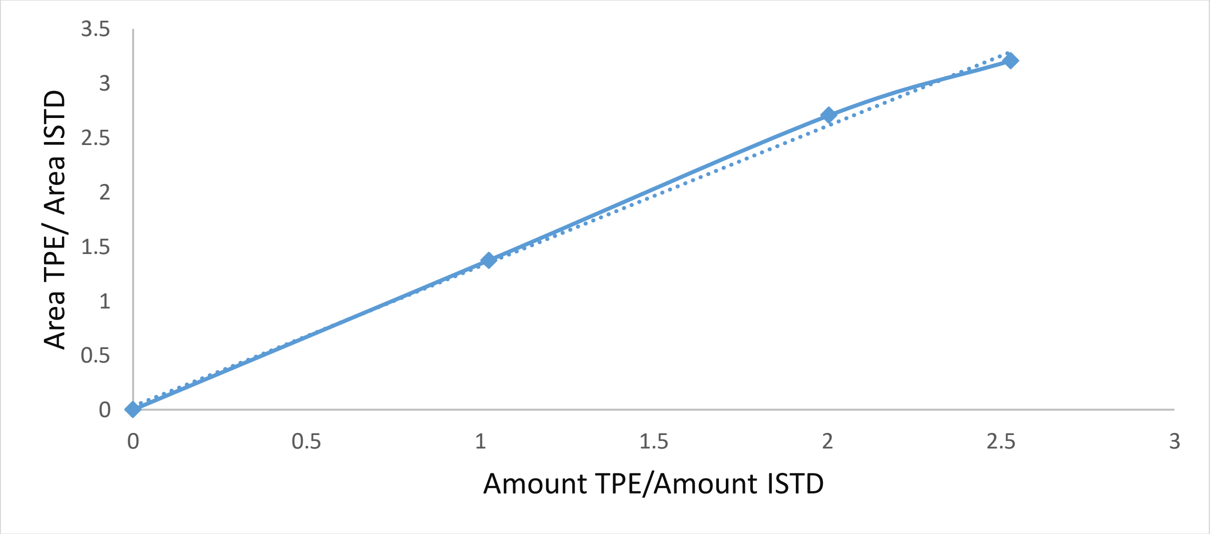

Figure B. 9. Calibration Curve for 1,2-diphenylethenylbenzene. Quantification was performed using GC- FID, using α-Methylnaphthalene as an internal standard. Regression coefficient: $R^2=0.999$; Linear equation: $y=1.287x-3.154E-2$. Retention time of 2,4,6-trimethylstyrene: 14.407 minutes

B.3. Extraction efficiency of probe molecules in the mixture

Control experiments were performed for the extraction of the probe molecules in the mixture prior to being subjected to reaction conditions. Due to the limited amount of 2,4,6-trimethylstyrene it was only quantified in the mixture with asphaltenes. Further information could be found in chapter 4, Section 4.3.1.2. All experiments were performed in duplicate. In Tables B.1 to B.5 the "-"sign indicates that no quantification was performed for the compounds.

Table B. 1. Extraction efficiency of the E-stilbene; Z-stilbene; Bibenzyl mixture

	Amount added at SATP			Quantification		Extraction efficiency	
Probe molecule: Asphaltenes mixture		x	s	x	s	x	s
	E-stilbene (mg/ml)	4.31	0.29	4.26	0.35	0.988	0.014
	Asphaltenes (mg/ml)	5.04	0.01	-	-	-	-
	ISTD(mg/ml)	1.99	0.01	1.96	0.00	1.000	0.000
	Z-stilbene (mg/ml)	1.01	0.06	0.91	0.16	0.901	0.105
	Bibenzyl (mg/ml)	0.98	0.01	0.90	0.07	0.922	0.082
Probe molecule: DHA: Asphaltenes mixture	Amount added at SATP			Quantification		extraction efficiency	
		x	s	x	s	x	s
	E-stilbene (mg/ml)	4.23	0.03	4.22	0.03	0.999	0.001
	Asphaltenes (mg/ml)	2.53	0.01	-	-	-	-
	ISTD(mg)	1.99	0.01	1.96	0.00	1.000	0.000
	Z-stilbene (mg/ml)	0.98	0.02	0.95	0.03	0.975	0.1
	Bibenzyl (mg/ml)	0.97	0.03	0.94	0.02	0.966	0.01
	DHA	2.54	0.00	-	-	-	-

Table B. 2. Extraction efficiency of DPE mixtures

	Amount added at SATP			Quantification		Extraction efficiency	
Probe molecule: asphaltenes		x	s	x	s	x	s
	DPE (mg/ml)	5.105	0.06	4.31	0.569	0.844	0.101
	Asphaltenes (mg/ml)	5.01	0	-	-	-	-
	ISTD (mg/ml)	1.99	0.01	1.96	0	1	-
Probe molecule: DHA: asphaltenes	Amount added at SATP			Quantification		Extraction efficiency	
		x	s	x	s	x	s
	DPE (mg/ml)	5.05	0.02	4.49	0.345	0.891	0.072
	DHA (mg/ml)	2.51	0.06	-	-	-	-
	ISTD (mg/ml)	1.97	0.01	1.96	0	1	-
	Asphaltenes (mg/ml)	2.52	0.04	-	-	-	-
Probe molecule:DHA	Amount added at SATP			Quantification		Extraction efficiency	
		x	s	x	s	x	s
	DPE (mg/ml)	5.05	0.02	4.79	0.23	0.950	0.053
	DHA (mg/ml)	5.01	0.05	-	-	-	-
	ISTD (mg/ml)	2.01	0.04	1.96	0	1	-

Table B. 3. Extraction efficiency of α-Methylstyrene mixtures

	Amount added at SATP			Quantification		Extraction efficiency	
Probe molecule: asphaltenes		x	s	x	s	x	s
	α-Methylstyrene (mg/ml)	3.99	399	3.134	0.48	0.786	0.01
	Asphaltenes (mg/ml)	5.03	0.03	-	-	-	-
	ISTD (mg)	0.95	0.02	1	0.00	1	0
	Cumene (mg/ml)	1.53	0.03	1.25	0.18	0.816015	0.136
Probe molecule: DHA: Asphaltenes	Amount added at SATP			Quantification		Extraction efficiency	
		x	s	x	s	x	s
	α-Methylstyrene (mg/ml)	4.03	0.01	3.12	0.111	0.775	0.026
	CUMENE (mg/ml)	1.58	0.05	1.181	0.008	0.750	0.0289
	ISTD (mg/ml)	0.99	0.01	1	0	1	0
	DHA (mg/ml)	2.47	0.04	-	-	-	-
	Asphaltenes(mg/ml)	2.51	0.00	-	-	-	-
Probe molecule: DHA	Amount added at SATP			Quantification		Extraction efficiency	
		x	s	x	s	x	s
	α-Methylstyrene (mg/ml)	3.98	0.04	3.347	0.087	0.842	0.029
	DHA (mg/ml)	5.01	0.02	-	-	-	-
	ISTD(mg/ml)	0.95	0.02	1	0	1	0
	Cumene (mg)	1.59	0.06	1.276	0.093	0.799	0.026

Table B. 4. Extraction efficiency of TPE mixtures

	Amount added at SATP			Quantification		Extraction efficiency	
Probe molecule: Asphaltenes		x	s	x	s	x	s
	TPE(mg/ml)	5.08	0.04	3.8	0.08	0.749	0.14
	Asphaltenes (mg/ml)	5.01	0.01	-	-	-	-
	ISTD (mg/ml)	1.98	0.01	1.96	0	1	0
Probe molecule: DHA: Asphaltenes	Amount added at SATP			Quantification		Extraction efficiency	
		x	s	x	s	x	s
	TPE (mg/ml)	5.05	0.06	3.35	0.09	0.663	0.025
	DHA (mg/ml)	2.505	0.04	-	-	-	-
	ISTD(mg/ml)	2.01	0.05	1.96	0	1	0
	Asphaltenes (mg/ml)	2.52	0.05	-	-	-	-
Probe molecule: DHA	Amount added at SATP			Quantification		Extraction efficiency	
		x	s	x	s	x	s
	TPE (mg/ml)	5.08	0.01	4.827	0.32	0.949	0.062
	DHA (mg/ml)	5.06	0.01	-	-	-	-
	ISTD (mg/ml)	2.05	0.13	1.96	0	1	0

Table B. 5. Extraction efficiency of 2,4,6-trimethylstyrene mixture. Note: further control experiments involving TMS probe molecules were not performed due to the limited amount of the compound.

Probe molecule: Asphaltenes	Amount added at SATP			Quantification		extraction efficiency	
		x	s	x	s	x	s
	2,4,6-trimethylstyrene(mg/ml)	4.18	1.13	3.501	0.453	0.854	0.122
	Asphaltenes (mg/ml)	4.2	1.13	-	-	-	-
	ISTD(mg/ml)	1	0.03	1	0	1	-

B.4. GC-FID chromatograms of some of the reaction products in methanol extract

Some of the chromatograms were represented as an example of the reaction results.

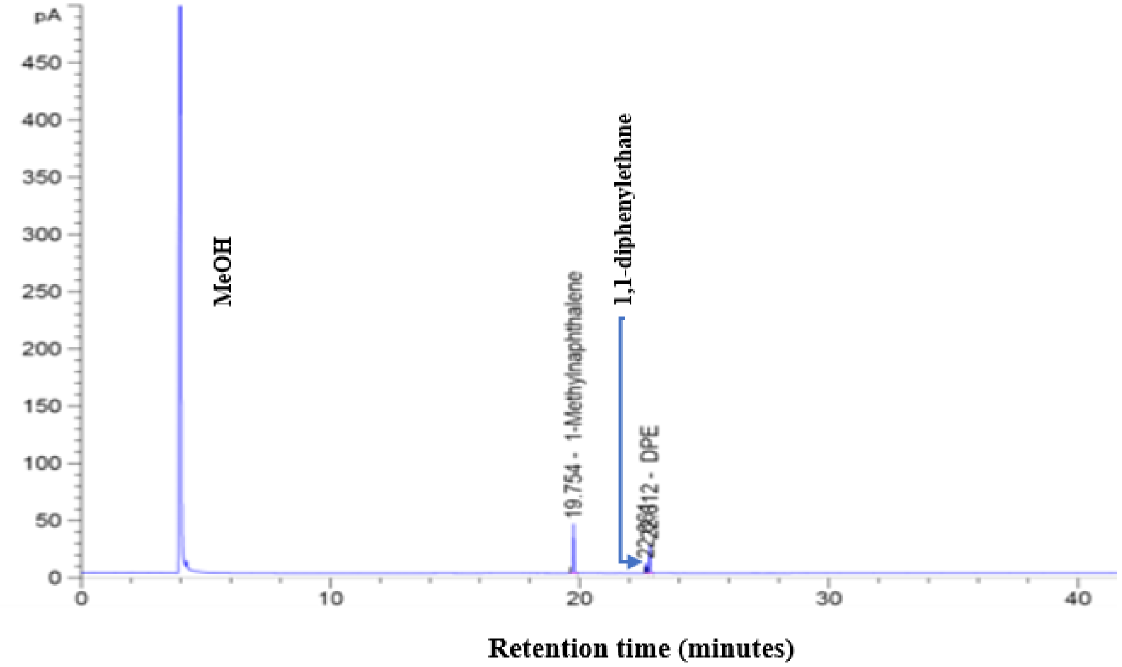

Figure B. 10. GC-FID chromatogram of the 1,1-diphenylethylene:asphaltene reaction products in methanol extract

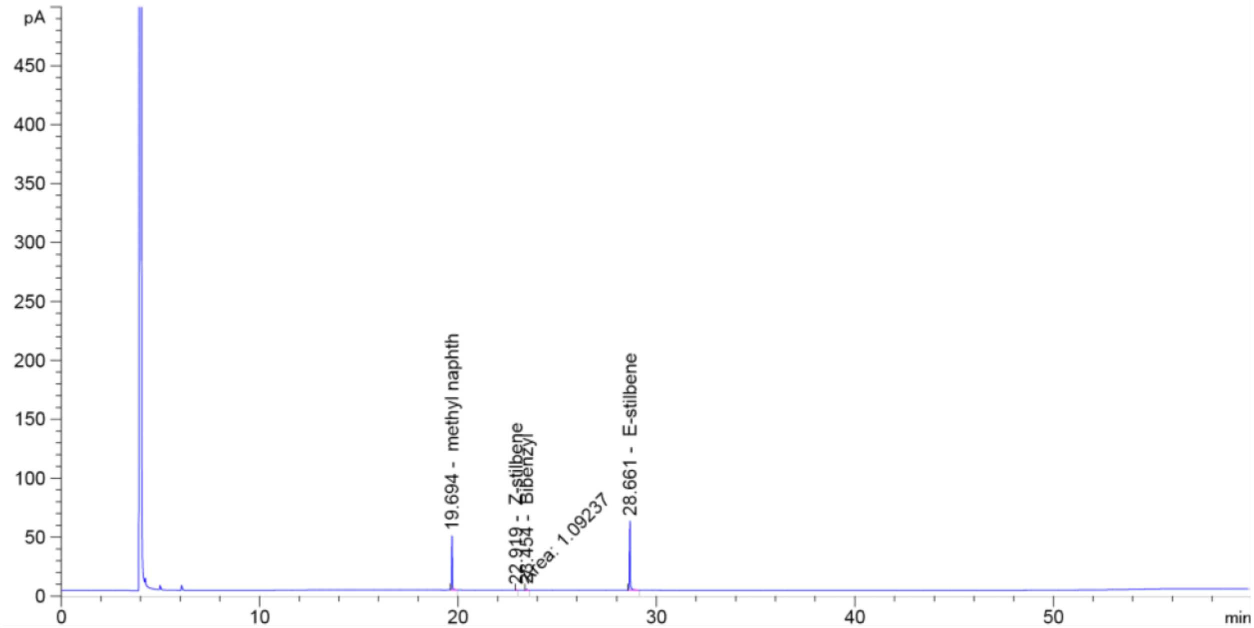

Figure B. 11. GC-FID chromatogram of the E-stilbene: asphaltene reaction products in methanol extract

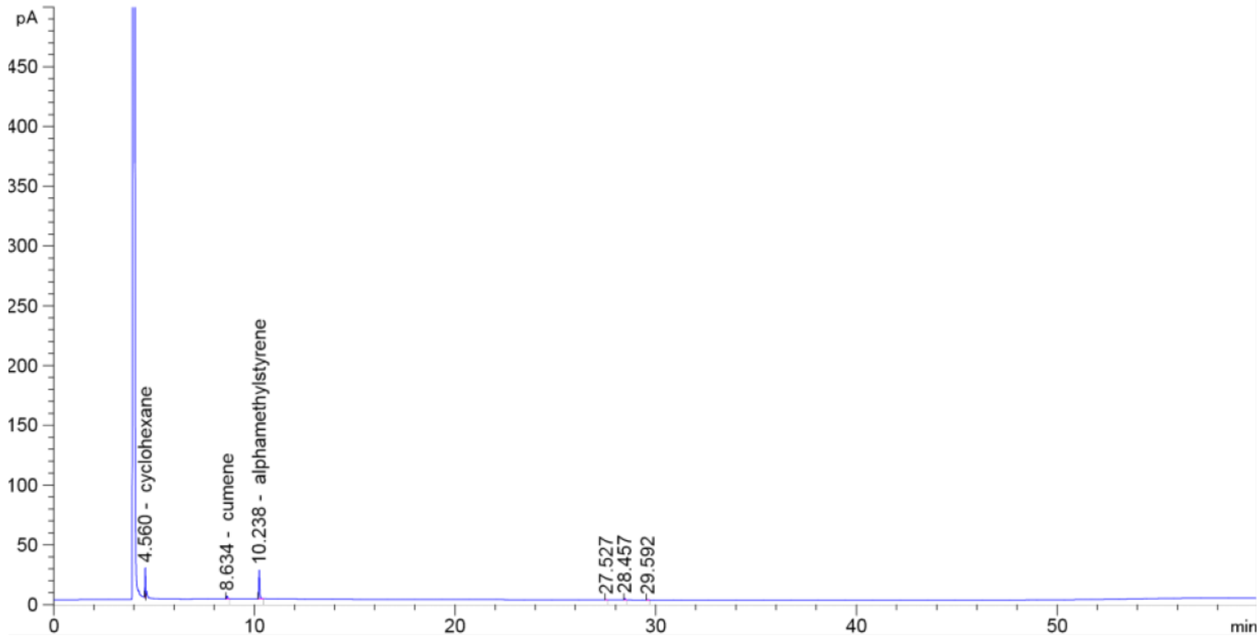

Figure B. 12. GC-FID chromatogram of the α-Methylstyrene: asphaltene reaction products in methanol extract

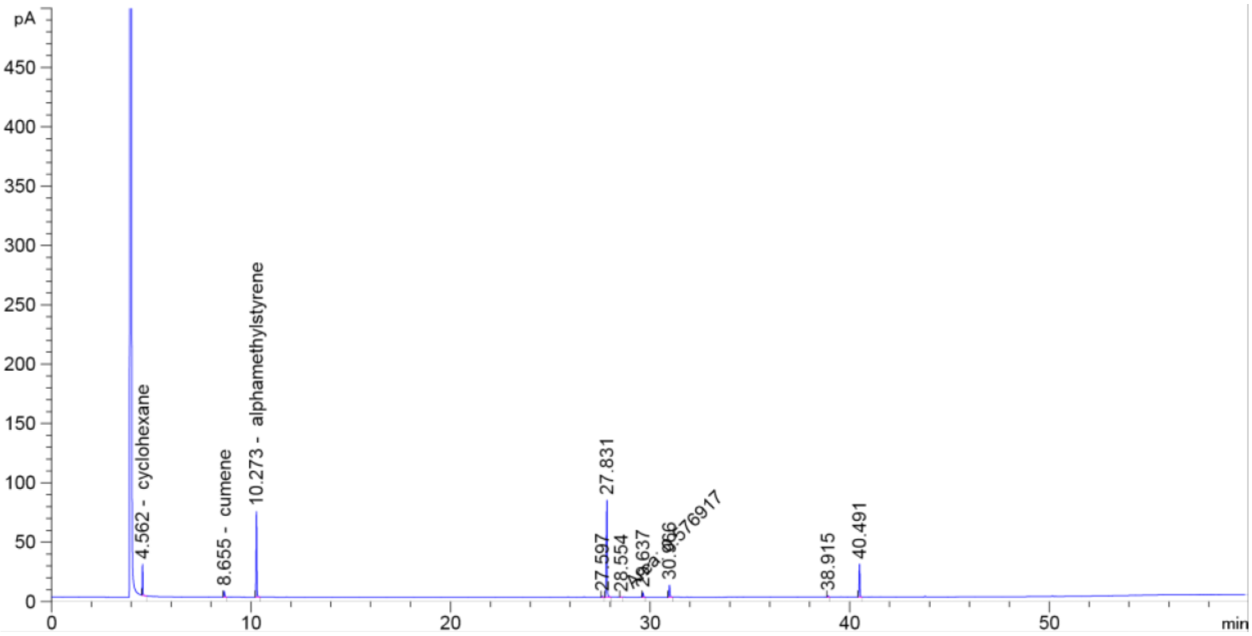

Figure B. 13. Chromatogram of the AMS:DHA reaction products in methanol extract. (Retention time in minutes (RT): 27.8 minutes- DHA; retention time 30.96 minutes- Anthracene)

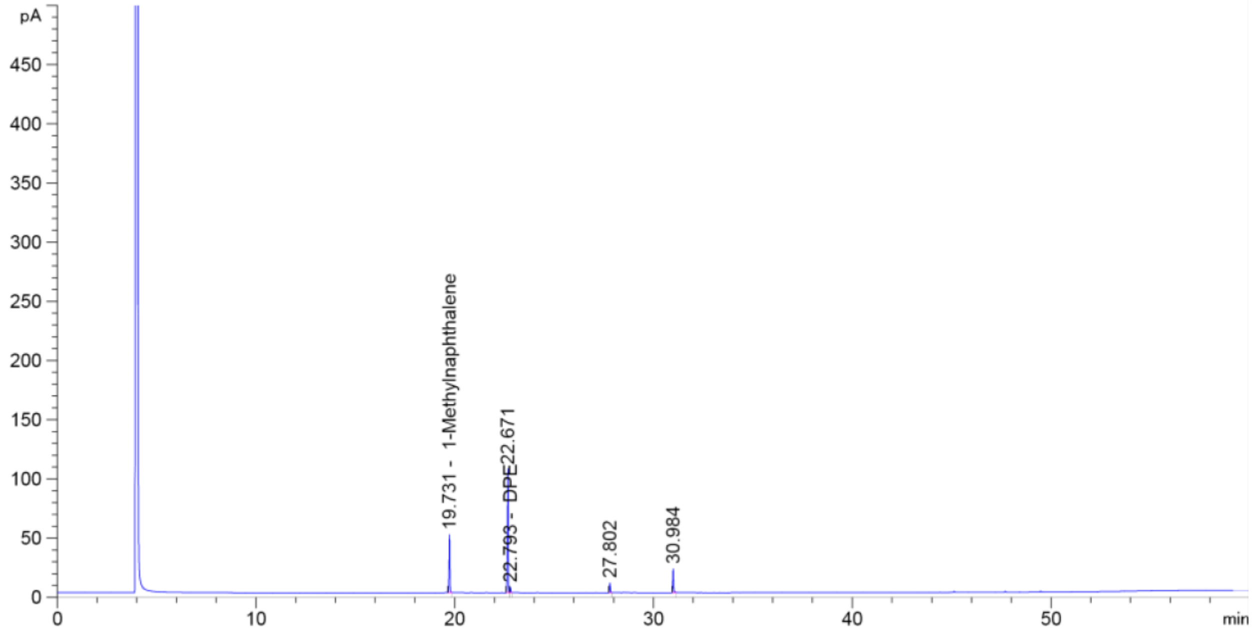

Figure B. 14. Chromatogram of DPE:DHA reaction products in methanol extract. (Retention time of 22.671-1,1diphenylethane; RT of 22.671-Dpe; RT of 22.8 -DHA; RT of 30.984 - anthracene)

B.5. Mass spectra of addition products obtained after AMS reaction with asphaltenes and DHA

Mass spectra results for the addition products obtained as a result of Experiments 10,11,12 are represented below. 2 mass spectra are represented for each compound, first the obtained mass spectra, second picture corresponds to the original mass spectra of the compound.

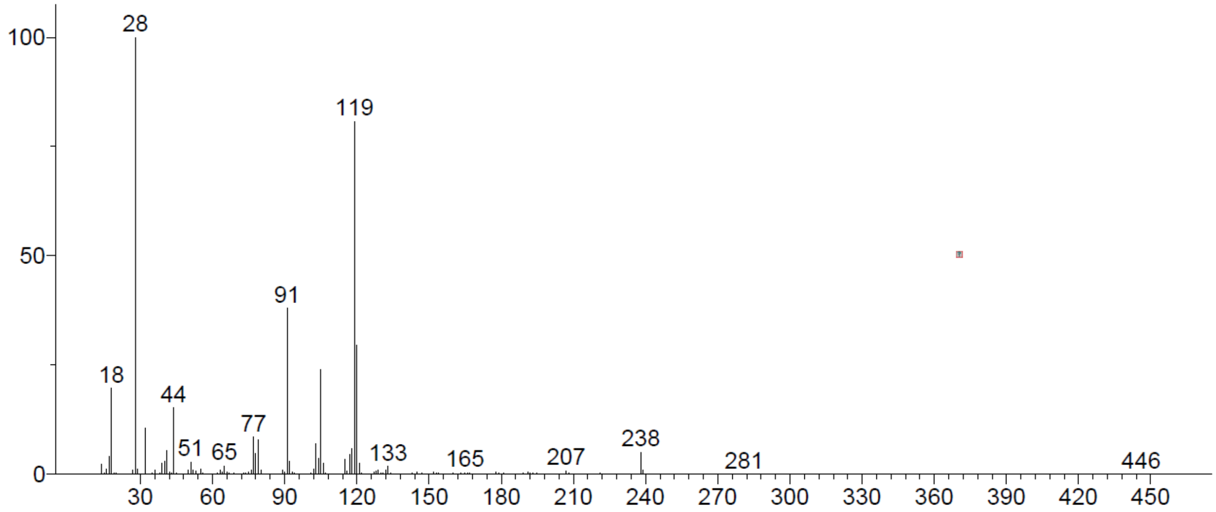

Figure B. 15. Mass spectra of the addition product A-1 in methanol extract

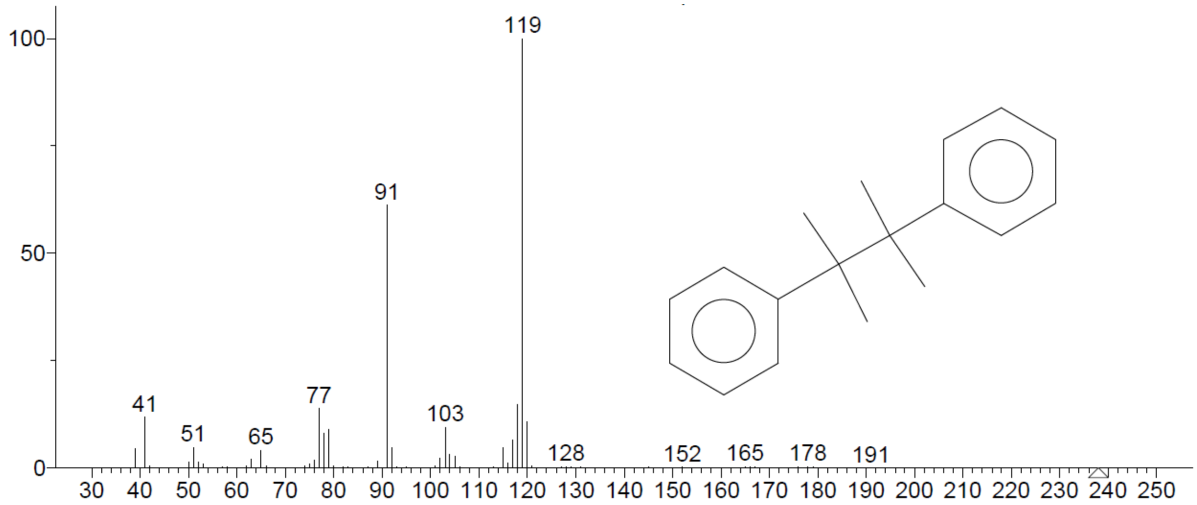

(replib) Benzene, 1,1'-(1,1,2,2-tetramethyl-1,2-ethanediyl)bis-

Figure B. 16. Mass spectra of the (2,3-Dimethylbutane-2,3-diyl)dibenzene that was suggested as a possible structure for A-1 product by NIST database

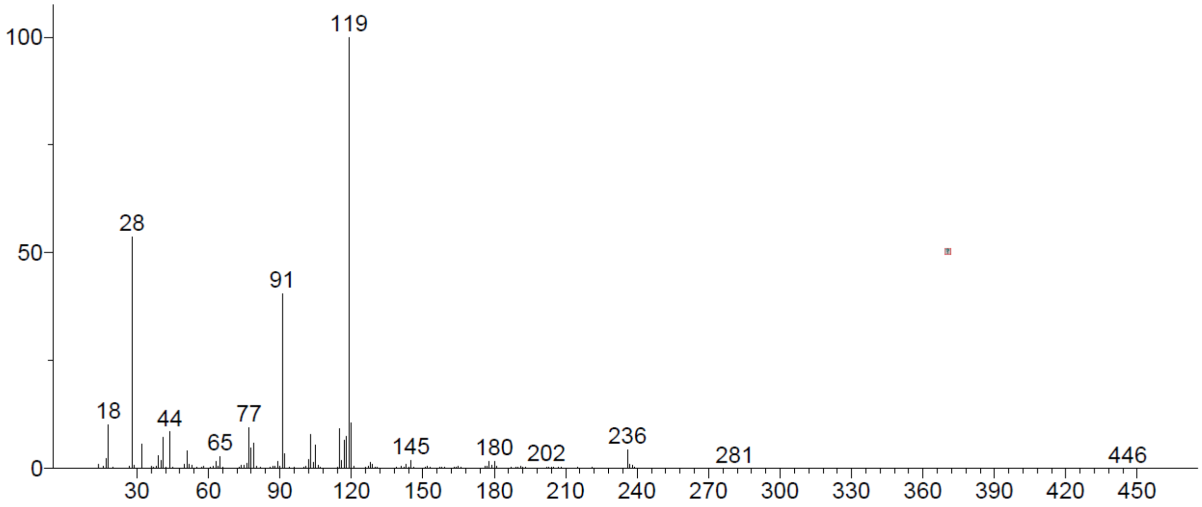

Figure B. 17. Mass spectra of the A-2 addition product in methanol extract

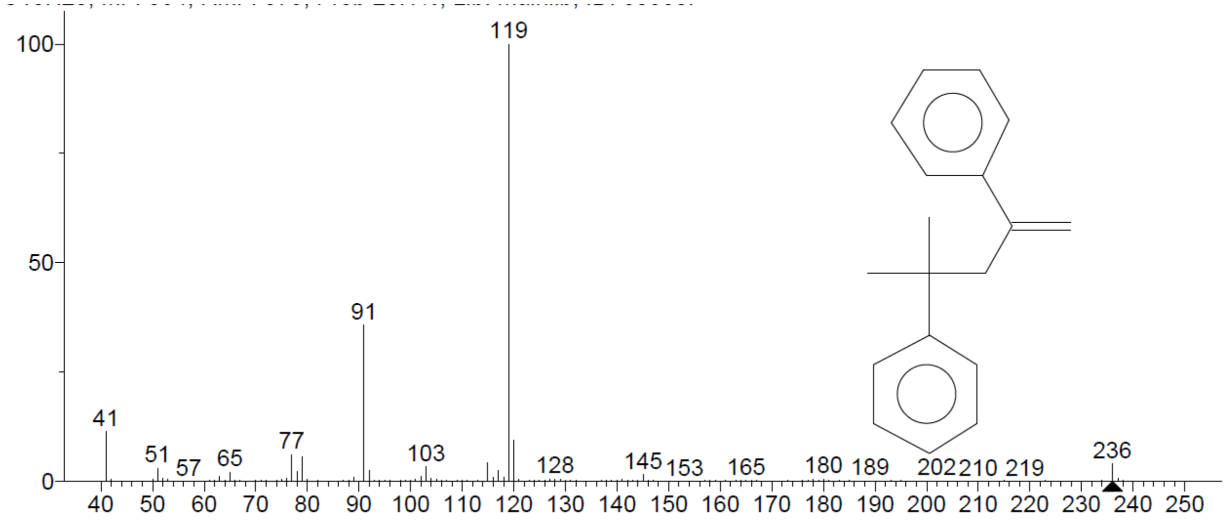

(mainlib) 2,4-Diphenyl-4-methyl-1-pentene

Figure B. 18. Mass spectra of (4-methylpent-1-ene-2,4-diyl)dibenzene that was suggested as a possible structure for A-2 product by NIST database

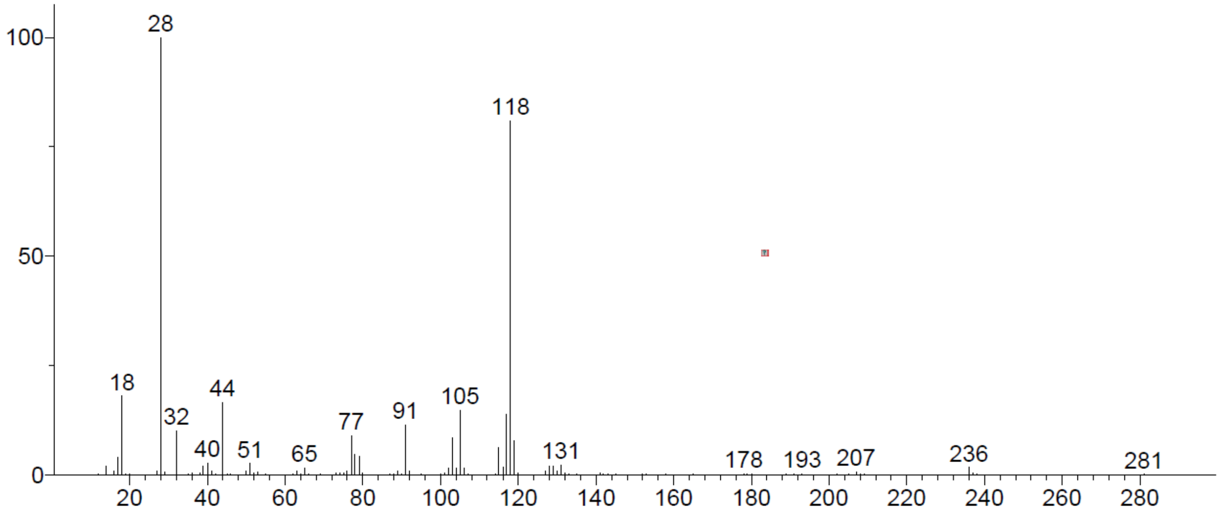

Figure B. 19. Mass spectra of the A-3 addition product in methanol extract

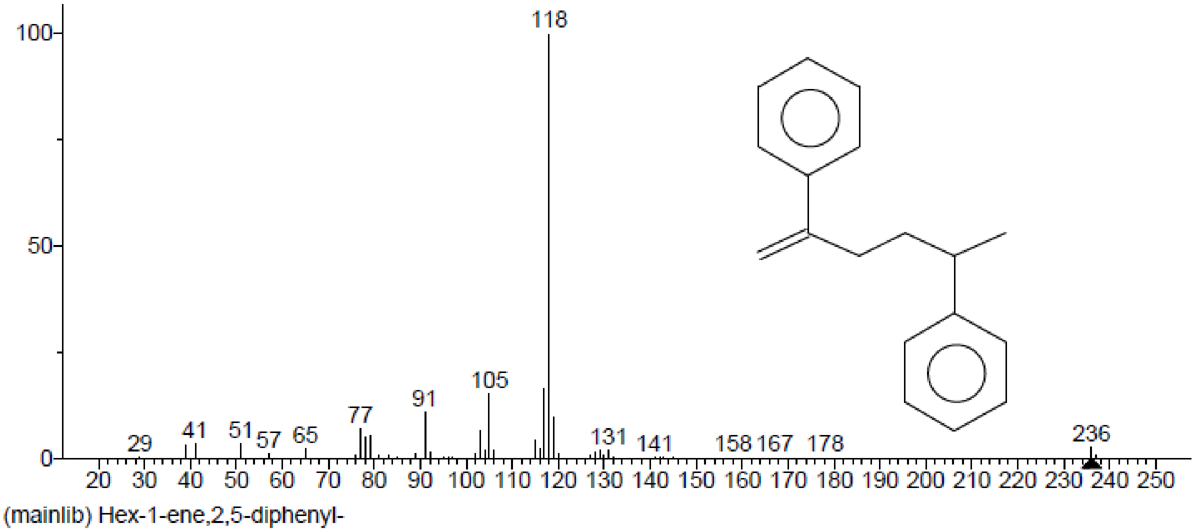

Figure B. 20. Mass spectra of hex-1-ene-2,5-diyldibenzene that was suggested as a possible structure for A-3 product by NIST database

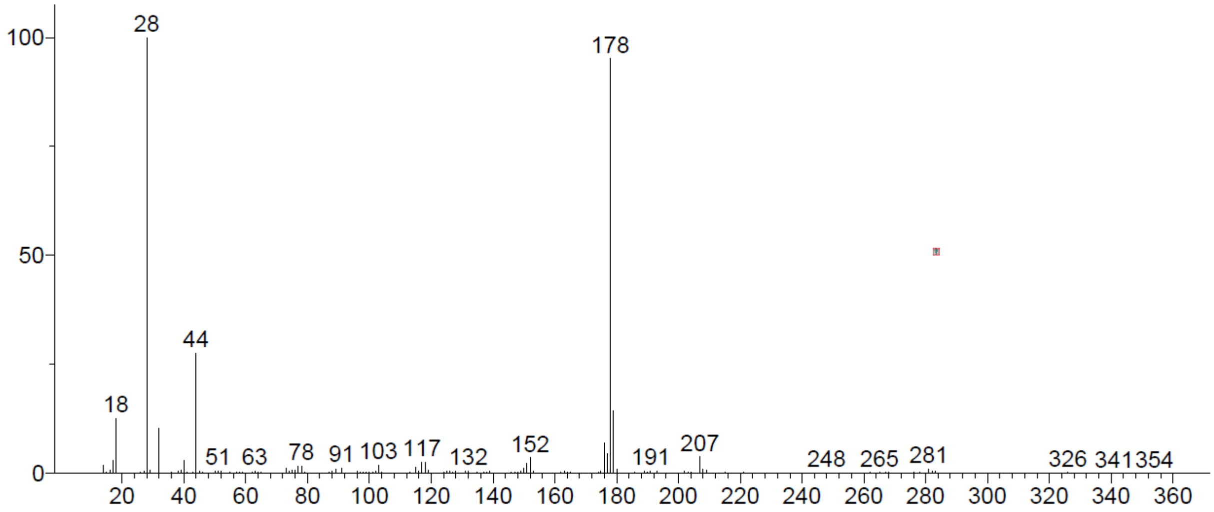

Figure B. 21. Mass spectra of the A-4 addition product in methanol extract

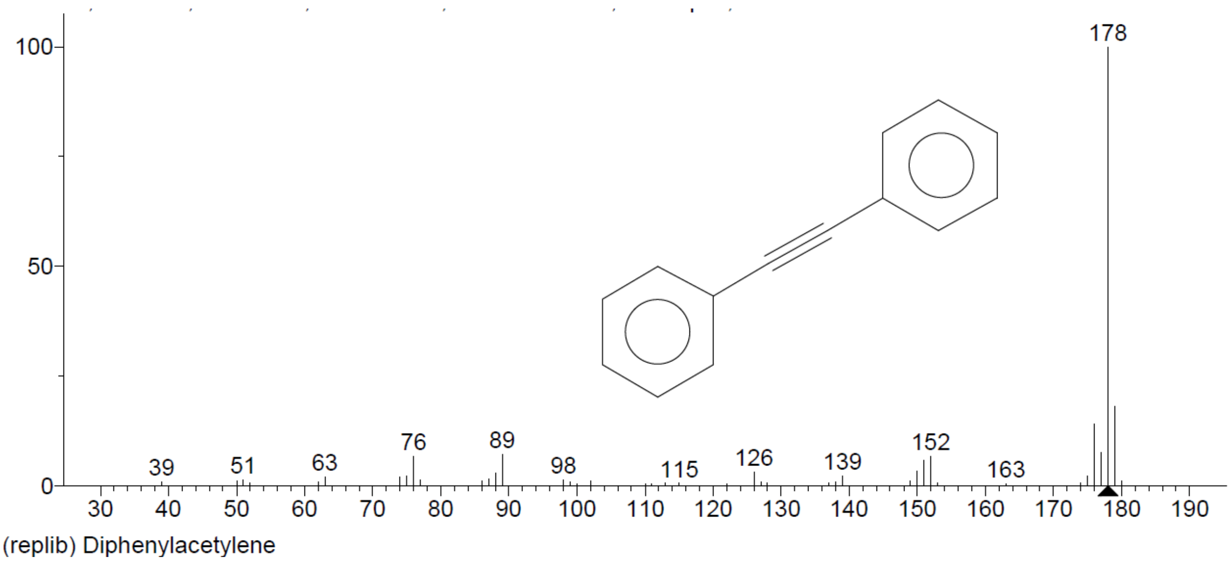

Figure B. 22. Mass spectra of 1,2-diphenylethyne that was suggested as a possible structure for A-4 product by NIST database

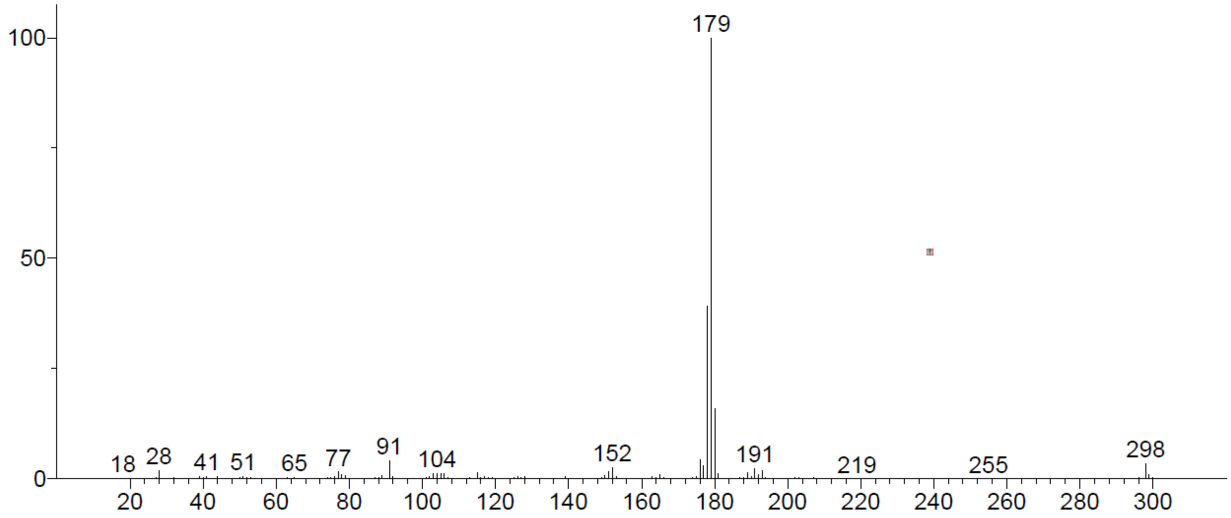

Figure B. 23. Mass spectra of the A-5 addition product in methanol extract

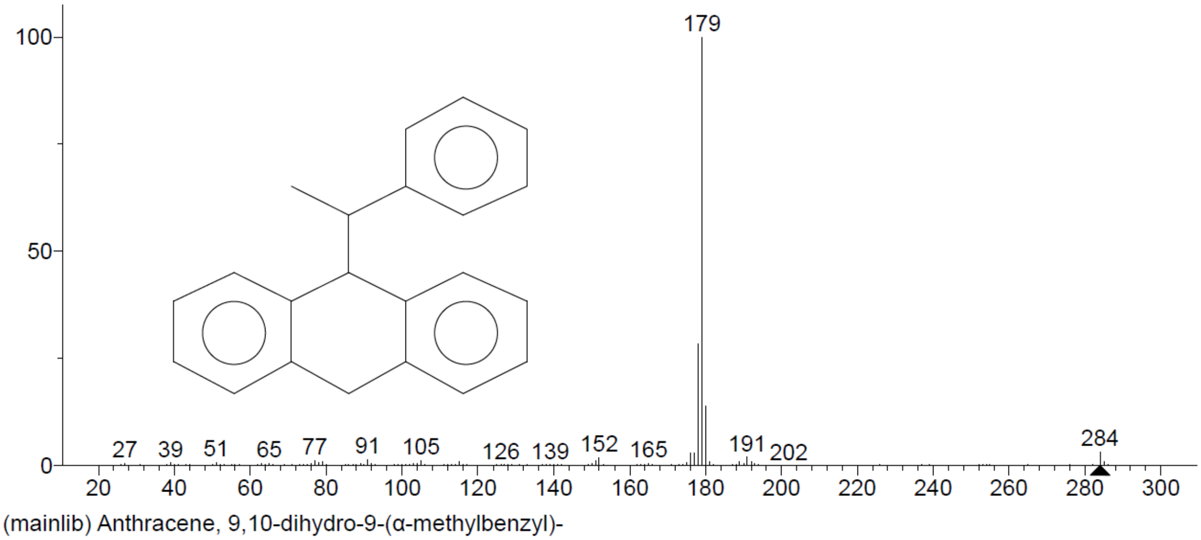

Figure B. 24. Mass spectra of 9-(1-phenylethyl)-9,10-dihydroanthracene that was suggested as a possible structure for A-5 product by NIST database

B.6. Mass spectra of the most abundant peak of TMS reaction with asphaltenes and DHA

Due to the absence of the probe molecule it was impossible to identify the compound obtained after reaction of TMS, asphaltenes and DHA. Mass spectra for the product is provided below.

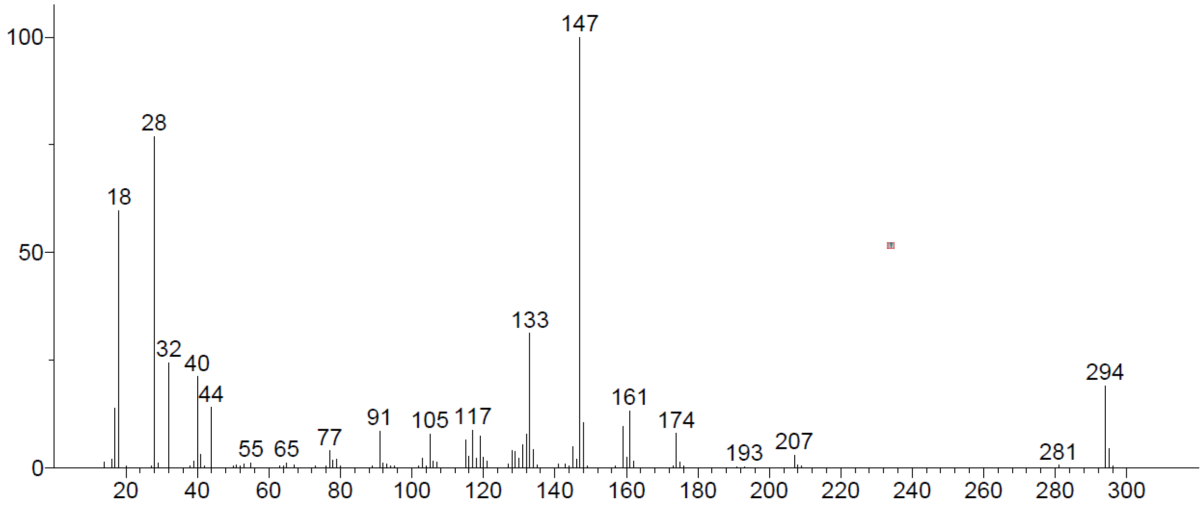

Figure B. 25. Mass spectra of the most abundant product in TMS reactions. Unidentified

Appendix C

Supplementary information of Chapter 5- Synthesis of hex-1-en-2-ylbenzene

C.1. Calibration data

To obtain the yield of the hex-1-en-2-ylbenzene it was necessary to perform the calibration for the compounds (Table C.1). Due to the absence of the hex-1-en-2-ylbenzene calibration was performed using 1-phenylpentan-1-one. More information can be found in Chapter 5, Section 5.2.3.

Table C. 1. Calibration data for 1-phenylpentan-1-one quantification

	Levels		
	1	2	3
1-phenylpentan-1-one			
Concentration (mg/ml)	1	2	3.1
Amount 1-phenylpentan-1-one/Amount ISTD	1.04	1.971	3.165
Area 1-phenylpentan-1-one/Area ISTD	0.896	1.916	2.941
ISTD			
Concentration (mg/ml)	1	1	1

The Figure C.1 represents the calibration curve for 1-phenylpentan-1-one built based on the data provided in Table C.1.

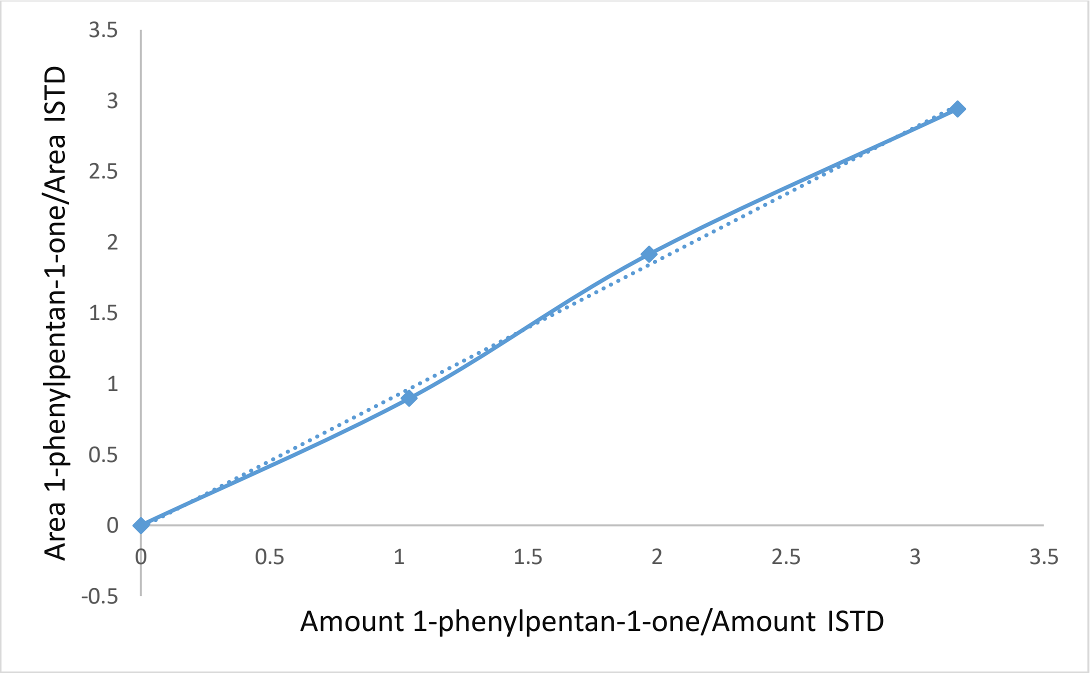

Figure C. 1. Calibration curve for 1-phenylpentan-1-one. Calibration was performed with parent compound 1-phenylpentan-1-one in the absence of hex-1-en-2-ylbenzene. As seen from the figure the regression coefficient: $R^2=0.998$. Linear equation: $y=0.9423x-0.0168$

C.2. Methylenation of 1-Phenylheptan-1-one

C.2.1. Introduction

It was initially decided to synthesize sterically hindered α-Methylstyrene derivative, such as 1-Phenylheptan-1-one, which has a long bulky alkyl chain attached to styrene in α-position. The procedure is based on the literature provided in Chapter 5, Section 5.1.

C.2.2. Procedure

To obtain sterically hindered alpha-alkyl vinyl aromatic compound the Tebbe methylenation of 1-Phenylheptan-1-one was carried out so as to produce (Oct-1-en-2-yl)benzene. Reaction procedure was based on the information given in chapter 5.

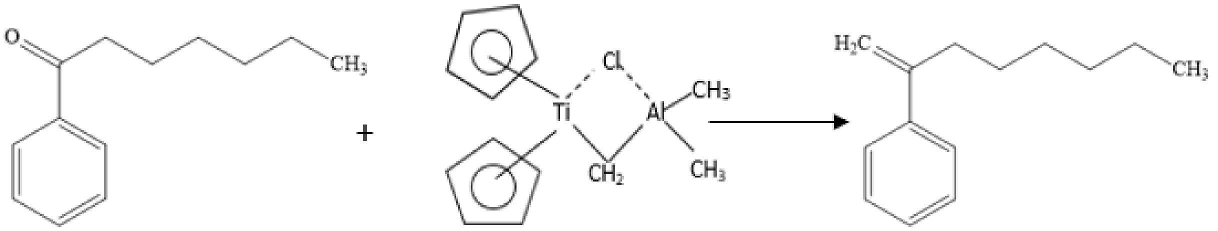

Figure C. 2. Basic representation of the reaction. Tebbe methylenation of 1-Phenylheptan-1-one to synthesize (Oct-1-en-2-yl) benzene.

Experiments were conducted based on the literature reported in Chapter 5. Procedure described in Chapter 5 was followed using different inputs. The first two attempts were made to synthesize (oct-1-en-2-yl)benzene from 1-Phenylheptan-1-one. The reaction was conducted twice, first time using dry ice and second time using conventional ice, while keeping all the other inputs unchanged. For that purpose, 117±3 mg of 1-Phenylheptan-1-one (0.61 mmol), THF 0.322 g were added to the tared 100ml round bottom flask. The mixture was cooled down to to -1°C, for 30 minutes using chiller. Tebbe reagent of 3.119±0.1 g (1.68 mmol) was added. The mixture was stirred for 1.5 hours. In the absence of ice (at the moment of reaction performance) the dry ice was employed at 350 rpm. The temperature inside the reaction vial was measured with temperature sensor and removed once the desired temperature was achieved. The mixture was diluted with 8 ml t-bumeO and quenched with 7 ml NaOH. Following the dyeing technique performed by Merck (1980) and Komsta et al., (2013) it was decided to use $KMnO_4$ (1.501g), K_2CO_3 (10,02g), 2.126 ml NaOH (1N), H_2O (150 g) to visualize the stains. Ehtyl acetate/hexane (3/50) mixture was used during the first run for the column chromatography as an eluent in the developing beaker to develop the TLC plate. However, to optimize the purification the eluent mixture ratio was optimized so as to move the products of the reaction down the column. In the second run reaction mixture was washed with the Hex/CH_2Cl_2 (1/20) for better dissolution of the compounds (later on defined as impurities or byproducts as it was not possible to determine them). Filtrate was washed with brine (NaCl solution) and dried over Na_2SO_4 in order to remove the remaining water content. The mixture was filtered using MF-Millipore Hydrophilic Filter papers with 0.22 µm pore size. The solution was concentrated using Heidolph Hei-Vap rotary evaporator at 130 mbar at room temperature, slowly bringing the vacuum pressure of 100 mbar so as to avoid rapid excessive evaporation of the compounds. The small-scale reaction was performed twice to prove the liability of the results.

Polarity indexes of the solvents were considered in order to provide optimal separation, following Snyder, et al. studies (Snyder et al., 2010).

C.2.3. Liquid Chromatography using stationary column

Liquid-solid adsorption technique was employed for that purpose, which is generally used for separation of non-ionic compounds dissolved in solvent. Liquid-solid chromatography (LSC) is a laboratory purification technique which is used to separate mixture of components dissolved in the solvent based on different rates of adsorption of the compounds on the stationary phase. As a result components of the mixture run at a different speeds with the eluent throughout the column due to the gravitation. Because the mobile phase is comprised of eluents that have uneven charge distribution, and therefore high polarities, they can readily move and penetrate through the stationary phase and separate analyte compounds from that phase.

It is a useful technique when separating components with similar or close boiling points. For that purpose, column chromatography was installed. Silica gel was selected to be the stationary phase for adsorption of the reaction mixture components. Ultra-pure Silica gel for liquid chromatography column was purchased from Acros Organics (Catalog Number: 360050010), with pore size 60 Å, and particle size 40-60 µm. Collected eluates were analyzed further using GC-MS. Slurry packing technique was used to pack the column. During the process the silica was not allowed to dry, supplying the eluent flow to the column constantly. Cotton plug was installed at the bottom and the top of the column. The analyte was added to the column evenly to ensure uniform distribution of sample down the column.

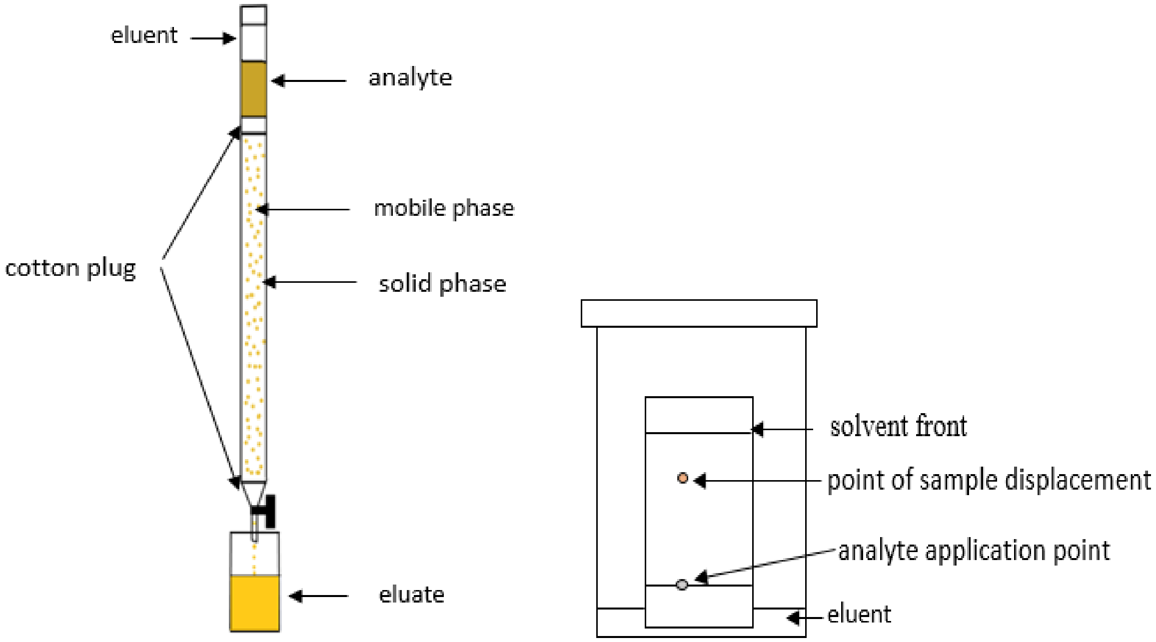

Figure C. 3. Setup of chromatography column and setup for TLC development (note: analyte dissolved in solvent was mixed with silica and dried then added to the column with eluent, however for the ease of the representation analyte was shown separately.)

Planar chromatography (PC): In planar chromatography the stationary phase of silica covers the solid sheet (Thin Layer Chromatography -TLC). The separation is optimized by changing the eluent mixture, depending on the polarity of the solvents employed. The optimal ratio is based on the results of TLC plates development. (Ganshirt, 1955; Burtis and Bruns, 2014)

TlC technique was performed as a laboratory technique to identify the components of the reaction mixture, its purity, and also was used for optimisation of the column chromatography. Ascending mode for TLC plates development was performed for the current study. Capillary action will move the eluent throughout the TLC plate, moving the components comprising the analyte as well. The analyte spot is added to the TLC plate with the capillary tube. The efficient eluent mixture ratio is selected after TLC plates development.

In the given case the ratio of the mixture was given in the article, however in case of side-products formation instead of the desired products, or in case if the product is stuck amongst the impurities, the eluent constituents as well as the ratio might be altered so as to move the components of the reaction down the column accordingly. It is important to know the retardation factor (Rf) which is the ratio of the distance travelled by component to the distance travelled by solvent on the TLC plate; (Poole 2003; Burtis and Bruns, 2014.)

$$R_f = \frac{\text{distance travelled by component}}{\text{distance travelled by eluent}} \qquad \text{Eq. C.1}$$

and the relative affinity of the component (K) (or capacity factor) for the eluent relative to silica column, which is defined as (Poole, 2012)

$$K = \frac{(1 - R_f)}{R_f} \qquad \text{Eq. C.2}$$

Based on the above-mentioned values, the suitable composition and ratio of polar to non-polar solvents in eluent are adjusted accordingly.

Figure C. 4. Reaction set ups for the test runs, from left to right:
-Reaction mixture at low temperatures using dry ice in the absence of ice as the coolant
-Liquid-liquid phase separation of immiscible organic-inorganic mixtures to define the side-products.
-Column setup for liquid-solid chromatography for product purification

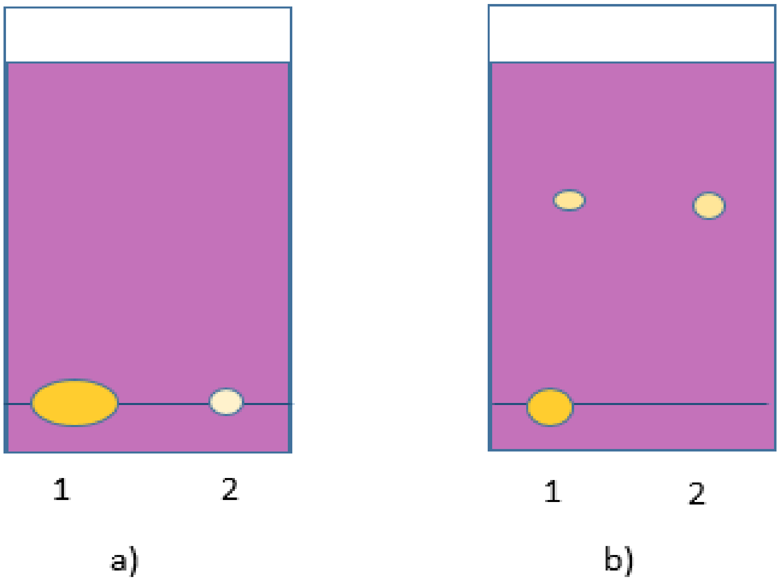

Figure C. 5. Visual Representation of thin layer chromatography (TLC) plates obtained after reaction run. The eluent moved the 1-Phenylheptan-1-one up the plate. The residual point is assumed to be impurities. As it was not possible to observe the peak using GC-MS.

1) - reaction mixture; 2) - parent ketone compound (1-Phenylheptan-1-one)

a) Initial state b) final state

Figure C. 6. Residue on filter papers; after water washing of reactions products (right), after drying mixture with Na_2SO_4 (left)

C.2.4. Results

Analysis of the fractions was performed using GC-MS technique. No peaks were observed using the GC-MS technique (Figure C.7), except for the parent compound 1-Phenylheptan-1-one and solvents comprising the eluent. That might be due to very heavy compounds present in the reaction mixture which might be either impurities, or reagent residuals, which are not the products of interest. The very low concentration of the reaction products might also be the case, however in the current study high yield of the product was of interest. For that purpose the eluates were allowed to stay for over 24 hours to observe the higher concentrations of the compounds within, however it was not possible to observe any peaks.

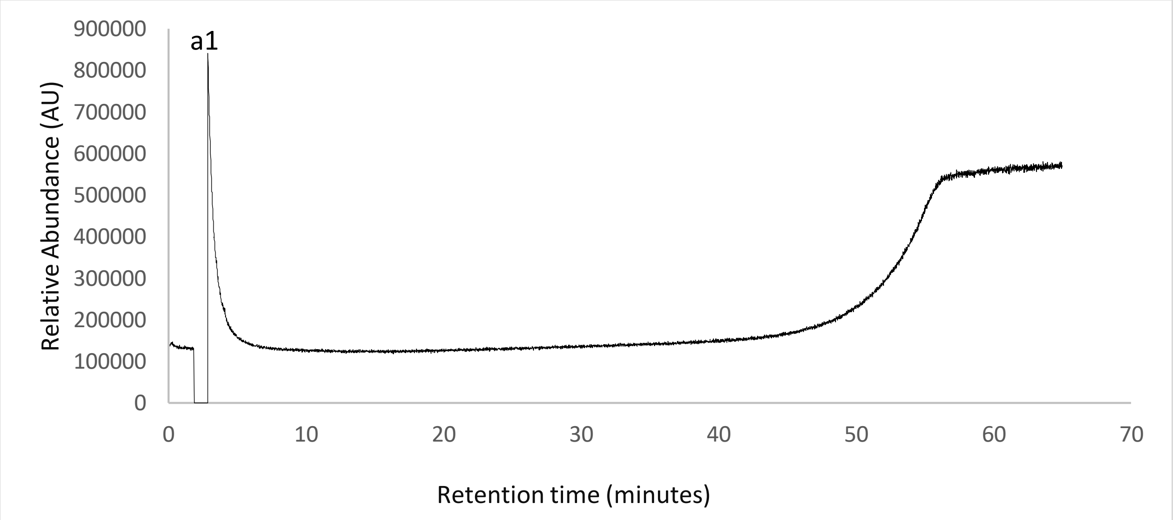

Figure C. 7. Chromatogram of the eluate with the most abundant peak after the reaction conduction. A1 peak shown in the chromatogram is the peak of the solvent comprising eluent CH_2Cl_2.

C. 3. References

Burtis, C.A. and Bruns, D.E., 2014. *Tietz fundamentals of clinical chemistry and molecular diagnostics-e-book*. Elsevier Health Sciences.

Ganshirt, H., 1955. Quantitative Evaluation of Thin-Layer Chromatography. *Thin-Layer Chromatography, A Laboratory Handbook*, pp.133-155.

Komsta, L., Waksmundzka-Hajnos, M. and Sherma, J. eds., 2013. *Thin layer chromatography in drug analysis*. CRC Press.

Merck, E., 1980. *Dyeing reagents for thin layer and paper chromatography*. E. Merck.

Poole, C.F. and Poole, S.K., 2012. *Chromatography today*. Elsevier.

Poole, C.F., 2003. *The essence of chromatography*. Elsevier.

Snyder, L.R., Kirkland, J.J. and Dolan, J.W., 2010. Basic concepts and the control of separation. *Introduction to Modern Liquid Chromatography*, pp.19-86.